



UiT The Arctic University of Norway

IVT-Faculty

Modeling and analysis of power system oscillations using real-time simulator.

Using MATLAB/Simulink and RT-Lab

Andreas Sandberg

Master's thesis Electrical Engineering – Master ELE-3900 [May 2022]

Table of Contents

1	Introduction	1
1.1	Background.....	1
1.2	Problem description.....	1
1.3	Previous work.....	2
1.4	Scope and limitations.....	2
2	Theory	4
2.1	Power system stability theory.....	4
2.1.1	Rotor angle stability	5
2.1.2	Frequency stability	9
2.1.3	Voltage stability	10
2.2	Control elements.....	10
2.2.1	Governor and turbine system.	10
2.2.2	Excitation system	11
2.3	Load modelling.....	13
2.4	Simulation software.....	14
2.4.1	RT-LAB	14
2.4.2	Power System Toolbox (PST).....	15
3	Modelling	16
3.1	The network model.....	16
3.2	Initial models	17
3.3	Changes applied.....	19
3.4	Load modelling.....	20
3.4.1	Alternative solution.....	23
3.5	Modeling Linear analysis	24
3.5.1	Tuning PST	24
3.5.2	Modeling the control elements.....	26

3.5.3	PST load change response.....	32
3.5.4	Dynamic response comparison.....	32
3.6	RT-Lab modeling	34
4	Simulations.....	38
5	Results	39
5.1	Linear analysis.....	39
5.1.1	No PSS implemented	39
5.1.2	Applying the PSS	47
5.2	Dynamic simulations of load changes with analysis.....	52
5.2.1	100MW applied to load in area 1	52
5.2.2	100MW applied to load in area 2	55
5.2.3	300MW applied to load in area 1, then 300MW applied to load in area 2	57
5.2.4	Testing the limits of the voltage 1000MWs added to load in area1.....	59
5.2.5	Concurrent 50MW increase at both loads	60
5.2.6	Concurrent 100MW increase at both loads	62
5.2.7	100MW increase of load in area1, while 100MW decrease of load in area 2 ...	62
5.2.8	400MW increase of load in area1, while 400MW decrease of load in area 2 ...	64
5.2.9	No PSS tests	67
5.3	RT lab	70
5.3.1	With PSS	70
5.3.2	Without PSS	77
6	Conclusion and future work	80
	References	81
	Appendix	84

List of Tables

Table 1:Generator data	19
------------------------------	----

Table 2: Load flow data variable step model	25
Table 3: Load flow data fixed step/RT model.....	25
Table 4: Load flow data PST model.....	26
Table 5: Steam turbine governor data	27
Table 6: PSS Data	29
Table 7: Exciter data	30
Table 8: No PSS eigenvalues, dampening and frequency	39
Table 9: With PSS eigenvalues, dampening and frequency.....	47

List of Figures

Figure 2.1-1 The different types of power system stability [5].....	4
Figure 2.1-2: Small signal rotor angle stability equilibrium points [11].....	6
Figure 2.1-3: Process of frequency stabilization after disturbance[17]	9
Figure 2.2-1: Steam turbine governor block diagram [2].....	10
Figure 2.2-2: Excitation control system [22]	11
Figure 2.2-3: Elements of PSS	12
Figure 2.2-4: Block diagram of PSS [2].....	13
Figure 2.4-1: Structure of simulator OP4510 [29]	15
Figure 3.1-1: Kundur two area	16
Figure 3.2-1: Generator control circuit	18
Figure 3.4-1: ZIP-load block diagram.....	20
Figure 3.4-2: Load response with and without LP filter	21
Figure 3.4-3: ZIP-load block diagram with LP filters.....	22
Figure 3.5-1: Initial K2A one line diagram from PST [2].....	24
Figure 3.5-2: Steam turbine governor block diagram [2].....	27
Figure 3.5-3: STG in MATLAB	27
Figure 3.5-4: Response of IEEE Governor versus premade governor in Simulink	28
Figure 3.5-5: PSS block diagram [2].....	29
Figure 3.5-6: Block diagram of DC1A exciter.....	30
Figure 3.5-7: Difference in response between DC1A for fixed-step/RT model and variable- step/PST model	31
Figure 3.5-8: PST Rotor speed deviation after 242MW change in load 1	32
Figure 3.5-9: Simulink Rotor speed deviation after 242MW change in load 1	32
Figure 3.5-10: PST Rotor angle after 242MW change in load 1	33

Figure 3.5-11:Simulink Rotor angle after 242MW change in load 1.....	33
Figure 3.6-1:Top level of RT-Lab(fixed-step) model	34
Figure 3.6-2:SM-subsystem	35
Figure 3.6-3:SC-subsystem	36
Figure 5.1-1:Compass plot of rotor angle terms of inter-area mode eigenvector without PSS	40
Figure 5.1-2: Real part of speed participation factor - inter-area mode without PSS	41
Figure 5.1-3: Dynamic speed deviations response of increase of active load in area 1 without PSS	41
Figure 5.1-4: Dynamic response of increase of active load in area 1 without PSS zoomed in	42
Figure 5.1-5:Compass plot of rotor angle terms of local machine mode eigenvector without PSS, Left for area 1 and right for area 2.....	43
Figure 5.1-6:Real part of speed participation factor- local area mode for area 1 No PSS	44
Figure 5.1-7:Real part of speed participation factor- local area mode for area 2 No PSS	44
Figure 5.1-8:Dynamic test of local mode oscillations by increasing the voltage in generator 1, No pss.....	45
Figure 5.1-9:Dynamic test of local mode oscillations by increasing the voltage in generator 1, No pss Zoomed in	45
Figure 5.1-10:Compass plot of rotor angle terms of inter-area mode eigenvector with PSS ..	48
Figure 5.1-11: Real part of speed participation factor - inter-area mode with PSS	48
Figure 5.1-12: Dynamic speed deviations response of increase of active load in area 1 with PSS	49
Figure 5.1-13: Compass plot of rotor angle terms of local machine mode eigenvector with PSS, Left for area 1 and right for area 2.....	49
Figure 5.1-14:Real part of speed participation factor- local area mode for area 1 with PSS...	50
Figure 5.1-15:Real part of speed participation factor- local area mode for area 2 with PSS...	50
Figure 5.1-16: Dynamic speed deviations response of increase of terminal voltage of generator 1 with PSS	51
Figure 5.2-1:Speed deviations after a 100MW load increase in area 1.....	52
Figure 5.2-2: Rotor angles with ref set to generator 1 after a 100MW load increase in area1	53
Figure 5.2-3: Voltage levels after a 100MW load increase in area1	53
Figure 5.2-4:Speed deviations after a 100MW load increase in area 2.....	55
Figure 5.2-5:Voltage levels after a 100MW load increase in area2.....	55
Figure 5.2-6:Speed deviations after a 300MW load increase in area 1.....	57
Figure 5.2-7:Voltage levels after a 300MW load increase in area1	57

Figure 5.2-8:Speed deviations after a 300MW load increase in area 2.....	58
Figure 5.2-9:Voltage levels after a 300MW load increase in area2.....	58
Figure 5.2-10:Speed deviations after a 1000MW load increase in area 1.....	59
Figure 5.2-11:Voltage levels after a 1000MW load increase in area1	59
Figure 5.2-12: Rotor angle after a 50MW concurrent load increase in both areas	60
Figure 5.2-13: Rotor speed deviations after a 50MW concurrent load increase in both areas	60
Figure 5.2-14: Rotor speed deviations after a 100MW concurrent load increase in both areas	62
Figure 5.2-15: Rotor angles after a 100MW load increase in area1 and a 100MW load decrease in area 2	63
Figure 5.2-16: Rotor speed deviations after a 100MW load increase in area1 and a 100MW load decrease in area 2	63
Figure 5.2-17: Rotor angles after a 400MW load increase in area1 and a 400MW load decrease in area 2	64
Figure 5.2-18: Rotor speed deviations after a 400MW load increase in area1 and a 400MW load decrease in area 2	64
Figure 5.2-19: Rotor angles after a 1000MW load increase in area1 and a 1000MW load decrease in area 2	65
Figure 5.2-20: Rotor speed deviations after a 1000MW load increase in area1 and a 1000MW load decrease in area 2	66
Figure 5.2-21:Rotor angles after a 100MW load increase in area 1 without PSS.....	67
Figure 5.2-22: Rotor angle after a 50MW concurrent load increase in both areas no PSS.....	68
Figure 5.2-23:: : Rotor speed deviations after a 100MW load increase in area1 and a 100MW load decrease in area 2 without PSS.....	68
Figure 5.3-1:Rotor angles after a 100MW load increase in area 1 RT/fixed step model versus Variable step model.....	70
Figure 5.3-2:Speed deviations after a 100MW load increase in area 1 RT/fixed step model versus Variable step model	70
Figure 5.3-3:Speed deviations after a 300MW load increase in area 1 RT	71
Figure 5.3-4:Terminal voltages after a 300MW load increase in area 1 RT.....	72
Figure 5.3-5:Terminal voltages after a 300MW load increase in area 1 RT Zoomed in	72
Figure 5.3-6:Rotor speed deviations after a 500MW load increase in area 1 RT	73
Figure 5.3-7:Terminal voltages after a 500MW load increase in area 1 RT.....	73

Figure 5.3-8:Rotor angles after a 200MW load increase in area 2 RT/fixed step model versus Variable step model.....	74
Figure 5.3-9: Speed deviations after a 200MW load increase in area 2 RT/fixed step model versus Variable step model	74
Figure 5.3-10: Rotor speed deviations after a 50MW concurrent load increase in both areas RT lab compared with variable step model.....	75
Figure 5.3-11: Rotor speed deviations after a 100MW load increase in area1 and a 100MW load decrease in area 2 RT lab compared with variable step model	76
Figure 5.3-12:Rotor angles after a 100MW load increase in area 1 No PSS RT/fixed step model versus Variable step model	77
Figure 5.3-13:Speed deviations after a 100MW load increase in area 1 No PSS RT/fixed step model versus Variable step model	77
Figure 5.3-14:Rotor angles after a 50MW concurrent load increase in both areas No PSS RT lab compared with variable step model.....	78
Figure 5.3-15: Rotor speed deviations after a 50MW concurrent load increase in both areas No PSS RT lab compared with variable step model	78
Figure 5.3-16: Rotor angles after a 100MW load increase in area1 and a 100MW load decrease in area 2 No PSS RT lab compared with variable step model.....	79
Figure 5.3-17: Rotor speed deviations after a 100MW load increase in area1 and a 100MW load decrease in area 2 No PSS RT lab compared with variable step model.....	79

Foreword

This master thesis presents the results of two years of master studies, at UiT The arctic university of Norway. A special thank goes to my supervisor, professor Sharma Charu. I would also thank professor Trond Østrem for a lot helping with the Simulink modelling. In addition I would like to thank Joe Chow for helping with the PST software.

Abstract

In this thesis a version of the Kundur two-area model has been developed for Simulink and real time simulator software and hardware from OPAL-RT. This model should be used for testing the rotor angle oscillations load variations create. A review of the different control elements found in basic power systems has been reviewed and implemented.

The main component that will be manipulated in the model is the active load, so a zip-load model had to be developed for Simulink to make the system work.

It was necessary to build multiple models of the same figure in Simulink, one fixed step version to run in RT-lab, and one variable step to do Simulink tests on.

Frequency and voltage stability are not a focus but are mentioned throughout because each of them do affect the system. The lack of secondary frequency reserves leads to never regain nominal rotor speed, and voltage stability affects the simulations done on the RT-lab model.

Linear analysis of the stability was done using PST software. The linear results were compared to the variable step model.

The results show that the different models behave similarly and manages to simulate what happens with the stability during load changes.

1 Introduction

1.1 Background

A few years ago, UiT Narvik bought a real time simulator unit from Opal-RT. The intent with acquisitions is to make it possible to do dynamic power system simulations. Because of the corona pandemic not much work has been done on the simulator. To mitigate this there was request a model that would be based on the classic Kundur Two area system that could be used to simulate and analyse oscillations caused by changes to the load.

Power systems are some of the most important structures that exist in the modern world. More integration of power system simulation can strengthen UiTs focus on power systems, since at the moment there is not much focus on simulation of dynamic power systems during the master's degree level.

1.2 Problem description

Small perturbations in load within a given power system can have significant effects on stability of a system. These disturbances result in oscillations. In general, these oscillations are characteristic of the system, and are acceptable if they have a decaying nature. In present work, oscillation dynamics will be studied, and a control algorithm will be developed to control these oscillations on real-time simulator.

Main Objective:

- Review of various types of oscillations
- Review of various control algorithms utilized for oscillations damping
- Studying and simulating oscillations in two-area four-machine model using MATLAB
- Implementing the suggested technique on real-time simulator

1.3 Previous work

A project based on stability analyses of the Kundur system was done during the autumn semester of 2021. It shared the same general problem description as the master thesis except that the testing of the model with the real time simulator was not a part of it. The tests done during the preproject was done using a MATLAB script program called Power System Toolbox(PST). The goal was to learn more about how to do dynamic power system simulations, how to analyse the simulation data and plot, and how to do modal analysis. The system model used was a slightly modified version of a two area model usually known as the Kundur two area model, most famously used in the book Power System Stability and Control [1], but the version of the model used was based on data from the PST toolbox manual[2] and graham book[3].

1.4 Scope and limitations

The main task of the project was to develop a MATLAB simulation model of the Kundur that was compatible with RT-Lab, and could have variable loads. Because of the lack of experience with both general dynamic power system modelling and Simulink modelling for high voltage systems, most of the effort went into making a model that could fulfill the tasks mentioned in the project description. Tuning of the control elements, like the PSS, could not be done within the timeframe so the focus will be one how these components work and how they affect the stability of the system.

To be able to do linear analysis of the oscillation modes the MATLAB script based software PST from the autumn project had to be used, since neither student or supervisor could find a way to get MATLAB to calculate the state space matrix of the model. This limited the amount of linear analysis that could be done, especially in relation to the actual model that was used in the real time simulator.

No major structural changes or additional elements were applied to the Kundur model.

The main theoretical focuses of this thesis are small signal rotor angle stability, oscillations, modes and load modelling. Frequency and voltage stability will be mentioned and superficially analysed when relevant.

There will be no large disturbance test, like short circuit test. The focus is on load variations so most of the tests will only look how variations in the load affect the system. The only exception will be tests for the local mode stability where changes in reference voltage will be applied, since there is only one load per area.

Since the rotor is a round rotor all saliencies will be ignored.

The only modes that are considered are local machine and inter area modes, the other kinds of modes are not relevant for the Kundur two area model.

2 Theory

2.1 Power system stability theory

Power system stability is the ability to return and maintain an equilibrium state in a electrical power system after a disturbance has been inflicted on the system [5]. A disturbance can be many different things, some of the most common are changes in load demand, loss of power production, or faults on transmission lines. One can broadly put disturbances in two groups, large and small. The small ones are changes in the system that are natural, expected and continuous, like variations in load flow. While large disturbances are usually faults or similar sudden and critical errors. It is critical that a power system is able to maintain stability during both small and large disturbances. [6]

Power systems are inertially nonlinear since their stability depends both on the initial condition of the system and the amount of disturbance that is applied. [7] The dynamics of the system can be divided into four different phenomena wave, electromagnetic, electromechanical and thermodynamic. This broad classification is based on mainly on their physical characteristic and their time frame. In this thesis the focus will be on the electromechanical dynamics which are caused by oscillations of the rotating masses of electrical machines. These have a time frame of milliseconds to almost a minute. [8]

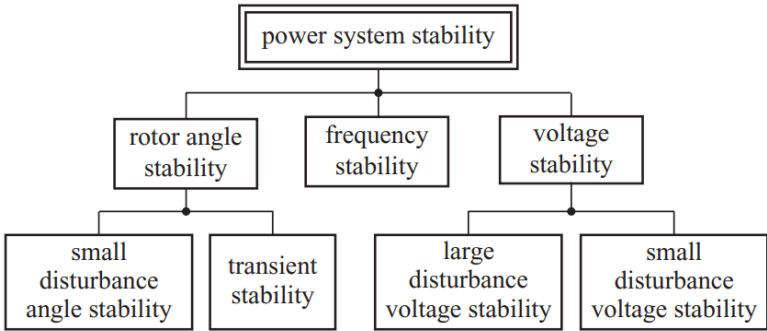


Figure 2.1-1 The different types of power system stability [5]

Based on what part of the system that is affected one can further divide up power system stability, into three main categories, rotor angle, frequency and voltage stability. Voltage and rotor angle stability and further be divided up based on the size of the disturbance applied to the system. [5]

2.1.1 Rotor angle stability

Rotor angle stability is the ability of interconnected synchronous machines within a power system to stay synchronised with each other after a disturbance has occurred. By studying the electromechanical oscillations that appear in the power system. These oscillations will impact the power output of the machines, which will lead to changes in the power flow of the system. The rotor angles are derived from the angular separation between the rotor and stator magnetic fields. The separation of these fields is decided by the torque output of the generator. The torque can be rewritten as the power output. [9]. It is the balance of electrical and mechanical torque/power in the system that decides if the rotor angle is stable.

The rotor oscillations in the synchronous machine can be explained by using the swing equation. [10]

$$M \frac{d^2 \delta}{dt^2} = P_m - P_e - P_D = P_{acc}$$

This second order formula can be written as two first order formulas

$$M \frac{d\Delta\omega}{dt} = P_m - P_e - P_D = P_{acc}$$

$$\frac{d\delta}{dt} = \Delta\omega$$

2.1.1.1 Small signal rotor angle stability

Small signal stability is when there are small disturbances applied to the network like a load flow change. The electrical air gap power can be expressed by [11]

$$P_e(\delta) = P_{E_q}(\delta) = \frac{E_q V_s}{x_d} \sin \delta.$$

The maximum air gap power and angle are the critical power and critical angle. The mechanical power can be treated as a horizontal line since it is independent of the load angle. [11]

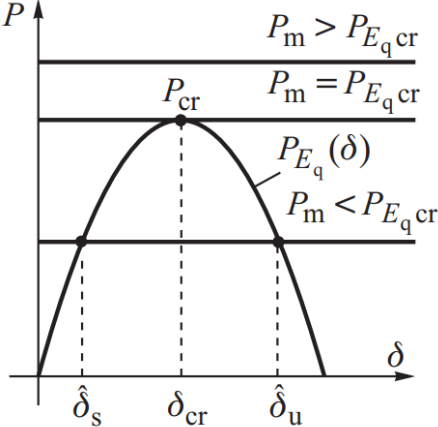


Figure 2.1-2: Small signal rotor angle stability equilibrium points [11]

If the mechanical power is greater than the critical electric power leads to the system not being able to uphold stability.

Only the left equilibrium point is stable, since if there is an increase in mechanical power a generator theoretically running at that point will reduce its electrical power. If there is a reduction in mechanical power there will be an increase in electrical power, creating instability. [11]

What differentiate small rotor angle disturbances from large transient disturbances mathematically is that it is possible to linearize the system.

2.1.1.2 Linearization and eigenvalues

By linearizing the system around an operation point, one can calculate the parameters of the swing equation. Finding the roots of the swing equation will give the eigenvalues. Using the eigenvalues and their characteristics one can deduce if the system is oscillatory or aperiodic. [12, 13]

The eigenvalues can be a real or a complex. How the system behaves will depend on which quadrant of the real/imaginary axis the eigenvalues belong to. [14]

- If the real value is positive there will be gain instead of damping leading to instability.
 - If it is only a real value the gain will be exponential, while if there are imaginary values the system will experience increasingly larger oscillations.
- If the real value is zero, there is no dampening or gain.
 - If it is only a real value the mode will be constant, while if there are imaginary values the system will experience standing oscillations
- If the real values is negative there will be dampening.
 - If the eigenvalue is only a real value there will be critical dampening, if it is a complex value the system will have oscillations decreasing oscillations. [14]

The eigenvalue can determine the frequency of the oscillations through $f = \text{imag}(\lambda) / 2\pi$. [14]

The eigenvalue also provides the relative damping ratio, which tells how much the oscillation gets dampened. [14]

$$\zeta = \frac{-\alpha}{\sqrt{\alpha^2 + \beta^2}}$$

The eigenvalues with the lowest dampening ratios are the ones that are the most interesting to analyse since they are the least stable ones. One unstable eigenvalue will lead to the entire system being unstable.

Often the minimum damping ratio is set to be 0,05 for a stable system for most modes, but for low frequency modes, like interarea modes it is set as high as 0,1 to be sure that the system is stable. [15].

Linearizing the behaviour makes analysis the oscillations in the system more precise, easier, and more organised. Non linearized simulations are still needed since power systems are inherently non-linear so comparing linear and nonlinear results are essential. [13].

In systems with multiple generators the equations and matrixes very complicate, so using computer software becomes a necessity, to derive the state space matrix, which will give the eigenvalues. [13]

2.1.1.3 Modes

The oscillations can be categorised as different modes, there are many kinds of modes, that can be identified by how they operate and what their frequency is. The two relevant to this thesis is local machine mode and interarea modes.

Local machine mode are oscillations that are associated with one generator or a small plant of generators swinging against the rest of the system. Usually, these oscillations mostly affect other generators that are electrically close. Local mode oscillations are usually between 0.7 and 2 HZ. [16].

Interarea mode are oscillations that are created when groups of generators that are electrically linked swinging against each other, for example two power plants connected with long transmission lines. In the Kundur model it would be the area 1 and 2 oscillating with each other. These oscillations are usually 0.1 and 0.8 HZ. [16]. These oscillations can lead to stability issues for the network since they are more complex and harder to control than local modes, since they depend on an analyse of the entire interconnected system, not just the individual generators, or area. Interarea oscillations are especially prevalent in systems with very long AC transmission lines. [16]

2.1.2 Frequency stability

Frequency stability is the ability for the system to maintain its set frequency, in most of the world it is at 50HZ for power system. The frequency of the system is proportional to the rotational speed of the synchronous machines. The frequency is primarily affected by changes in the active load of the system.

If a disturbance occurs there are two/three phases of frequency control that will recover the system frequency to its nominal value.

If the load increases, the power output from the generator will not change instantaneously so the compensation energy will come from the kinetic energy in the rotor. This leads to the dip in speed. The opposite will happen if the load shrinks.

The primary control response is from the governors that will increase the power output from the generator, which in turn will increase the speed. This period last for 30 seconds. Primary reserves will not return the system to set nominal frequency. The secondary control which is the automatic generation control where power reserves will be automatically applied to return the system to set frequency. In some systems one might need to apply some extra power reserves manually to return the system to the exact nominal frequency. [17]

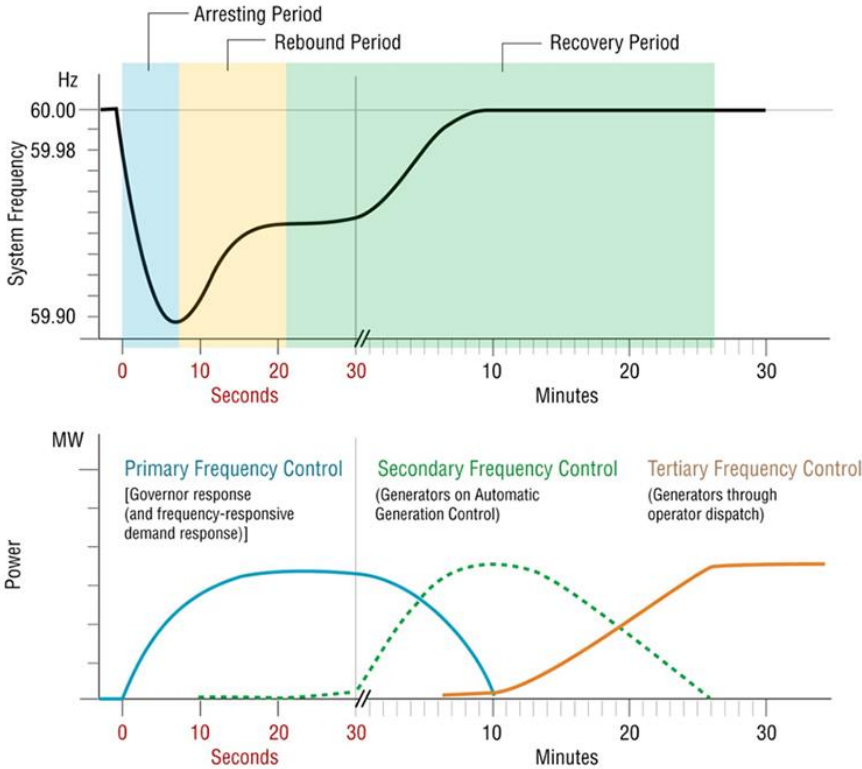


Figure 2.1-3:Process of frequency stabilization after disturbance[17]

2.1.3 Voltage stability

Voltage stability the ability of power system to keep the voltage of the network buses within a certain tolerance during standard conditions or after a disturbance. The biggest influence on the voltage stability is the power flow in the network, especially the reactive power, because of long highly reactive transmission lines. For a practical power system, one will use dynamic reactive elements to keep the voltage stable. The voltage stability is not a major focus of this thesis, since these dynamic elements are not in the figure, but it needs to be taken account for since if the load voltage deviate too much it can crash the system. [18]

2.2 Control elements

2.2.1 Governor and turbine system.

The function synchronous generator’s turbine systems is to convert either the kinetic energy from water (Hydroplants) or the thermal energy from steam to mechanical energy. In a steam turbine this is done by creating steam by heating water in a boiler using either a fossil fuel or a nuclear reactor. The steam creates a high temperature and pressure that makes the rotor move creating mechanical energy. [19]

The governor’s task in a steam turbine is to regulate this process by doing three function, speed/load control overspeed control and overspeed trip. The speed/load control is to control the speed of the rotor after a change in load, as described in the frequency subchapter. A speed drop of 4-5% is provided by the control function which makes the machines in the system work in parallel with each other. Overspeed control prevents the rotor from overspeeding during loss of load, and the overspeed trip is a last defence against critical load loss, it trips the boiler to protect it from damage. [20]

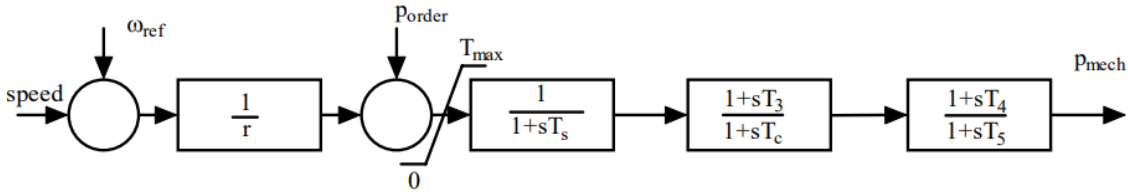


Figure 2.2-1: Steam turbine governor block diagram [2]

There are many configurations of STGs. Most of them are based on the principle shown in figure X. To derive the mechanical power out the load reference minus $\Delta \omega$ divided by the speed droop is sent through two or more transfer functions which are derived from the inertia of the mass of steam in the different parts of the steam turbine system. [21]

2.2.2 Excitation system

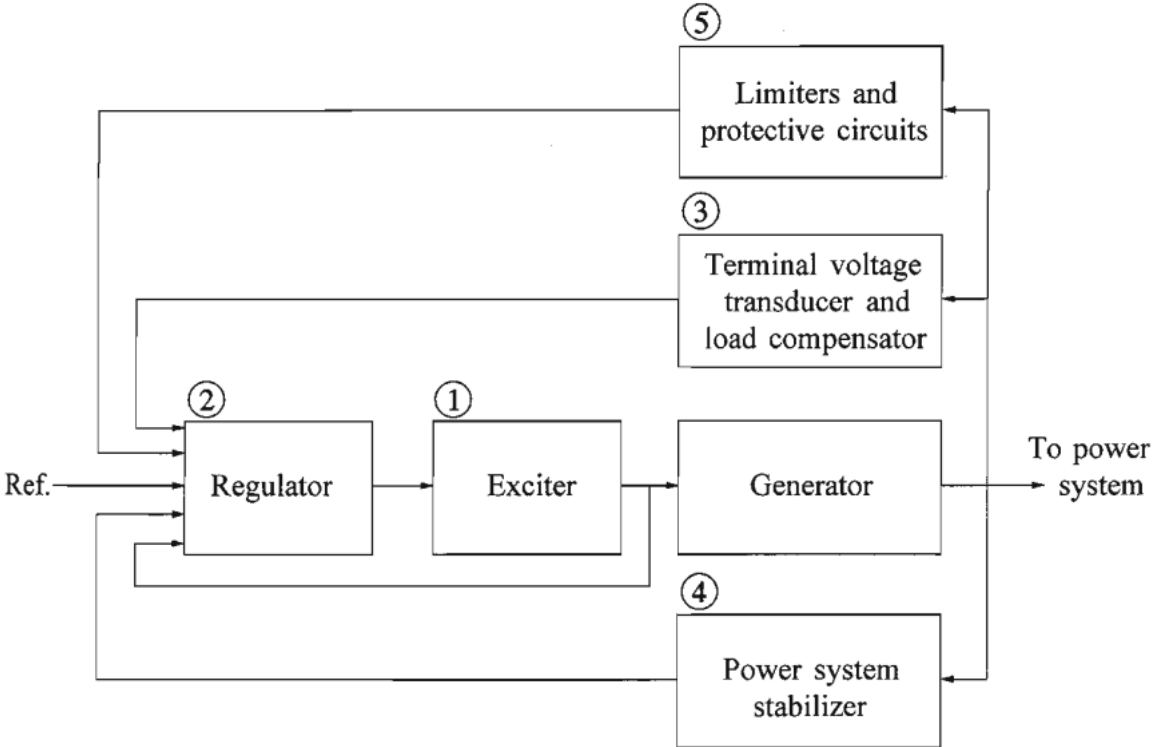


Figure 2.2-2:Excitation control system [22]

The excitations systems functions are to provide current to the generators field windings, enhance stability and to control voltage and reactive power flow. It does this by controlling the terminal voltage through automatically adjusting the field current. Figure XX shows the five components of the excitation system. The regulator (AVR) and the PSS are the elements that regulates to maintain stability.

There are three main categories of excitation systems, DC, AC and static. The AC are today mostly used on smaller generators, while static exciters are used on high power generators. DC had mostly been phased out because of weak dynamic properties on high power generators, and communication problems between the different exciters in the system. [23]

2.2.2.1 Power system stabilizer

The power system stabilizer (PSS) provides additional control by applying dampening torque to the rotor oscillations to counteract them. Without PSS the voltage regulators can introduce negative feedback to the system which will lead to loss of small signal stability. [24].

The general structure could be described as this

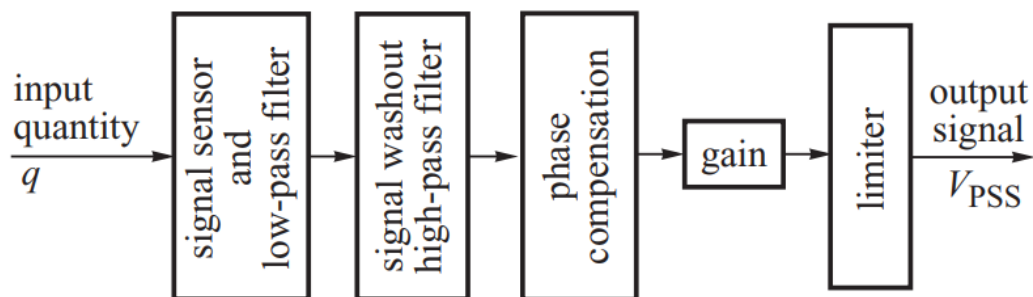


Figure 2.2-3: Elements of PSS

The low-pass filter helps with filtering out high frequency noise.

The high-pass filter work as a washout circuit which prevent the PSS from being active the rotor during steady state. [24].

The phase compensation is a lead and lag filter that compensates for the phase lag of the input signal and the high- and low-pass filter in the PSS. [Jan 384]. For the dampening torque to be satisfying it needs to be in phase with the rotor's speed deviations. [ROBUST 59-60].

The gain amplifies the signal, and the limiters keeps the output from disturbing the AVR. [25].

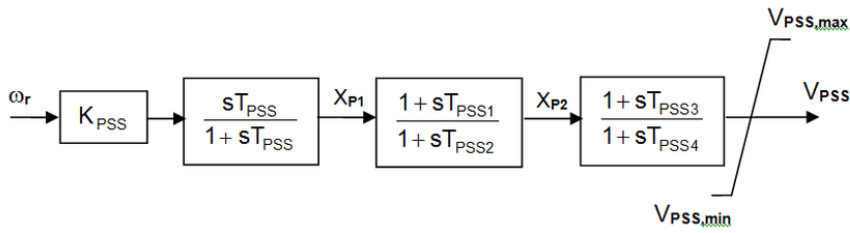


Figure 2.2-4: Block diagram of PSS [2]

The input quantity could be many different elements, the most common ones are rotor speed deviation, electrical power and frequency. Speed is the input that it is the easiest to tune, but on long shafts it can be a challenge since

Power based PSSs are easier to measure but a single input power PSS assumes that the mechanical power is constant.

2.3 Load modelling

Load models describe the mathematical relations between the load and the load voltage.

The most basic load models are the constant power, current and impedance models. The sum of the three constant load models is the ZIP load model. It gives a more realistic representation of big power system loads which are a combination of many different smaller loads.

$$P = P_0 \left[a_1 \left(\frac{V}{V_0} \right)^2 + a_2 \left(\frac{V}{V_0} \right) + a_3 \right]$$

$$Q = Q_0 \left[a_4 \left(\frac{V}{V_0} \right)^2 + a_5 \left(\frac{V}{V_0} \right) + a_6 \right]$$

P_0 , Q_0 and P_0 are the initial conditions also called the nominal values of the load, while the a_1-6 are the percentage each constant model represent for either the active or reactive load. A_1 and A_4 is the coefficient for the constant impedance load, A_2 and A_5 for the constant current, and A_3 and A_6 for the constant power.

For active loads the constant current load is the dominant model, while for reactive loads the constant impedance load model is the most dominant. The constant power model has a stiff load voltage characteristic which makes it good for load flow analysis but lacking for dynamic simulations. [26]

2.4 Simulation software

2.4.1 RT-LAB

RT-Lab is a real time simulator software created by the Canadian company Opal-RT. The main function of the software is to do real time simulations of electrical circuit, control circuit and power systems. RT-Lab can run real time simulations based on MATLAB/Simulink or SystemBuild models (like PSS/E). A real time simulator runs in real time (clock time). Simulink in itself is not a real time simulator since it tries to run simulations as fast as the CPU of the computer it is on allows it too. By remodelling a Simulink model according to RT Labs set up and putting in the rt lab opcomm signal blocks the model will be able to run in real time with RT-Lab. [27]

The basic structure of a RT-Lab model is that the Simulink model should be split into different subsystems based on function. The console subsystem contains the elements the measurement and any block or switch that needs manual changes during the simulations needs to be in the console. There can only be one console in the system. The computational elements will either be put into a master or slave subsystem. The master needs to be in the system and can only be one, the slave subsystem can be used to split up the system to run over multiple cores. The OpComm communication blocks are used to make the different subsystem communicate with each other while run by rt lab. The Simulink model has to be running in discrete mode with fixed time step intervals. [29]

RT-lab does not use the host pc to run the simulation it uses its own proprietary range of simulators. For this project a OP4510 simulator was used. It is the entry level simulator from OPAL-RT, it is a FPGA and Intel based simulator. [29]

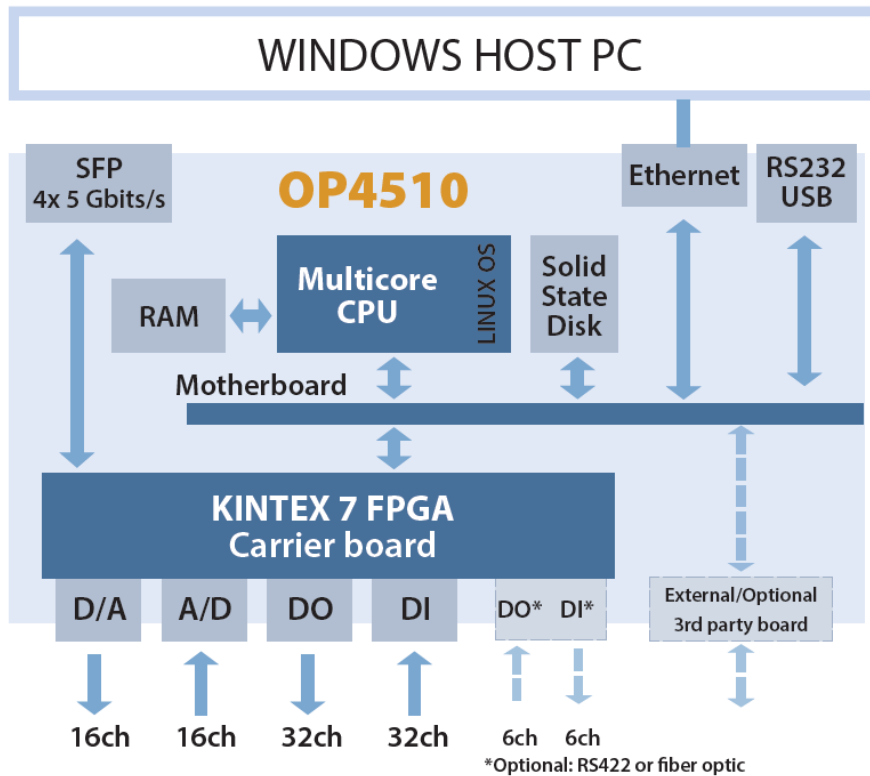


Figure 2.4-1: Structure of simulator OP4510 [29]

The Simulink model will be linked to the RT LAB software, and the RT LAB software will build and load the system into the simulator. The simulation will then be ready to run. To send out the plots one can either use standard MATLAB Tofile/Toworkspace blocks or RT labs own custom blocks.

2.4.2 Power System Toolbox (PST)

Power system toolbox is a MATLAB script-based power system analysis software, developed by Joe Chow and Graham Rogers. PST is not compatible with RT-LAB since it is a script based, and not Simulink based. It allows for many different types of simulations and calculations, including load flow analysis, linear analysis and to dynamic simulations. [2]

3 Modelling

3.1 The network model

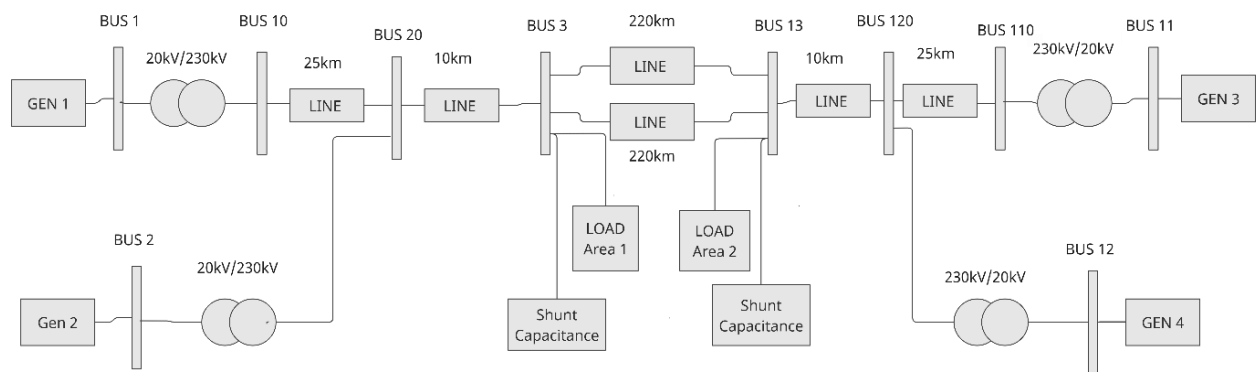


Figure 3.1-1: Kundur two area

To test the oscillation modes the Kundur two area model (K2A) was chosen. It consists of two mirrored areas connected through two parallel transmission network lines. Each area consists of 900MVA two steam turbine generators, two 20/230kV transformers, one load and one shunt capacitor. All the generators and transformers in the system have the same data. [30]

Some of the data has been changed from the original K2A figure, most notably the shunt capacitances have been increased with 150MVar each, this has been done to improve the voltage stability.

The K2A model was chosen because of the symmetrical nature of the network, and the small size. The symmetry makes it easier to analyse the different effect the various factors have on both the interarea and local oscillations, without the two modes interfering with each other. Changes in one of the generators will lead to local modes, while load changes in load will create interarea oscillations. The base power of the system is 100 MVA, the base voltages are 20kV for the generator buses, and 230kV for the rest of the network. [30]

Area 2 is a deficit area since the production total production at around 1400MW is smaller than the load 1767MW, so a surplus at around 400MW needs to be from area 1 needs to be transferred. Taking losses into account shows that the K2A model is quite stressed even at steady state since there is not a lot of surplus active power. Long distance systems that are

heavily stressed, like K2A are very susceptible to oscillations, this makes the control system response paramount.

3.2 Initial models

The modelling started with deciding if the model should be made from the ground up or chosen from a set of premade versions made by MATLAB/Simulink. It was decided to go with one of the premade versions. Building the figure from scratch in Simulink without much experience in modelling of dynamic power systems in software would take too much time.

The decision to make a variable step model was done to make it easier to test changes done to the model since the variable simulation takes significantly shorter time than fixed step simulations. Running a fixed step simulation can also introduce transients and ringing that could make the data harder to read, having a variable step example will then make it easier to identify these software/simulation disturbances.

For the variable step version power_PSS [31] was chosen as the basis.

Simulink had applied some changes to the model, primarily the shunt capacitors had been increased with 187MVAR each to improve the voltage profile [31]. Gen 1 is the swing machine/bus, while in the standard K2A model it is Gen 3.

The fixed step model was built on power_KundurTwoAreaSystem premade model from Simulink [32].

It has the same values and structure as power_PSS, but all the continuous elements have been replaced by discrete elements. The only additional elements added are snubber loads added between the generators and transformers, they are there to help the simulation run, without them voltage transients will terminate the Simulation.

The generator control system is composed of:

A DC1A exciter with a slightly modified structure.

Three types of PSSs that can be switched between, speed, power and multiband frequency

A tandem-compound steam prime mover. Which includes a speed governing system, a four-stage steam turbine, and a shaft with up to four masses.

The generator model used is a premade block, that receives the mechanical power from the speed governing system and the field voltage from the exciter circuit. The generator sends out its stator voltage, rotor speed, rotor speed deviation, rotor angle, electrical power and load angle back into the control circuit and to the measurement units.

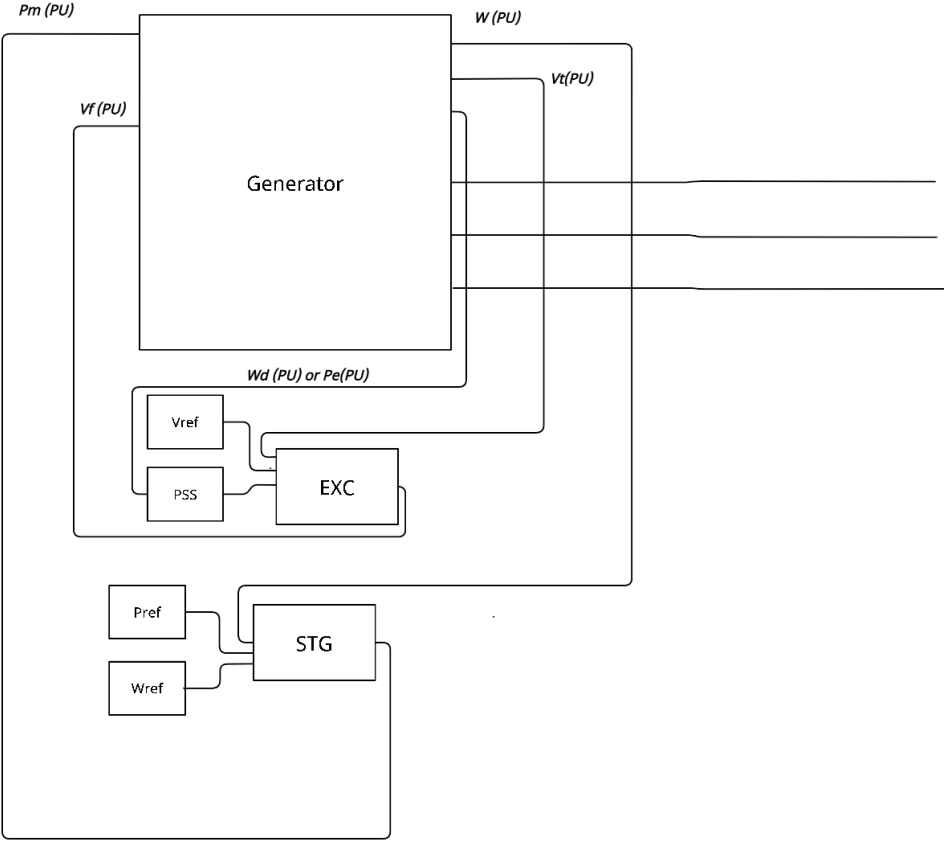


Figure 3.2-1:Generator control circuit

Table 1:Generator data

Generator data	Gen 1	Gen 2	Gen 3	Gen 4
Bus number	1	2	11	12
Type	PV	PV	Swing	PV
Power MW	700	700		700
Voltage pu	1	1	1,03	1,03
Base MVA	900	900	900	900
Leakage Reactance X_l (pu)	0,2	0,2	0,2	0,2
Stator resistance R_s (pu)	0,0025	0,0025	0,0025	0,0025
d-axis synchronous reactance x_d (pu)	1,8	1,8	1,8	1,8
d-axis transient reactance x'_d (pu)	0,3	0,3	0,3	0,3
d-axis subtransient reactance x''_d (pu)	0,25	0,25	0,25	0,25
d-axis open-circuit time constant T'_{do} (sec)	8	8	8	8
d-axis open-circuit subtransient time constant T''_{do} (sec)	0,03	0,03	0,03	0,03
q-axis synchronous reactance x_q (pu)	1,7	1,7	1,7	1,7
q-axis transient reactance x'_q (pu)	0,55	0,55	0,55	0,55
q-axis subtransient reactance x''_q (pu)	0,2	0,2	0,2	0,2
q-axis open-circuit time constant T'_{qo} (sec)	0,4	0,4	0,4	0,4
q-axis open circuit subtransient time constant T''_{qo}	0,05	0,05	0,05	0,05
inertia constant H (sec)	6,5	6,5	6,5	6,5

3.3 Changes applied

First thing done with the models was to remove the components related to large disturbance simulations, this included combining the two parts of line 1 to be just one line.

Gen 3 was made to be the swing machine instead of gen 1. This will increase the active load production in area 2, which reduces the transferred power therefore also the losses between the areas.

For this project hardware implementation will not be done, but for future project that might use hardware it was decided that the system frequency would be changed from 60HZ to 50HZ. All the frequency depended blocks and components was changed so that they run at 50HZ.

3.4 Load modelling

The loads in the system are all constant impedance loads and all of them are static. The standard RLC load block in Simulink does not allow for changes in either impedance or power rating during a simulation. The RLC load blocks were therefore replaced with Three-Phase dynamic blocks [33]. The new blocks allow for external control of the load's active and reactive power using either constant blocks or other signal generating blocks. The huge weakness with this external control is that it sets the loads to be operating at constant power. During testing this often led to very unstable results. To mitigate this, it was decided to build an external zip model control system for each load.

$$P = P_0 \left[a_1 \left(\frac{V}{V_0} \right)^2 + a_2 \left(\frac{V}{V_0} \right) + a_3 \right]$$

$$Q = Q_0 \left[a_4 \left(\frac{V}{V_0} \right)^2 + a_5 \left(\frac{V}{V_0} \right) + a_6 \right]$$

The set active and reactive effects are known and is modelled with stair signal generator blocks which would allow changes in the load during simulation. All the coefficients are gain blocks, but since reactive loads are in most cases modelled to have constant impedance a_5 and a_6 are set to be zero. The nominal voltage will be 1 since it is a pu system.

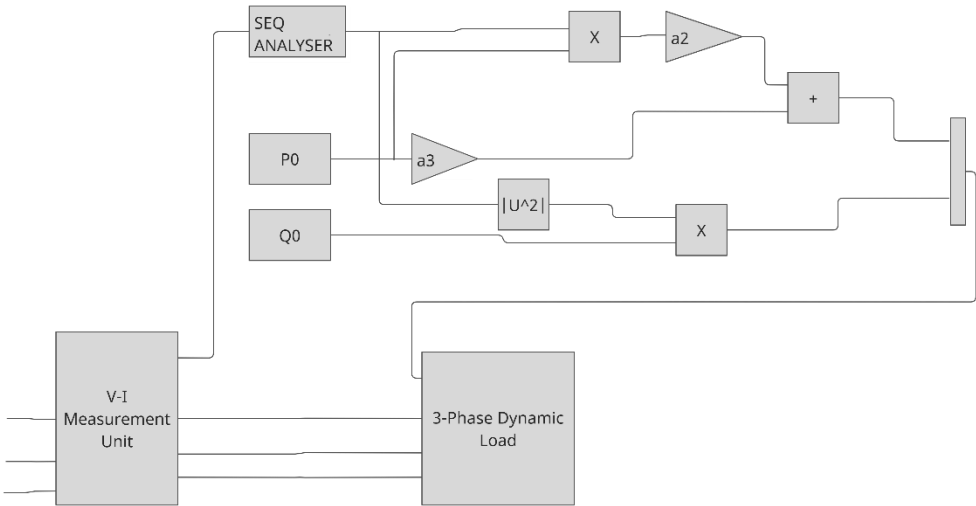


Figure 3.4-1:ZIP-load block diagram

To find the variable load voltage there is need for a three phase V-I measurement block that measures the voltage and outputs it. In the variable step version of the measurement block one can directly output the load voltage magnitude in pu, but that is not possible on the fixed step

model, it can only output voltage three phase signals in pu. To get the single-phase RMS magnitude signal a Sequence Analyzer block is used. A weakness with this block is that it during initial condition it stays static for one time cycle, 0.02 sec, this creates some extra initial disturbance.

In the variable step model this load model system works as it should, but in the fixed step model there is some 50HZ ringing in the circuit. This ringing spreads to other parts of the system, like the exciter, power transferred and terminal voltages for the generators. What part of the load model is creating the ringing was not conclusively proven during testing, but it was clear from tests that the transient changes in both the load references and voltage are influencing the ringing.

Implementing a constant impedance model led to feedback in the system, while if it was modelled as a constant current load, it had still ringing, but the system did not ring enough for feedback to occur. The exponential nature of the constant impedance model makes the actual reactive higher than both the reference and the constant current model. To prevent feedback a low pass filter was implemented inside the zip model. The filter removes unwanted high frequencies and makes the time response slower. To reduce the ringing further a low pass filter can be added to the load references to increase the switching time of load changes.

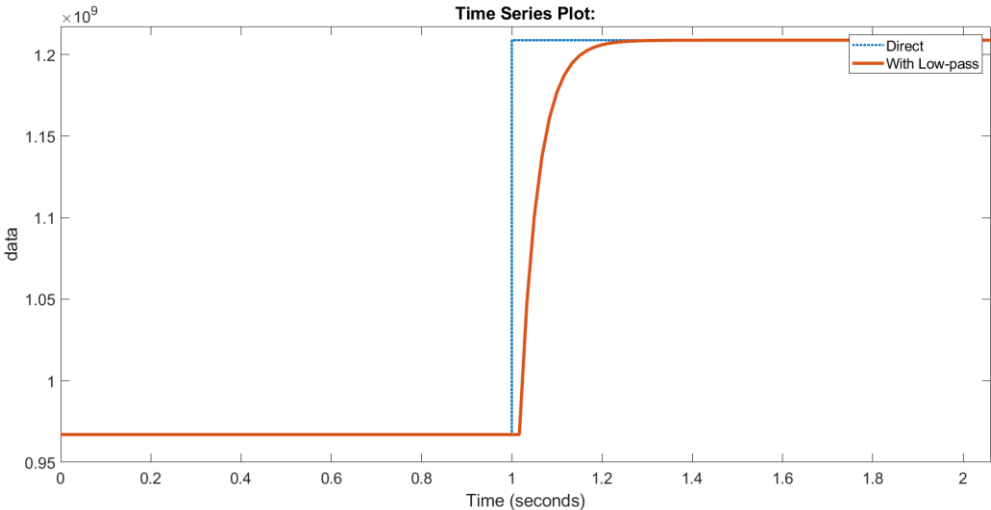


Figure 3.4-2: Load response with and without LP filter

Both filters were tuned in such a way that they do not change the actual system response much, but only remove the ringing. The time constant for the load reference filters are set to 0,05 seconds, and the time constant for the lowpass filter inside of the ZIP model is set to 0,1 seconds.

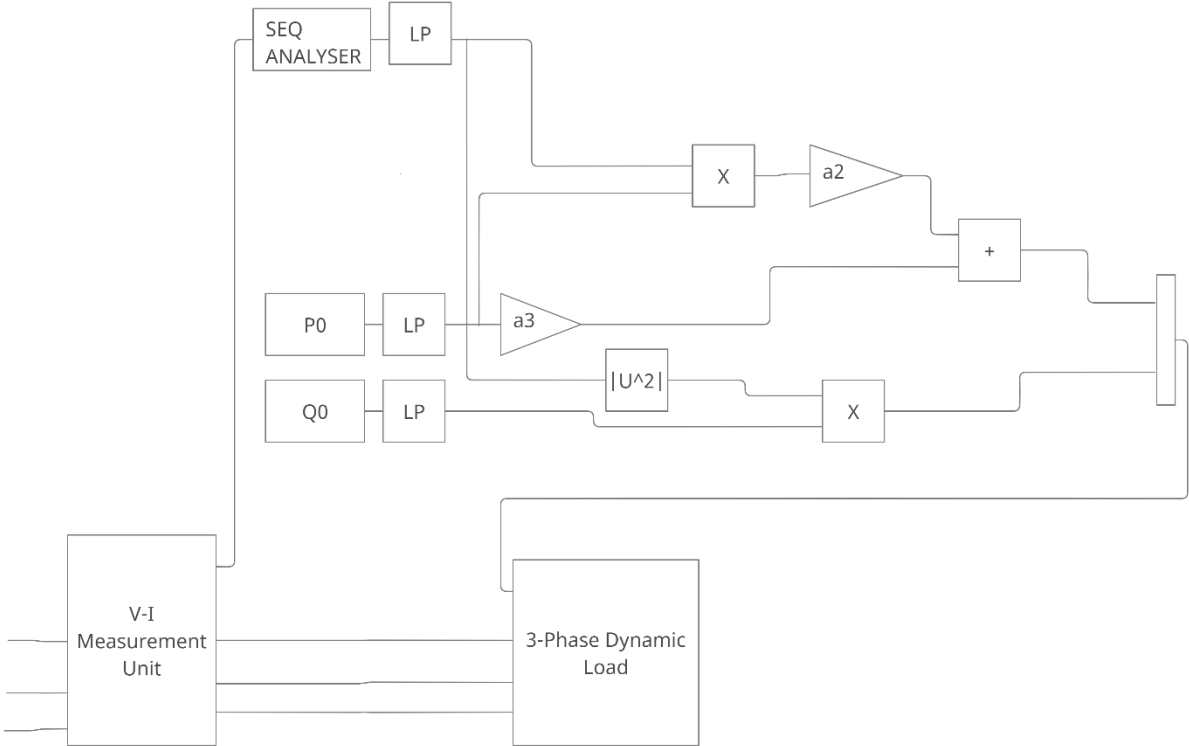


Figure 3.4-3::ZIP-load block diagram with LP filters

These filters were not added to the variable step model.

3.4.1 Alternative solution

An alternative way of creating a load that could be changed during simulations would be to implement switches that would turn of and on extra smaller loads in parallel with the original load. Two major disadvantages with this model that made it less ideal for this project than the model chosen was transients from the switches and the way RT-lab models need to be structured. During a RT-Lab simulation the only part available to the user is the console system which should only have source and measurement blocks in it. Switches are allowed, but RLC three phase load blocks are not. This would make it only possible to change the timing of the load changes but not the amount of load change. To edit the load values, one would have to delete the system from the simulator, edit it with MATLAB, rebuild the model and reload to the machine again in RT-Lab, and then run it. This process would take more than 10 minutes for each change one wanted to implement, while the system chosen would only take around 1 minute. The chosen model is also more user friendly since it is easier to read and how much load there is in the model at exact time points since it is controlled by a few stairs signal blocks.

3.5 Modeling Linear analysis

During modelling the biggest challenges faced was how to linearly analyse the system. The root of the problem was the process of extracting the solid-state space matrix of the system. Using the linear analyser [34] in Simulink produced a that gave very high eigenvalues, that led to extremely high frequencies for modes. Trying some of the other methods MATLAB has for finding state space matrixes gave the same results.

As a final measure it was decided that PST was going to be used to do the linear analysis. The problem with PST is that it is set up differently than the Simulink model.

3.5.1 Tuning PST

The first thing done was to change the structure of the PST model, in the PST version the loads are on their own buses which have a nominal voltage of 115kV.

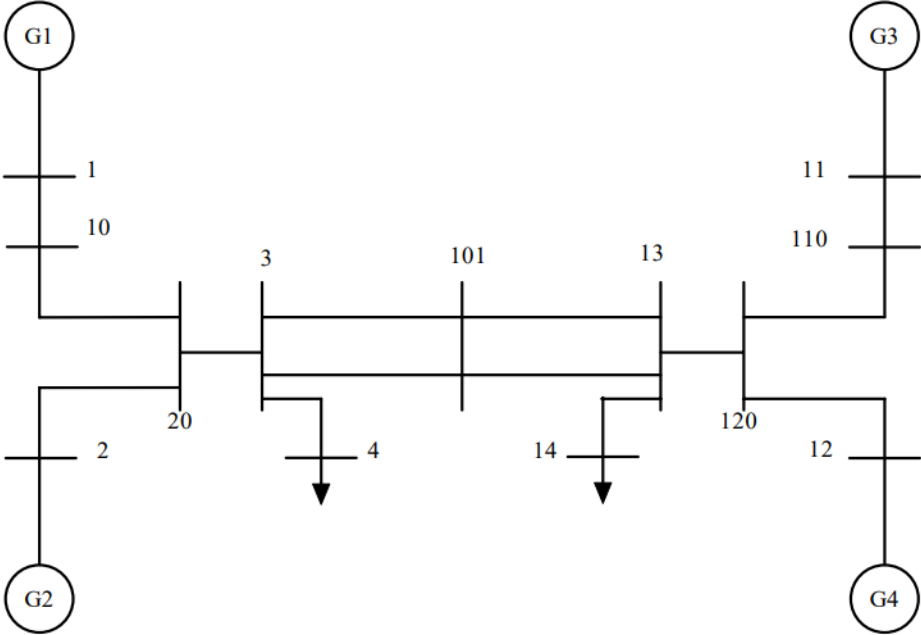


Figure 3.5-1:Initial K2A one line diagram from PST [2]

To maintain steady state voltage stability the transformers for the loads have tap changing capabilities. Since there are no tap changing transformers in MATLAB 2020b the transformers and extra buses were removed from the PST model through deleting the lines of codes referencing them and moving all the load data to bus 3 and 13. Then by manually tuning the conditions of the generators and buses in the d2asbeegg.m script the load flow got to be very similar to the one in variable step Simulink model. To get the loadflow data from PST lfdemo script was run.

Table 2: Load flow data variable step model

Type	Bus	Volt Mag	Volt ang	P [MW]	Q [MVar]
SM	BUS1	1	25.29	700.00	92.36
SM	BUS2	1	15.26	700.00	123.34
DYN load	BUS3	0.9891	30.45	967.00	100.00
RLC load	BUS3	0.9891	30.45	0.00	-342.41
Bus	BUS10	0.9918	48.55	0.00	0.00
SM	BUS11	1.0300	0.00	721.68	130.43
SM	BUS12	1.0000	-9.84	700.00	32.56
DYN load	BUS13	1.0091	5,58	1767.00	100.00
RLC load	BUS13	1.0091	5,58	0.00	-509.19
RLC load	BUS13	1.0091	5,58	0.00	-509.19
Bus	BUS20	0.9866	38.49	0.00	0.00
Bus	BUS110	1.0159	23.42	0.00	0.00
Bus	BUS120	1.0017	13.49	0.00	0.00

Table 3: Load flow data fixed step/RT model

Type	Bus	Volt Mag	Volt ang	P [MW]	Q [MVar]
SM	BUS1	1	25,03	700	81,56
Snubber	BUS1	1	25,03	1	-10
SM	BUS2	1	15,02	700	111,87
Snubber	BUS2	1	15,02	1	-10
RLC Load	BUS3	0,9894	30,23	0	-342,65
DYN load	BUS3	0,9894	30,23	967	100
Bus	BUS10	0,9919	48,3	0	0
Swing	BUS11	1,03	0	725,6	120,47
Snubber	BUS11	1,03	0	1,06	-10,61
SM	BUS12	1	-9,91	700	22,39
Snubber	BUS12	1	-9,91	1	-10
Dyn load	BUS13	1,0093	5,51	1767	100
RLC Load	BUS13	1,0093	5,51	0	-509,3
Bus	BUS20	0,9869	38,26	0	0
Bus	BUS110	1,0158	23,39	0	0
Bus	BUS120	1,0017	13,43	0	0

Table 4: Load flow data PST model

BUS	Volt Mag	Volt ang	GEN P [MW]	GEN Q [MVar]	Load P [MW]	Load Q [MVar]
1	1	25,353	700	93,324	0	0
2	1	15,0961	700	122,623	0	0
3	0,99	0,0782	0	0	967	100
10	0,99	18,581	0	0	0	0
11	1,03	0	713,695	127,308	0	0
12	1	-9,867	700	27,867	0	0
13	1,011	-24,589	0	0	1767	100
20	0,986	8,290	0	0	0	0
101	1,024	-12,661	0	0	0	0
110	1,016	-6,54	0	0	0	0
120	1,002	-16,566	0	0	0	0

3.5.2 Modeling the control elements

PST has a very limited array of governors, exciters and PSSs compared to what can be build in Simulink, so it was natural to replace or change the control elements in the Simulink model with the ones from PST.

The generators are set up in the same way as the Simulink version, with the same values.

3.5.2.1 Governors

The governors in the PST model were modelled after the IEEE TGOV1 model, but with some slight modifications. How it works is explained in section 2.2.1 The values chosen were based on the premade values from PST.

Modelling this in Simulink was done by deleting the original governor model and using two low-pass filters and one lead/lag filters.

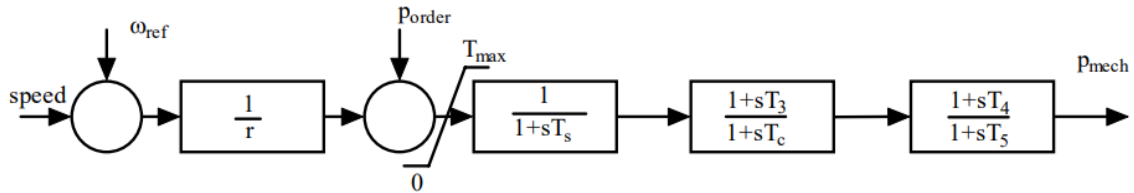


Figure 3.5-2: Steam turbine governor block diagram [2]

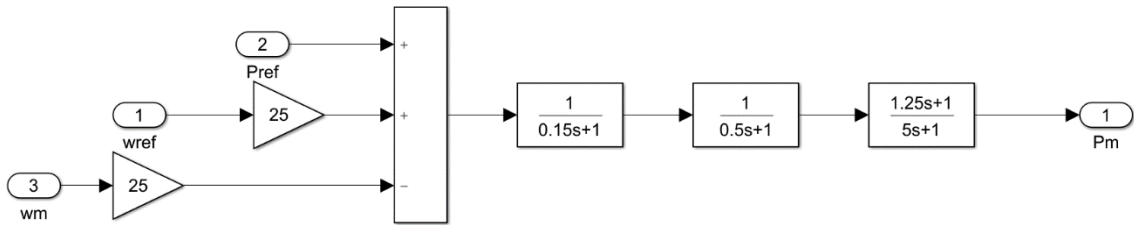


Figure 3.5-3: STG in MATLAB

Table 5: Steam turbine governor data

variable	speed set point ω_f (pu)	steady state gain $1/r$ (pu)	maximum power order T_{max} (pu)	servo time constant T_s (sec)	HP turbine time constant T_c (sec)	transient gain time constant T_3 (sec)	time constant to set HP ratio T_4 (sec)	reheater time constant T_5 (sec)
Amount	1	25	1	0.15	0.5	0	1,25	5

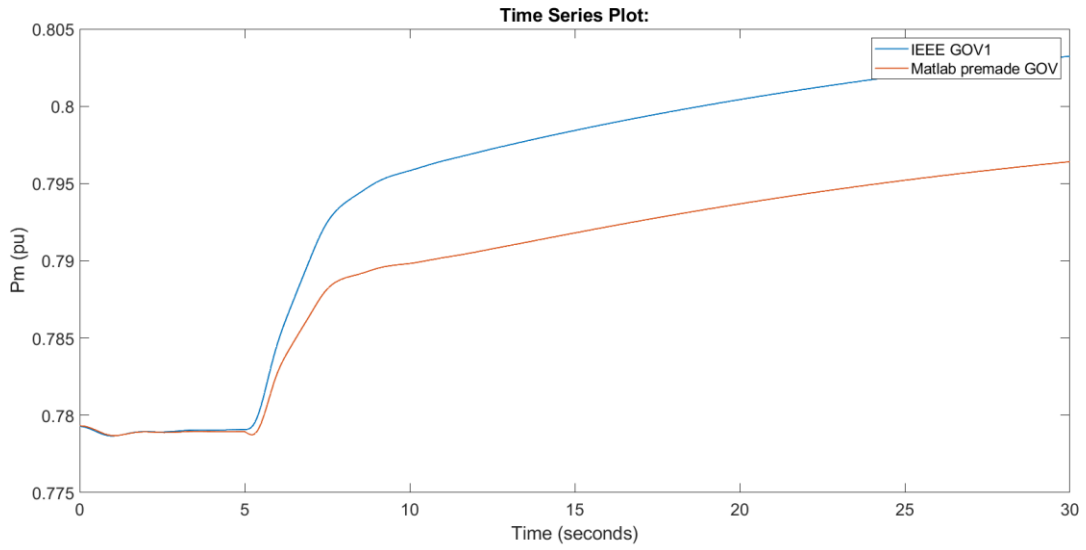


Figure 3.5-4: Response of IEEE Governor versus premade governor in Simulink

From the plot one can see that the IEEE GOV1 that has now been implemented has a faster and better response compared to the more complicated model that came premade in the Simulink figure.

3.5.2.2 PSS

The PSS was the same in both models, the values from the Simulink figure were transferred to the PST model.

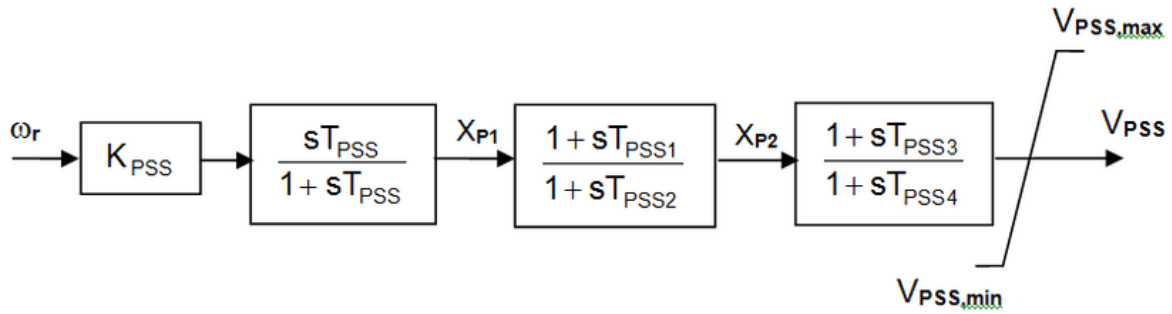


Figure 3.5-5:PSS block diagram [2]

Table 6:PSS Data

PSS	
Gain K _{pss}	30
Washout time constant T _{PSS}	10
First lead time constant T _{PSS1}	0,05
First lag time constant T _{PSS2}	0,02
Second lead time constant T _{PSS3}	3
Second lag time constant T _{PSS4}	5,4
Maximum output limit V _{PSS,max}	0,15
Minimum output limit limit V _{PSS,min}	-
	0,15

3.5.2.3 Exciter

The exciter model was chosen to be a IEEE DC1A model, the values were from derived from PST. For the variable step model there was no issue in implementing a DC1A model, since there is a block for that exact model.

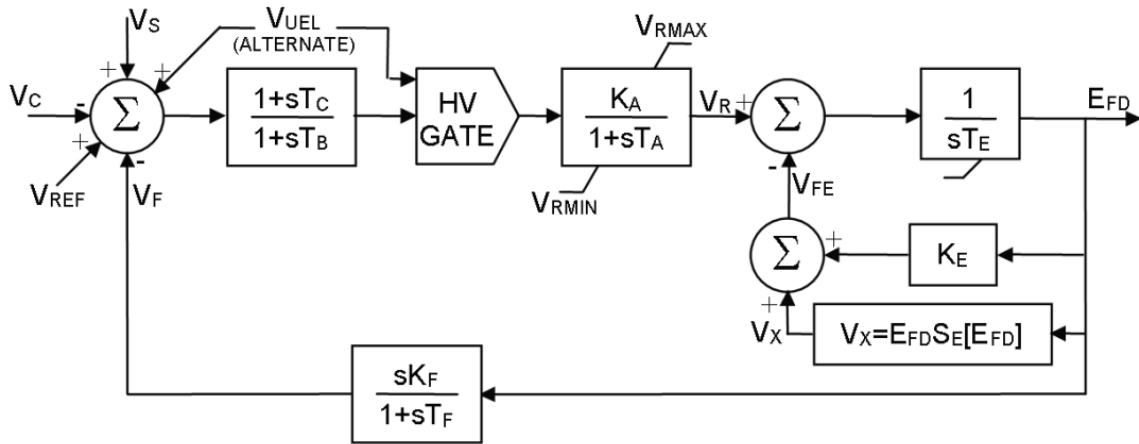


Figure 3.5-6: Block diagram of DC1A exciter

Table 7: Exciter data

Exciter data	
Input filter time constant TR	0,02
Voltage regulator gain KA	200
Voltage regulator time constant TA	0,01
Transient gain reduction lead time constant TB	0
Transient gain reduction lag time constant TC	0
Max voltage regulator output VRmax	5
Min voltage regulator output Vrmin	-0,9
Exciter constant KE	1
Exciter time constant TE	0,05
Field voltage E1	3,1
Exciter saturation function Efd1	0,33
Field voltage E1	2,3
Exciter saturation function Efd2	0,1
Damping filter gain	0,005
Damping filter time constant	1,5

For the fixed step model, the original exciter was kept since the DC1A block only works with variable step(continuous). The original exciter was already a DC1A exciter but the way the

model is structured regarding saturation is different. The values of the exciters were changed to be the same as the other models.

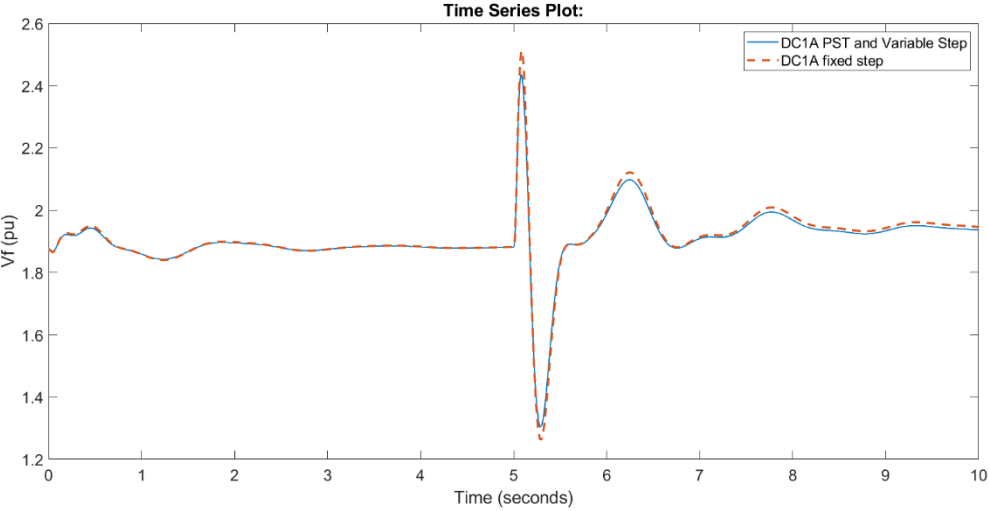


Figure 3.5-7: Difference in response between DC1A for fixed-step/RT model and variable-step/PST model

The plots show that the response from the different versions of the DC1A are in essence the same, the most noticeable difference is a higher transient for the fixed step version.

3.5.3 PST load change response

PST have low pass filters for the loads to slow the step response, this lowpass filter was set so that it has almost a pure step response to compare it with the variable step figure. [2]. Editing l mod con in the dsabgp.m script allows for a faster response.

3.5.4 Dynamic response comparison

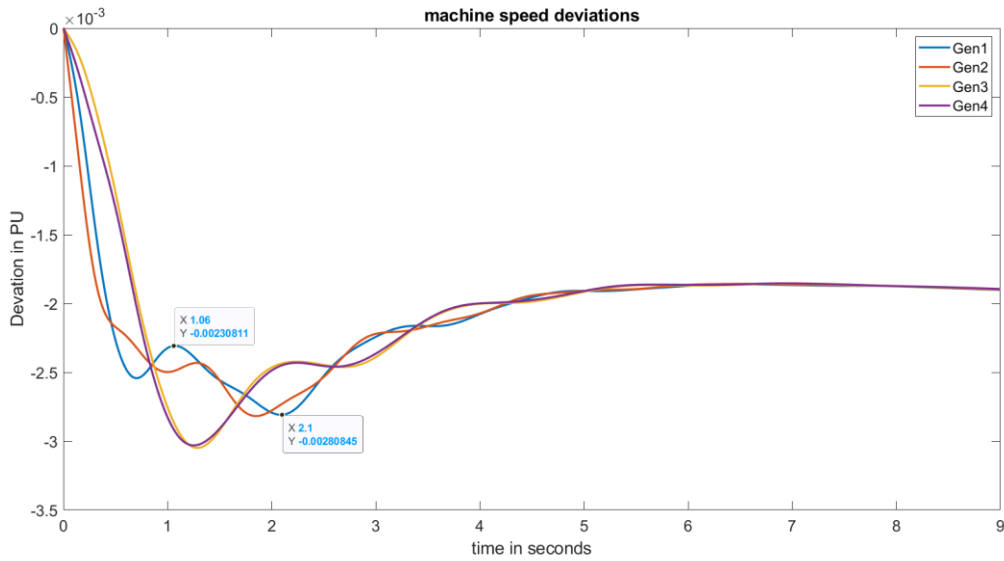


Figure 3.5-8: PST Rotor speed deviation after 242MW change in load 1

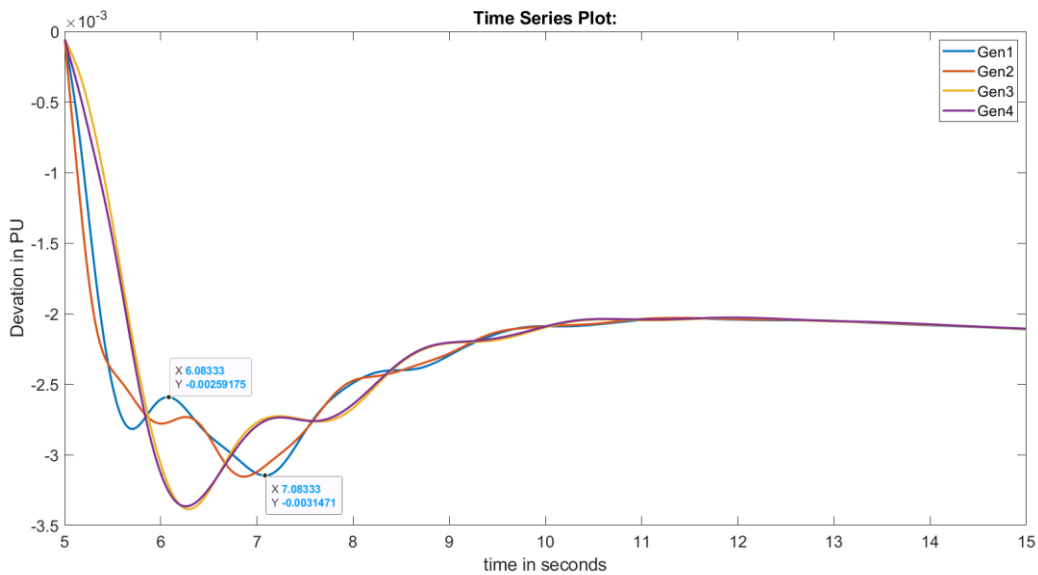


Figure 3.5-9: Simulink Rotor speed deviation after 242MW change in load 1

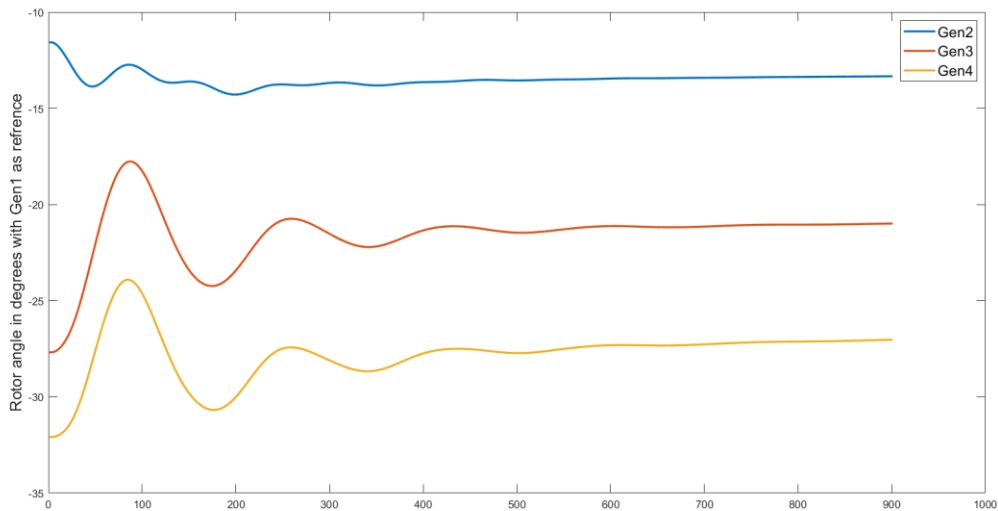


Figure 3.5-10:PST Rotor angle after 242MW change in load 1

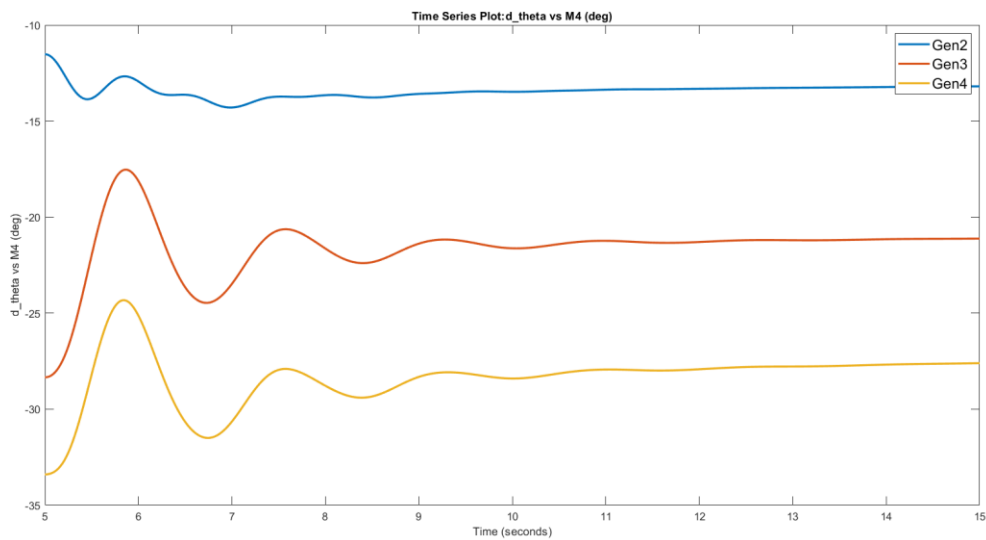


Figure 3.5-11:Simulink Rotor angle after 242MW change in load 1

Comparing the responses for the speed deviation and rotor angles for the PST and variable step model shows that they behave almost the same. There is a bit of a difference in terms of amplitude of the swings, but this might be from the small differences in load flow, the Simulink model not being at nominal frequency, and the lowpass filter in the PST model. The differences are negligible so the PST can therefore be used to do the linear analysis.

3.6 RT-Lab modeling

To make the fixed step model into being compatible it needs to be split into one subsystem for the computational elements and one for the control signals and measurements. It is important that the POWERGUI block is kept at the top page, and not in one of the subsystems. The long-distance lines blocks were replaced with RT-labs own version of those blocks who behave the same expect that they can be put between a master and slave system. Each area was put into their own subsystems the outputs of them are the different measurements and the long-distance lines, and the inputs are the for the reference load value signals.

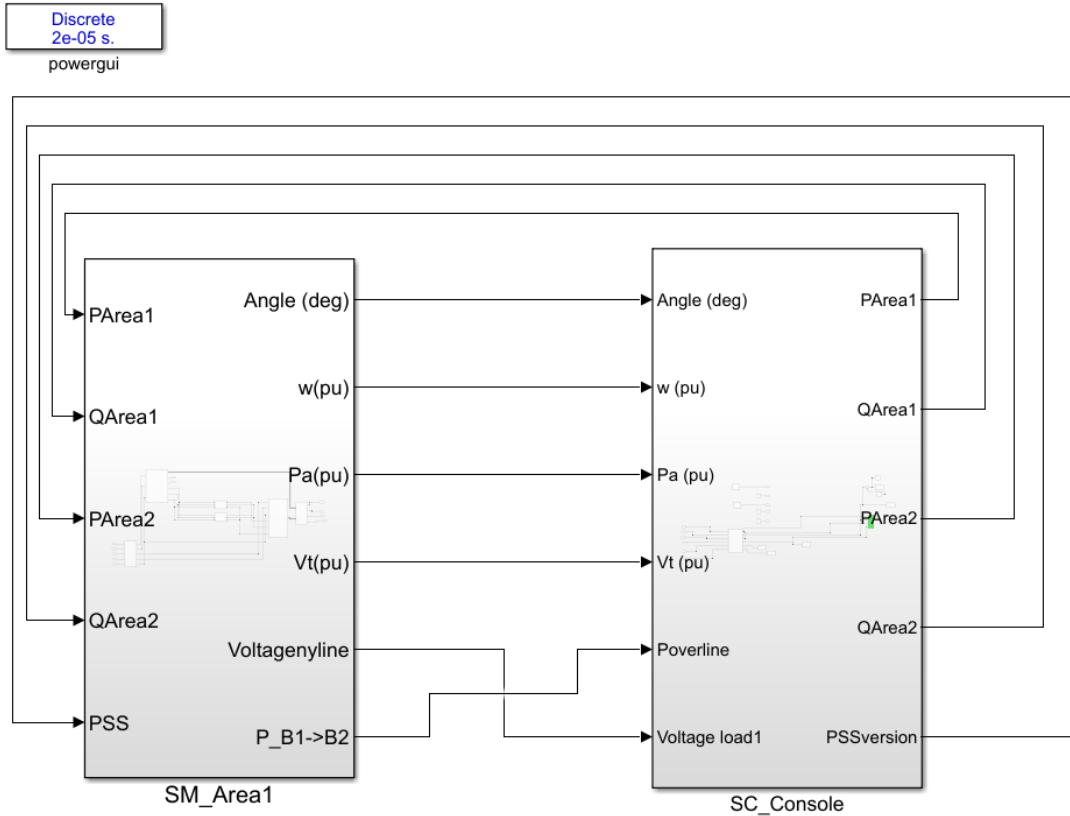


Figure 3.6-1: Top level of RT-Lab(fixed-step) model

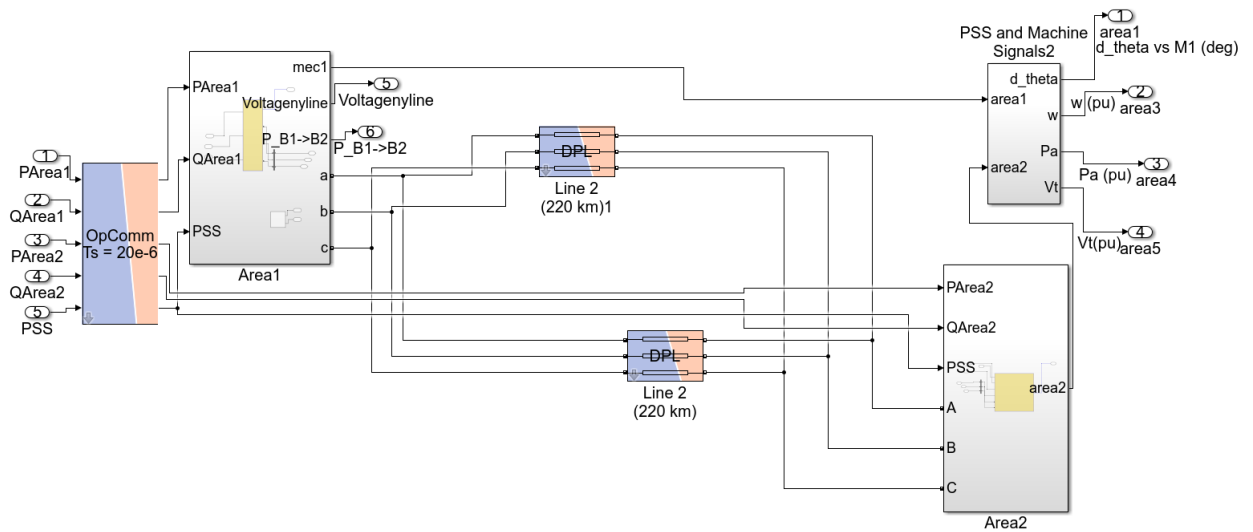


Figure 3.6-2:SM-subsystem

The original idea was to have area 1 as the master system, and area 2 as the slave system, but this configuration had problems being loaded onto the RT lab simulator. To make the model load the two-area subsystem were put into one main subsystem that would be the SM system for the model.

The console was set up in a simple way, where the signals from the SM is received through an OpComm block. One scope is used to monitor the simulation when it is running, looking at some of the most important units, speed, angle and terminal voltage. The load controlling blocks are modelled as stair signal blocks, that can both regulate the amount of change, and at which time the change is applied. These signals are sent into the SM system and there they also must go through an OpComm block. The data is saved using Tofile blocks.

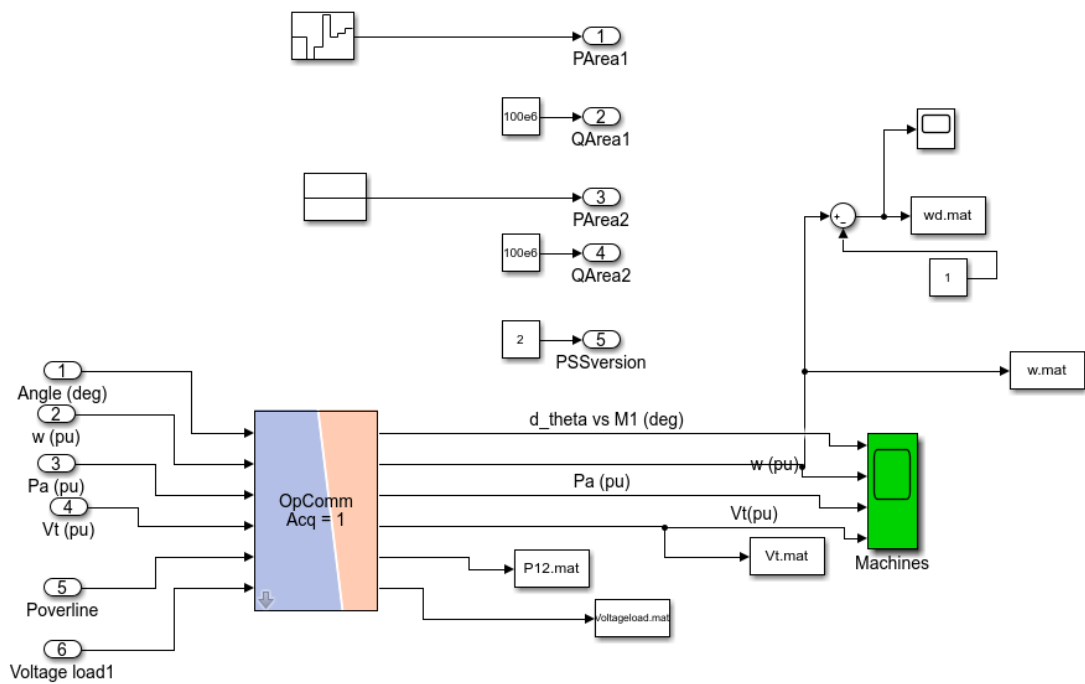


Figure 3.6-3:SC-subsystem

When running the model in RT-lab it was not running in real time, and that led to the results being distorted on the time axis. The model was running about 15 times too slow, but the plotting seemed to be trying to keep real time, meaning that the transients periods ran too fast compared to the Simulink simulations. The timing of the applied changes was correct, but the system returned to steady state way too fast. Trying to run the same system with the same system showed that there were small variations in how much the time got distorted.

Trying other unrelated premade models that came with RT-Lab gave similar errors, it seems like the simulator is having issues running in real time. The amount of slowdown was dependent on the size of the model. The version of the of the K2A model presented here has already been stripped down by removing a lot of the measurement units, the original version ran about 30 times too slow.

To make the model compatible with RT lab the fixed time step T_s was set to 20 us which is the minimum that is allowed with RT lab.

Getting the rt lab simulation to run in real time could not be achieved. To make the results comparable with the Simulink model's plots a setting called Time factor was adjusted to 15 which makes the simulator run the simulations slower. This mitigated the problem of a distorted time axis. To save the results from the simulations the Tofile blocks were implemented in the console. Opal RTs own Tofile block was tested, it is made to be less stressful on the system and it also export data with less stepping. The issue with the block is that even with the Time factor set there were some errors with the timing.

It seems to be stretching the time axis for the entire plot, so that even the timing of the load change gets delayed. While simulation was running the scopes showed the timing to be correct and looking at the MATLAB Tofile blocks also gave the right time. The big advantage with the RT-lab block is that it is less stressful on the system, and it records data at a greater frequency, making the plots smoother.

4 Simulations

The simulations and test that will be run are

- Linear analysis in PST compared to dynamic simulation in variable step Simulink model
 - No PSS
 - With speed PSS implemented
- Dynamic simulations of load changes with analysis
 - Load change in Area 1 with PSS
 - Load change in Area 2 with PSS
 - Concurrent load change in each area with PSS
 - Concurrent opposite load change in each area with PSS
 - Load change in Area 1 without PSS
 - Concurrent load change in each area without PSS
 - Concurrent opposite load change in each area with PSS
- Comparing results from RT-Lab to results from variable step Simulink model
 - Load change in Area 1 with PSS
 - Load change in Area 2 with PSS
 - Concurrent load change in each area with PSS
 - Concurrent opposite load change in each area with PSS
 - Load change in Area 1 without PSS
 - Concurrent load change in each area without PSS
 - Concurrent opposite load change in each area with PSS

5 Results

5.1 Linear analysis

5.1.1 No PSS implemented

Using PST running the svm_mgen script the eigenvalues for the different modes, and corresponding frequency and dampening coefficient were found. Most of the modes were non-oscillating, having a dampening factor of 1 and a frequency of zero, these have been omitted. See appendix for full results.

Table 8: No PSS eigenvalues, dampening and frequency

Mode	Eigenvalue	Dampening factor	Frequency (HZ)
7	-0,236545190648605-0,653677477470661i	0,340274299	0,104036002
8	-0,236545190648605+0,653677477470661i	0,340274299	0,104036002
13	-1,89398618517934-0,0115270144289232i	0,99998148	0,001834581
14	-1,89398618517934+0,0115270144289232i	0,99998148	0,001834581
17	0,135428096532491-3,73054972227586i	-0,036278553	0,593735429
18	0,135428096532491+3,73054972227586i	-0,036278553	0,593735429
21	-0,338283003665267-6,4595046180094i	0,052298139	1,02806209
22	-0,338283003665267+6,4595046180094i	0,052298139	1,02806209
23	-0,383190573999045-6,53953899101425i	0,058495625	1,040799956
24	-0,383190573999045+6,53953899101425i	0,058495625	1,040799956
30	-12,4561278215243-0,742338432545845i	0,99822886	0,118146831
31	-12,4561278215243+0,742338432545845i	0,99822886	0,118146831
32	-8,09349833848268-11,2323729467225i	0,584599139	1,787687677
33	-8,09349833848268+11,2323729467225i	0,584599139	1,787687677
35	-4,79256745441988-14,9464521168633i	0,305336422	2,378801736
36	-4,79256745441988+14,9464521168633i	0,305336422	2,378801736
41	-57,5027242972703-13,2045167116713i	0,974633286	2,101564106
42	-57,5027242972703+13,2045167116713i	0,974633286	2,101564106
43	-57,7800236505628-13,3166896460597i	0,974454572	2,119416983
44	-57,7800236505628+13,3166896460597i	0,974454572	2,119416983
45	-59,8506226756496-16,0366480552302i	0,965926948	2,552311809
46	-59,8506226756496+16,0366480552302i	0,965926948	2,552311809
47	-60,8926953517108-17,8175994673518i	0,959757175	2,835759029
48	-60,8926953517108+17,8175994673518i	0,959757175	2,835759029

Looking at the eigenvalues, the only modes that have positive real values are 17 and 18, indicating instability. The dampening factor is negative which means the modes are amplifying, meaning that the rotor angle should oscillate itself to crash the system by reaching critical angle. The frequencies of the modes are 0.59 HZ, indicating it being interarea oscillations. To test this a compass plot of the rotor angle state terms of the eigenvector is produced using PST.

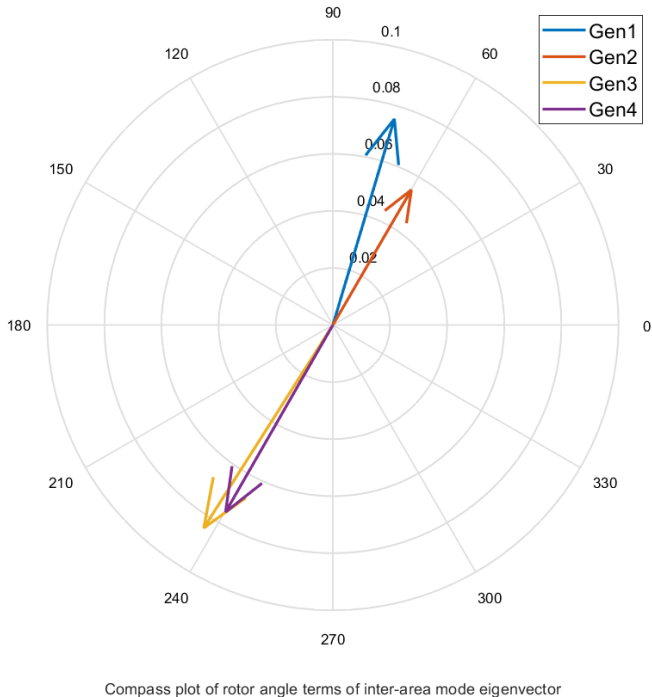


Figure 5.1-1: Compass plot of rotor angle terms of inter-area mode eigenvector without PSS

This shows that this mode is an inter area mode since the generators in area 1 are oscillating against the generators in area two. Gen 1 has some phase shift compared to gen2 and the generators of area 2, this indicated that the inter area mode will have some phase shift when plotted using dynamic simulation.

Plotting the speed participation for the inter-area mode will show the sensitivity of the mode when there is applied more damping at the shaft of the generators.

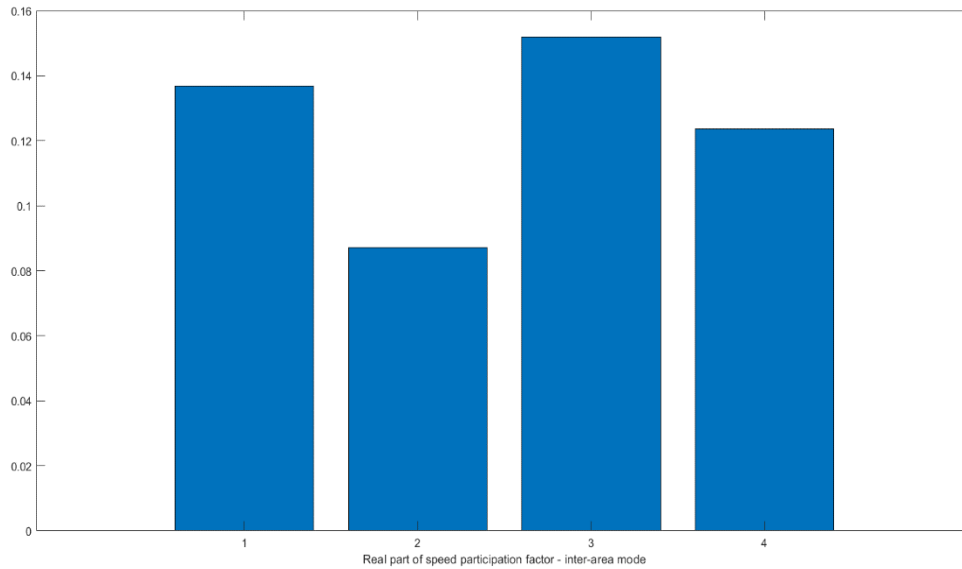


Figure 5.1-2: Real part of speed participation factor - inter-area mode without PSS

All the real parts of the speed participation factor are positive and are somewhat equal. Adding dampening torque with a PSS to any of the generators will contribute to reducing the inter area oscillations.

To test these calculations a dynamic simulation is run using the variable step Simulink model.

Running the variable step Simulink figure with an increase of the active load in area 1

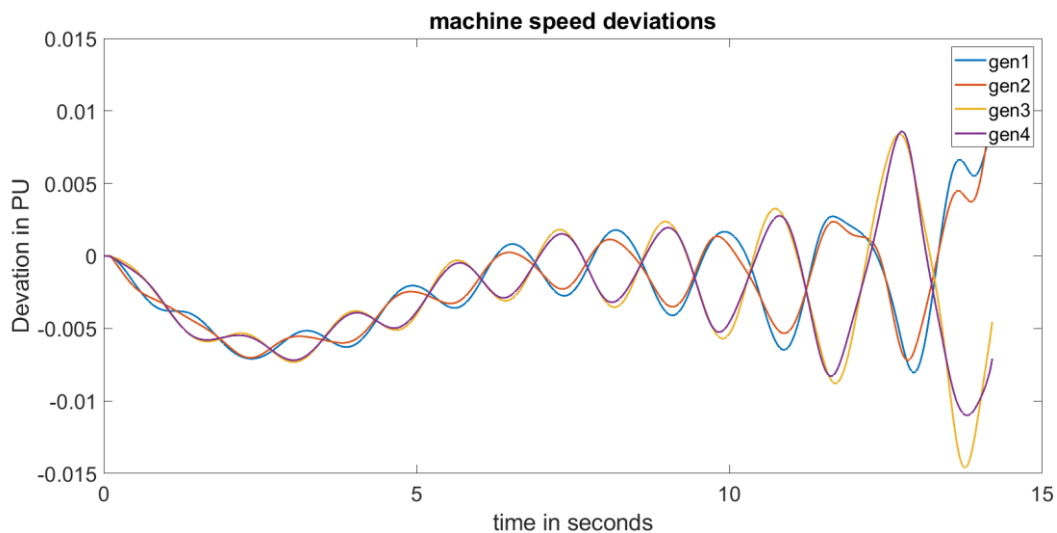


Figure 5.1-3: Dynamic speed deviations response of increase of active load in area 1 without PSS

The plot shows that the system is unstable since the oscillations are increasing and the system crashes. The inter area mode is the dominant mode since the generators in area 1 are oscillating against the ones in area 2.

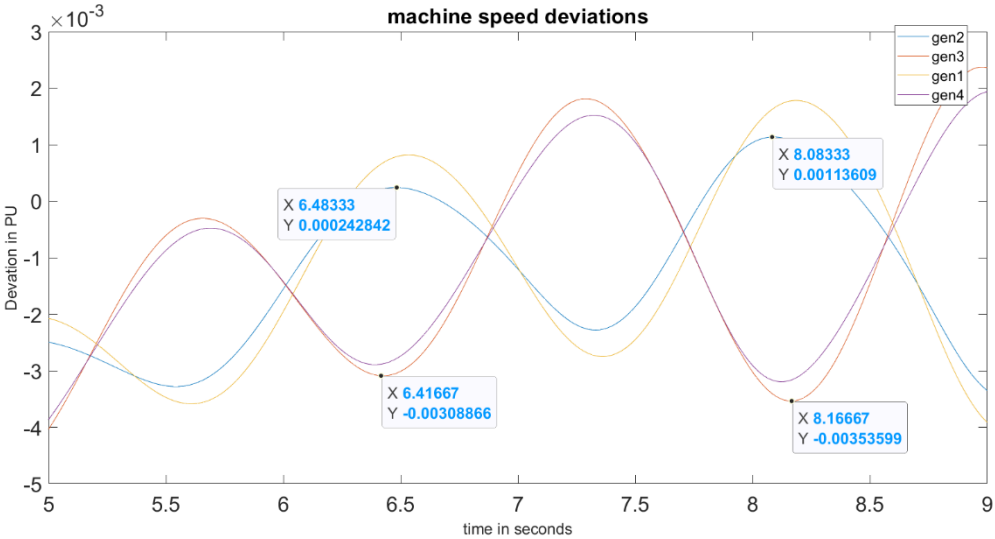


Figure 5.1-4: Dynamic response of increase of active load in area 1 without PSS zoomed in

The peaks of the speed deviations of generator 2 and 3 gives a cycle of 1.6 seconds, which is 0.625 HZ.

The theoretical value of 0.594HZ from PST is within margin of error. The difference might come from slight differences in the models, the other modes shifting the plots, or that the points placed down on the peaks are not placed completely accurate.

The phase shift between gen1 and gen2 is shown on the plots too. Gen1 is lagging behind gen2. There is some phase shift between gen3 and gen4 too, but it is less.

Looking at table 8, modes 21 to 24 have a quite a low dampening factor of 5,23% and 5,58% this is almost at the lower recommended limit of 5%. The frequencies of the modes, 1,03 and 1,05HZ, indicates that they are local modes.

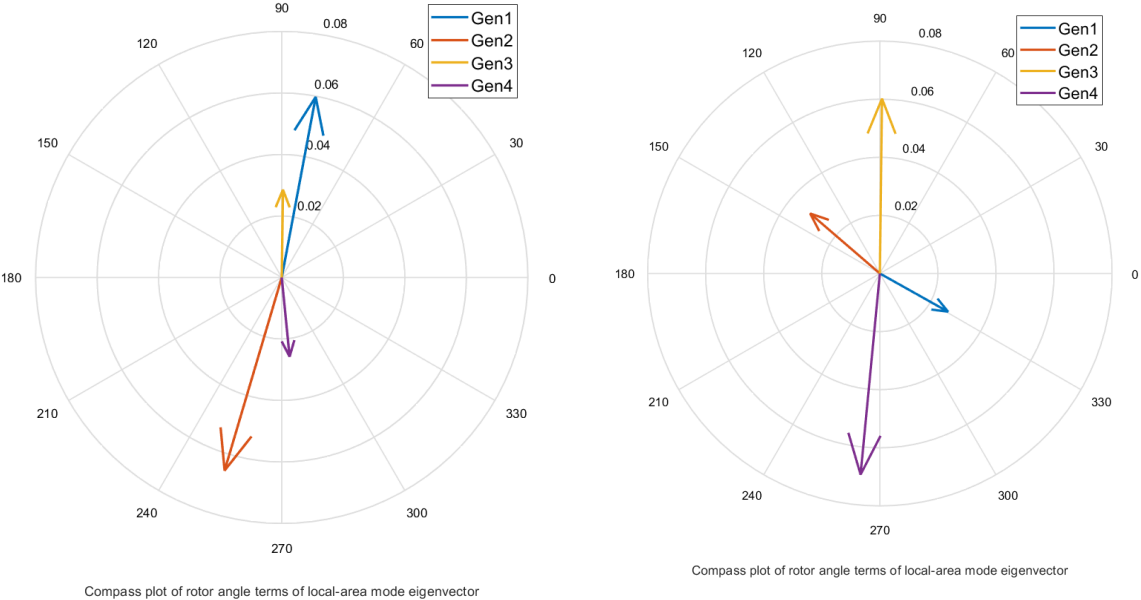


Figure 5.1-5:Compass plot of rotor angle terms of local machine mode eigenvector without PSS, Left for area 1 and right for area 2

The compass plots of the rotor angles show that the generators who are in the same area are oscillating against each other. The magnitude of the lines shows which generator the mode has the greatest effect on. Figure x representing mode 21 and 22 proves that these are the modes for local oscillations in area 1, and vice versa for figure x and mode 23 and 24.

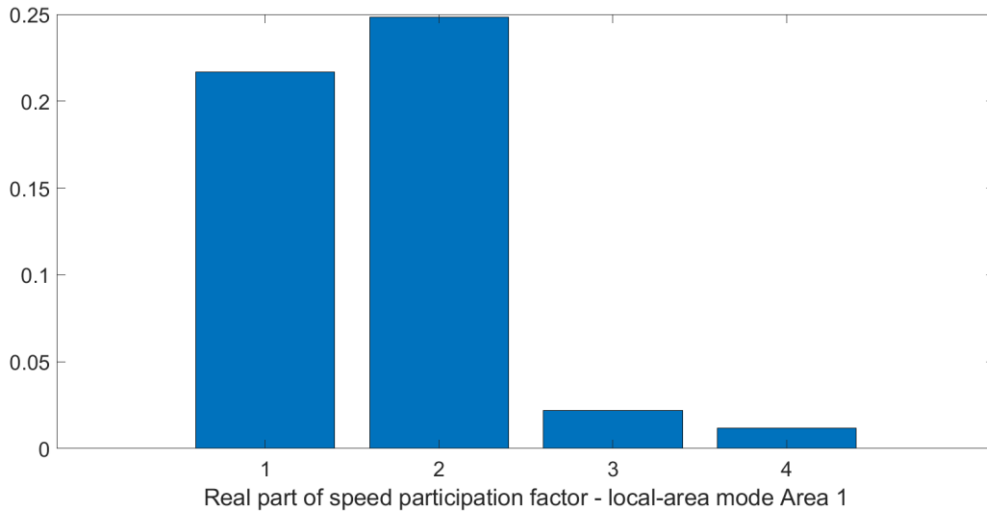


Figure 5.1-6: Real part of speed participation factor- local area mode for area 1 No PSS

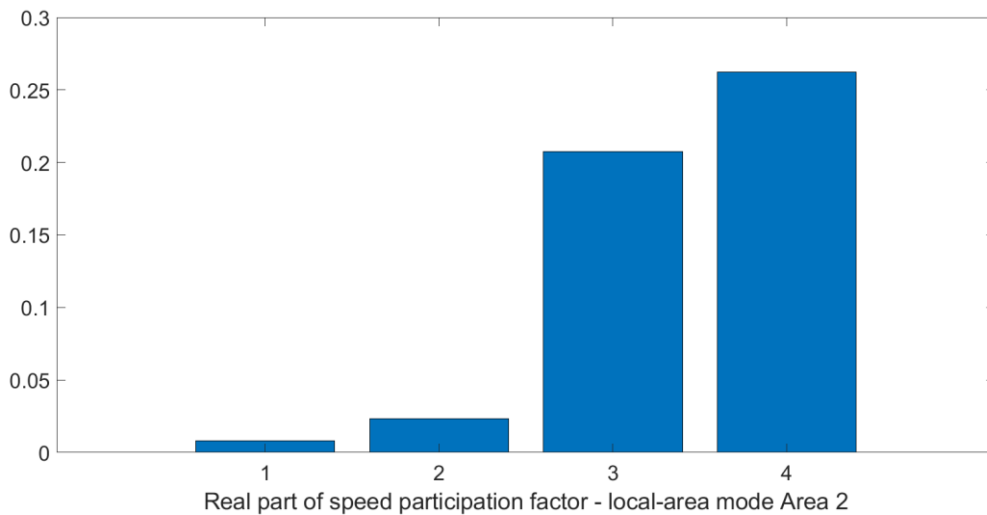


Figure 5.1-7: Real part of speed participation factor- local area mode for area 2 No PSS

The participation factors show that applying dampening torque to the generators in the area related to the mode is the most efficient way to dampen local oscillations. Applying dampening torque to the generators in the other area will have a positive effect, but at a much minor scale. This also shows that the local modes are not completely isolated to only affect the area where they occur. To isolate them more the transmission lines would need to be even longer.

To test these calculations a dynamic simulation is run.

Running the variable step Simulink figure with an increase of generator 1's terminal voltage.

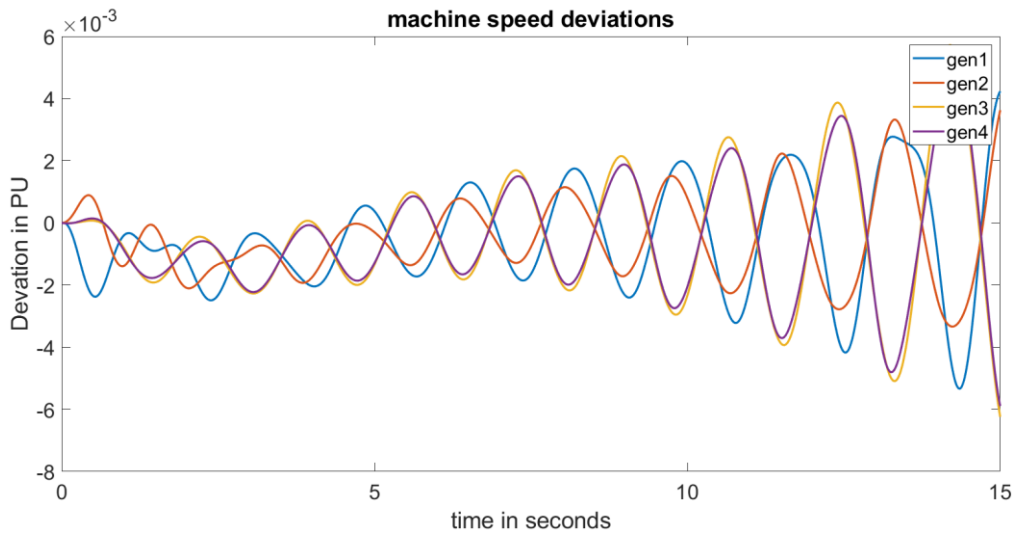


Figure 5.1-8: Dynamic test of local mode oscillations by increasing the voltage in generator 1, No pss

The machine speed deviations show that after the disturbance to generator 1 is applied generator 1 and 2 starts oscillating against each other, local mode. After the two first seconds this mode is dampened, and the inter area oscillation becomes dominant and destructive like in the previous example. The dynamic results affirms that it is the inter area mode that is unstable, and not the local mode.

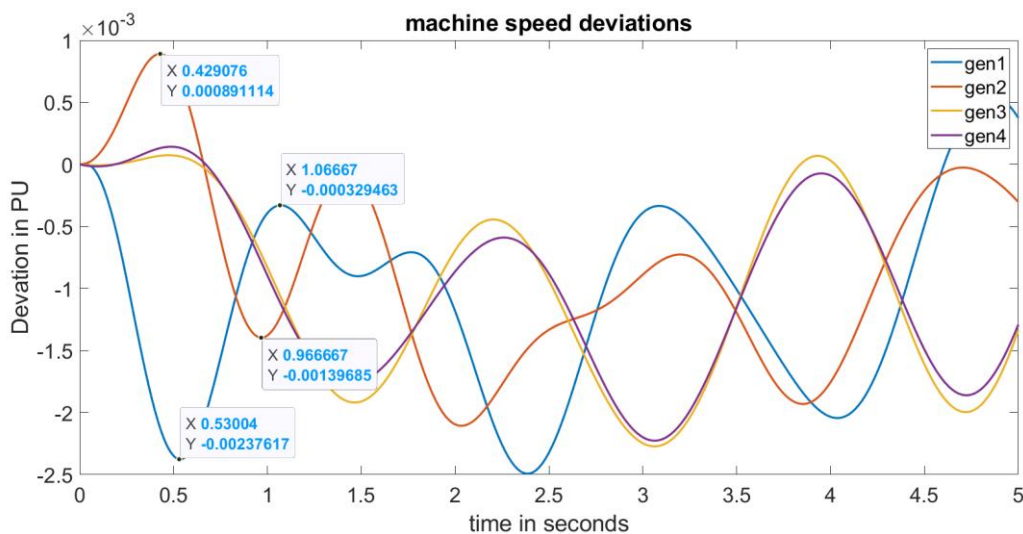


Figure 5.1-9: Dynamic test of local mode oscillations by increasing the voltage in generator 1, No pss Zoomed in

Analysing the peak values of generator 2 gives a mode frequency of 0.93HZ, which is lower than the 1,03HZ calculated by PST. Interference from the inter area mode and the dampening will influence the dynamic simulation, making it less accurate than the linear analyze when looking at the individual modes.

5.1.2 Applying the PSS

Doing the simulation now with the speed based PSS.

Table 9: With PSS eigenvalues, dampening and frequency

Mode	Eigenvalue	Dampening factor	Frequency (HZ)
14	-0,681981959264422-0,048238481977079i	0,997507784	0,007677393
15	-0,681981959264422+0,048238481977079i	0,997507784	0,007677393
18	-1,20116822937311-0,646725847732529i	0,880488554	0,102929615
19	-1,20116822937311+0,646725847732529i	0,880488554	0,102929615
25	-0,830011152197177-3,83468733139147i	0,21154939	0,610309444
26	-0,830011152197177+3,83468733139147i	0,21154939	0,610309444
27	-3,97266343977213-0,0551206697091946i	0,999903756	0,008772727
28	-3,97266343977213+0,0551206697091946i	0,999903756	0,008772727
35	-0,899638718645128-8,67421818401753i	0,103160752	1,380544701
36	-0,899638718645128+8,67421818401753i	0,103160752	1,380544701
37	-0,928575257389513-8,808460896895i	0,104837635	1,401910093
38	-0,928575257389513+8,808460896895i	0,104837635	1,401910093
39	-6,82211400644901-10,9693681501595i	0,528119352	1,745829164
40	-6,82211400644901+10,9693681501595i	0,528119352	1,745829164
41	-4,08590703546631-15,0155713227772i	0,262564174	2,389802399
42	-4,08590703546631+15,0155713227772i	0,262564174	2,389802399
53	-58,303372338224-14,2005586691046i	0,971596156	2,260089107
54	-58,303372338224+14,2005586691046i	0,971596156	2,260089107
55	-58,5345526355117-14,2730480162136i	0,971534368	2,271626145
56	-58,5345526355117+14,2730480162136i	0,971534368	2,271626145
57	-60,1458604385401-16,4135635100999i	0,964722495	2,612299766
58	-60,1458604385401+16,4135635100999i	0,964722495	2,612299766
59	-61,0631350283081-18,058746292844i	0,958943571	2,874138739
60	-61,0631350283081+18,058746292844i	0,958943571	2,874138739

All the eigenvalues have negative real parts meaning that the system should be stable. Modes 25 and 26 have a frequency of 0,61 HZ which indicates they are the interarea modes.

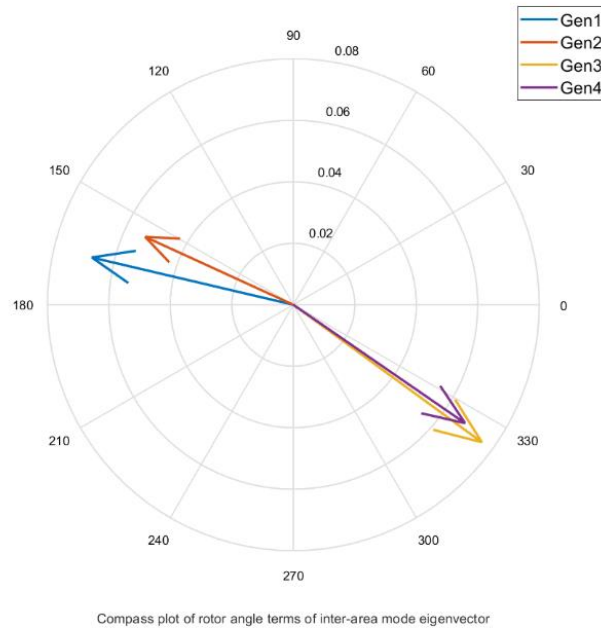


Figure 5.1-10: Compass plot of rotor angle terms of inter-area mode eigenvector with PSS

The compass plot of the rotor angles state terms show the generators in area 1 oscillates against the ones in area 2, proving modes 25 and 26 being the interarea modes.

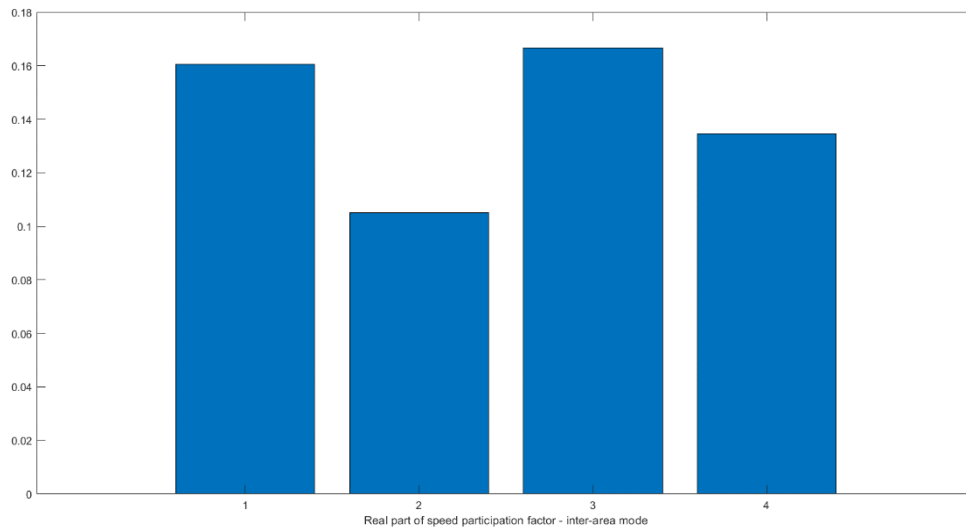


Figure 5.1-11: Real part of speed participation factor - inter-area mode with PSS

The participation factors still shows that there is room for more potential dampening. A 20% dampening coefficient is over the minimum of 10% that is recommended for inter area modes. Applying more dampening is not needed but could help improve the response.

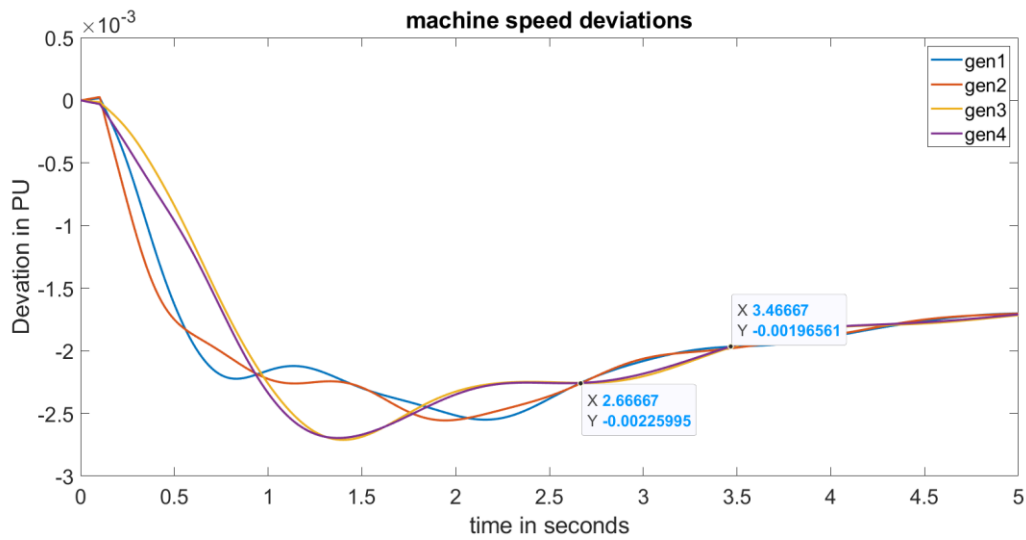


Figure 5.1-12: Dynamic speed deviations response of increase of active load in area 1 with PSS

The dynamic simulation shows that the system is stable after a change in the active load. The frequency for the inter area oscillations are 0.625HZ, which is within the margin of error.

The modes with the weakest dampening are 35 to 38, with 10,32 and 10,48 percent damping respectively. Their frequencies, 1,38 and 1,4 HZ, indicates that they are the local modes, and the compass plots proves that they are.

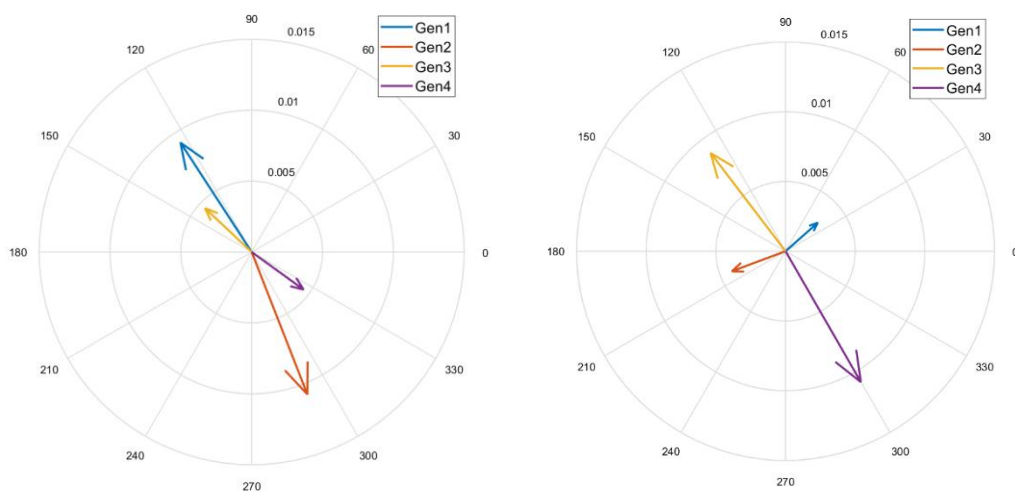


Figure 5.1-13: Compass plot of rotor angle terms of local machine mode eigenvector with PSS, Left for area 1 and right for area 2

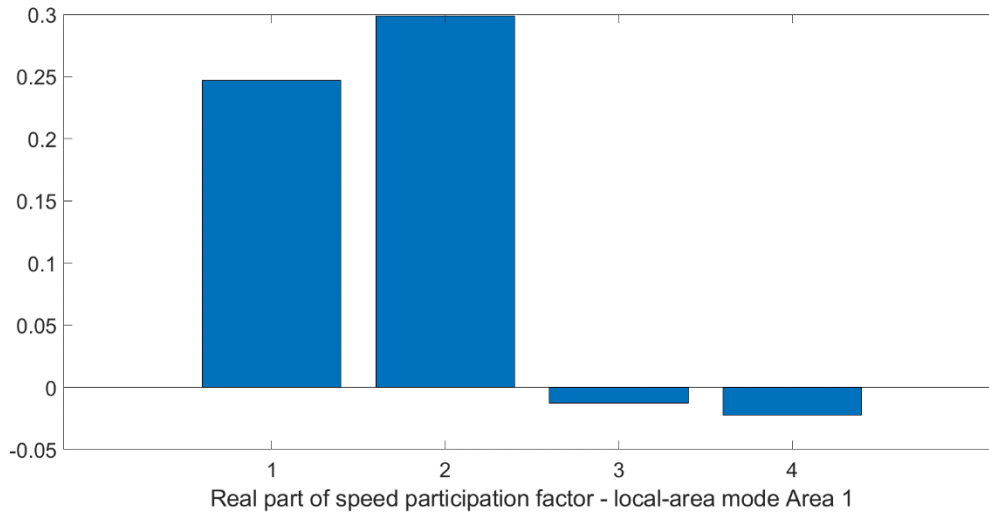


Figure 5.1-14: Real part of speed participation factor- local area mode for area 1 with PSS

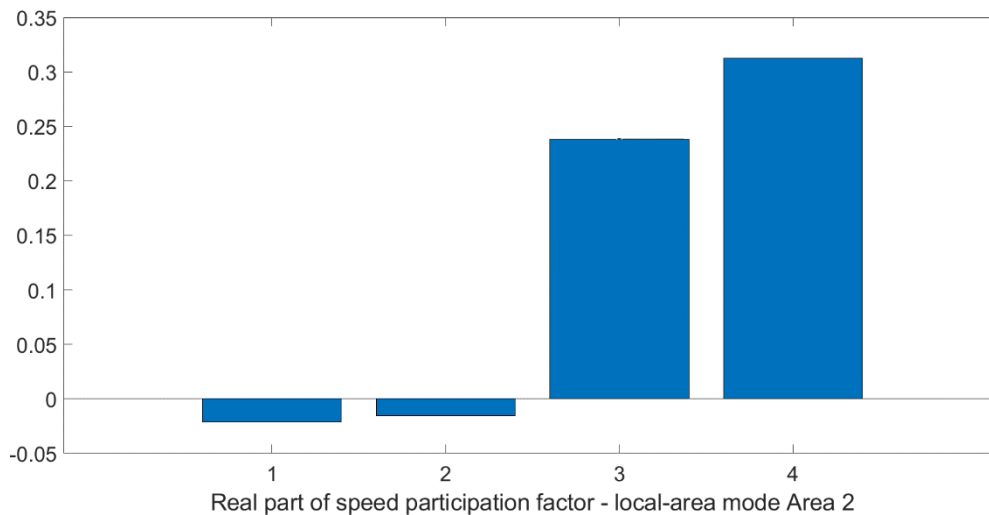


Figure 5.1-15: Real part of speed participation factor- local area mode for area 2 with PSS

The participation factor of local area mode deviates from the no PSS simulations, the factors for the generators in the opposite area are negative. A negative participation factor means that dampening torque applied to them will increase the mode and lower its damping coefficient. As the system stands now applying more dampening torque would make the system more stable since the negative factors are small compared to the positive factors.

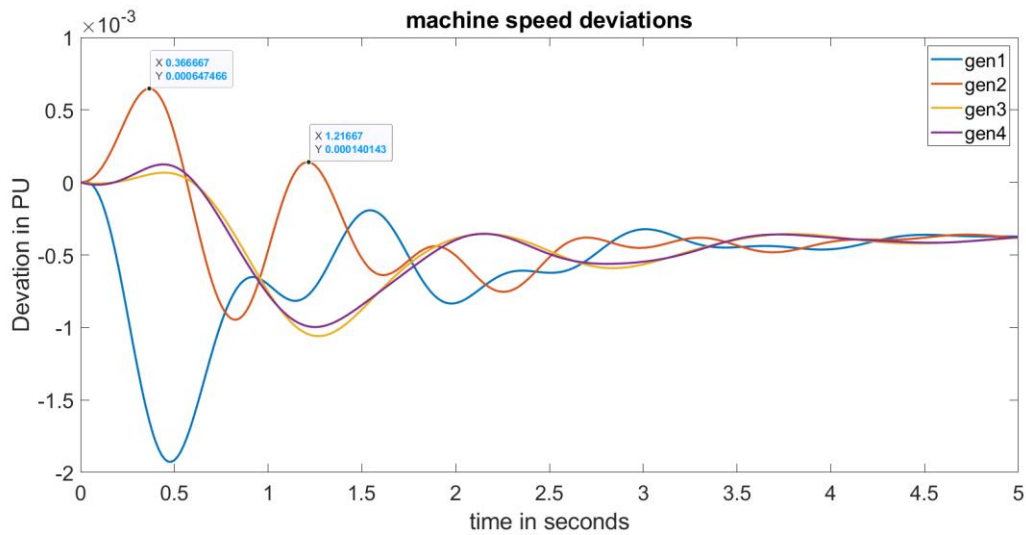


Figure 5.1-16: Dynamic speed deviations response of increase of terminal voltage of generator 1 with PSS

The dynamic simulation shows the local mode being dominant during the first few cycles with a frequency of 1.18 HZ. Like the no PSS simulation the local mode gets dampened out, but unlike the no PSS example the inter area mode does not become completely dominant and all the oscillations gets dampened after 5 seconds.

5.2 Dynamic simulations of load changes with analysis

5.2.1 100MW applied to load in area 1

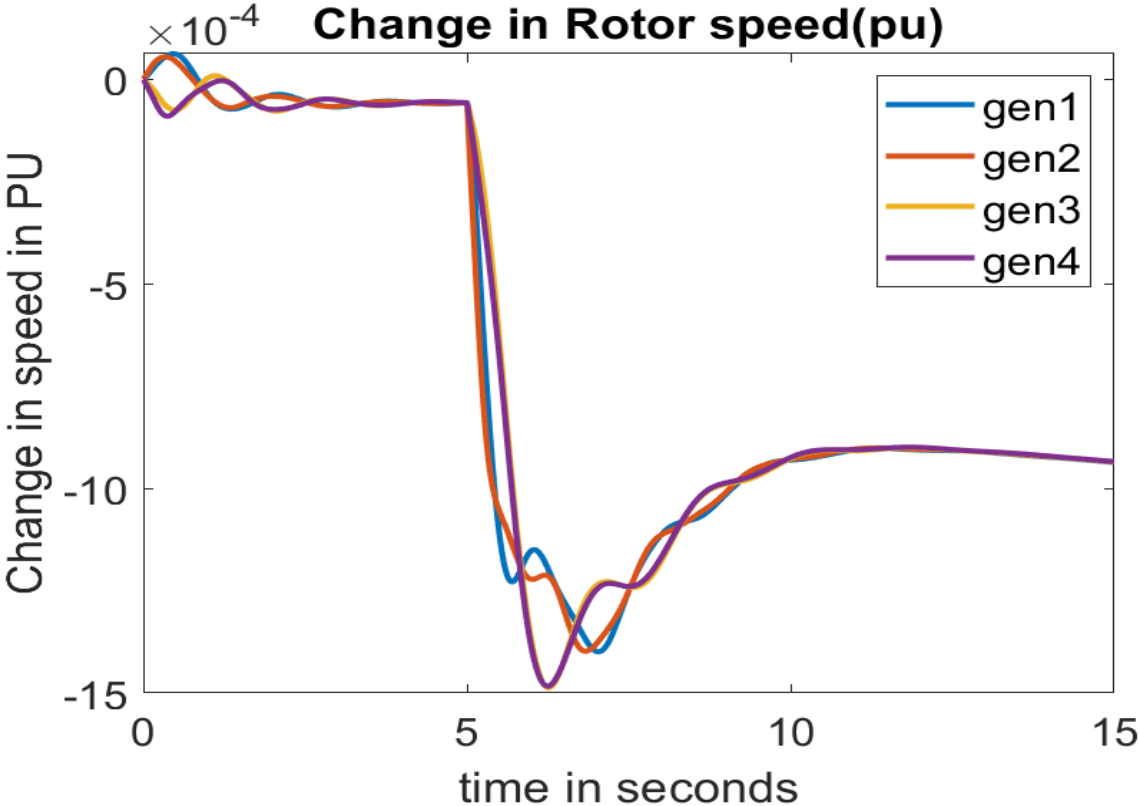


Figure 5.2-1: Speed deviations after a 100MW load increase in area 1

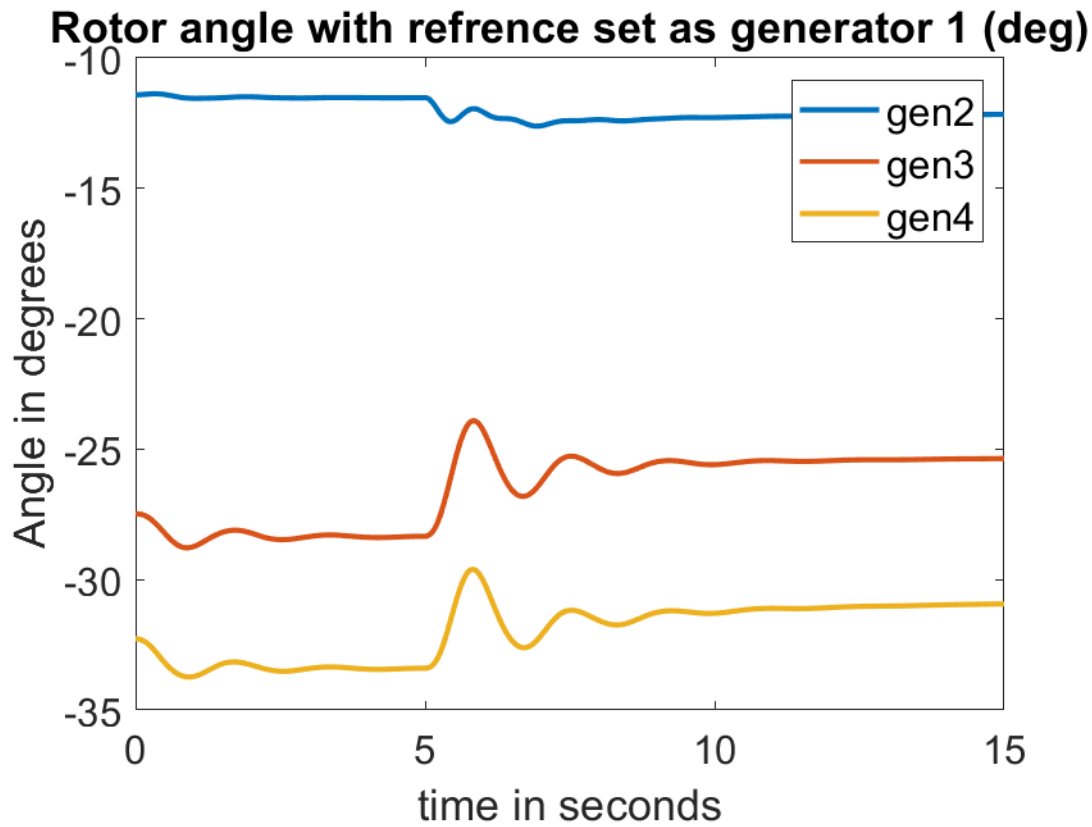


Figure 5.2-2: Rotor angles with ref set to generator 1 after a 100MW load increase in area1

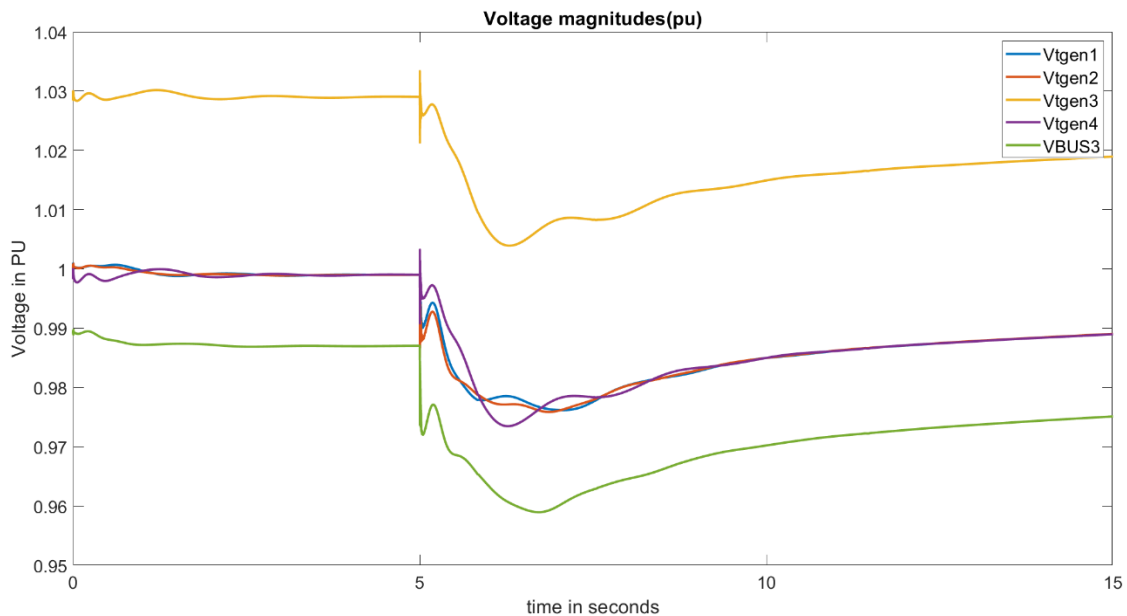


Figure 5.2-3: Voltage levels after a 100MW load increase in area1

Applying positive load changes leads to what is expected, the frequency/rotor speed and bus voltages drops, while the active amount of power produced increases. The rotor angle plot shows the generators in area 2 oscillating against the generators in area 1. The interarea

modes are dampened after around 5 seconds, which is a satisfying result, the minor oscillations lasting around 5 seconds should not do any harm to the system. The lack of secondary reserves are shown too, after stabilizing the frequency is not returned to nominal value, and if it simulation is run longer the frequency will very slowly keep dropping.

5.2.2 100MW applied to load in area 2

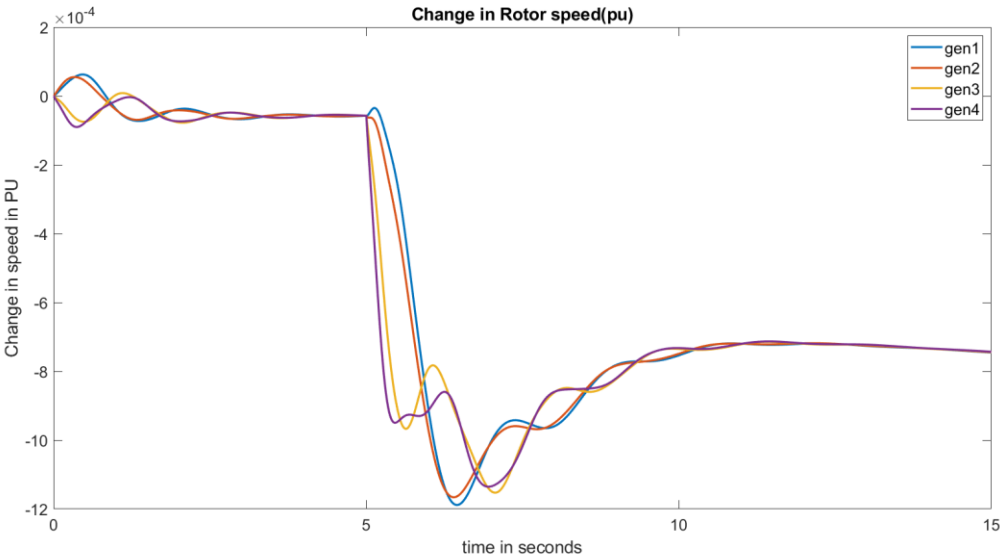


Figure 5.2-4: Speed deviations after a 100MW load increase in area 2

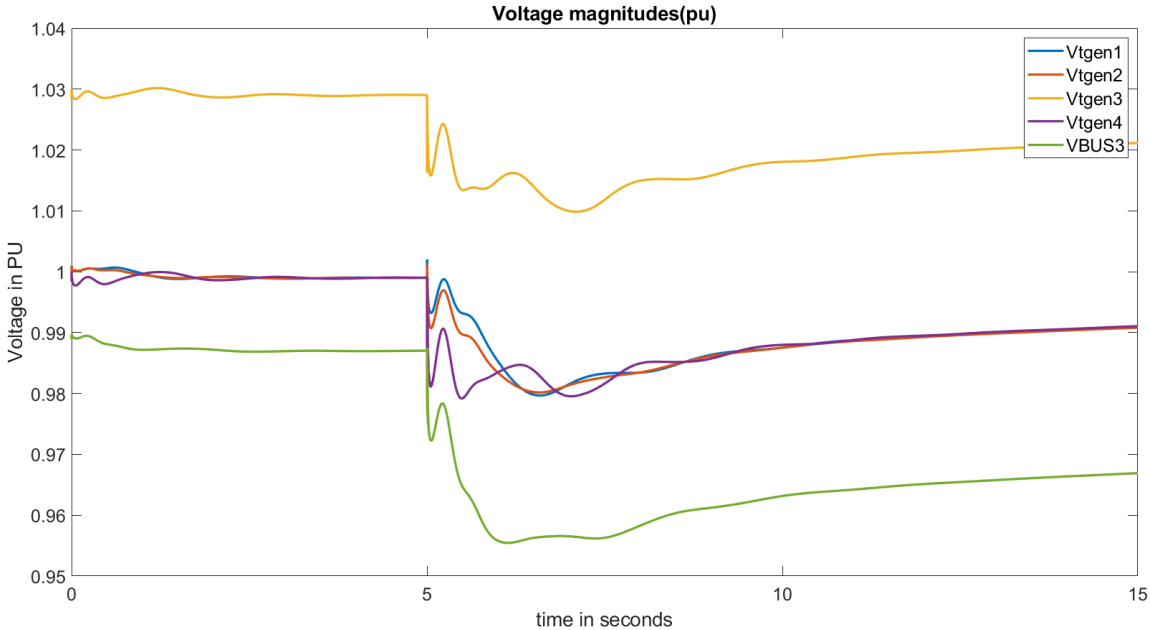


Figure 5.2-5: Voltage levels after a 100MW load increase in area2

Comparing the results from the 100MW change in area 1 to an 100MW change in area 2 shows that the voltage for the load buses get more reduced, and the rotor angle oscillations are larger. The more power transferred over the transmission lines leads to higher active and reactive losses and making the system more stressed. These losses lead to the low voltage at

the load busses which means the voltage stability is in danger of crashing. According to [16] more stress on long distance transmission will lead to stronger inter area modes.

The change in frequency is lower when the change is in area 2, even though the extra active power needed from the transmission lines losses should drop the speed more than when the load in area 1 changes. The lower speed drop can be caused by the network structure.

Generator 3 is the swing bus and usually produces more power than the other generators, so the close approximation to the load change might help the frequency response.

5.2.3 300MW applied to load in area 1, then 300MW applied to load in area 2

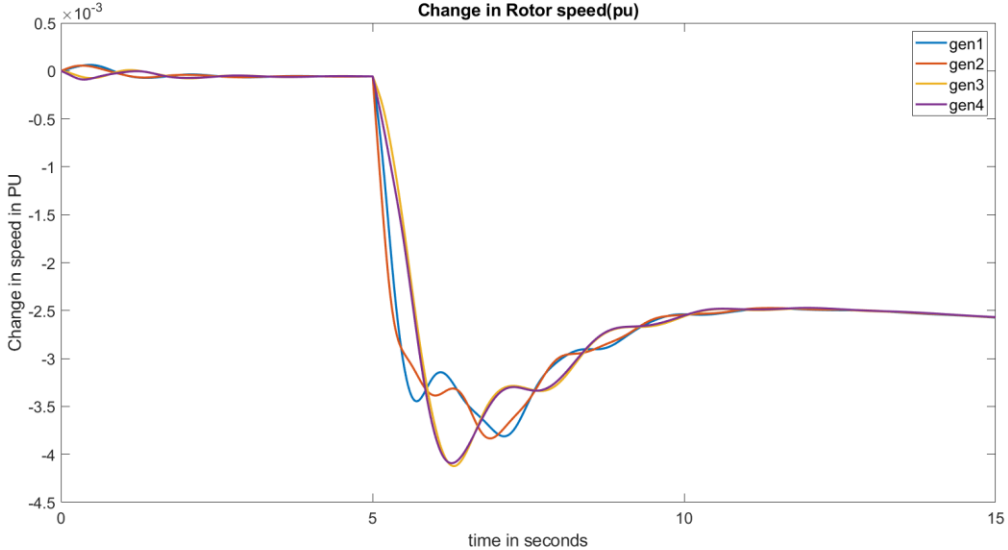


Figure 5.2-6: Speed deviations after a 300MW load increase in area 1

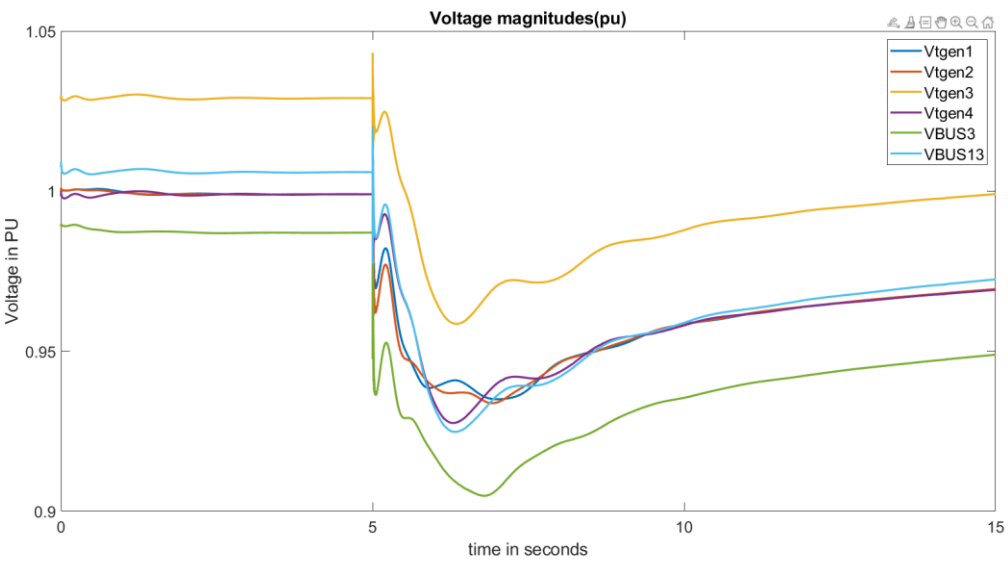


Figure 5.2-7: Voltage levels after a 300MW load increase in area 1

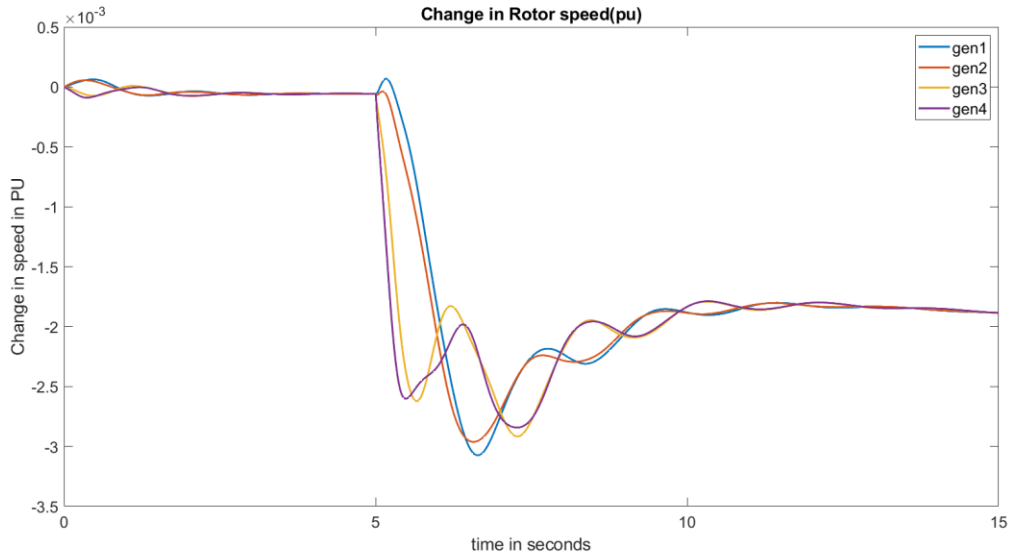


Figure 5.2-8: Speed deviations after a 300MW load increase in area 2

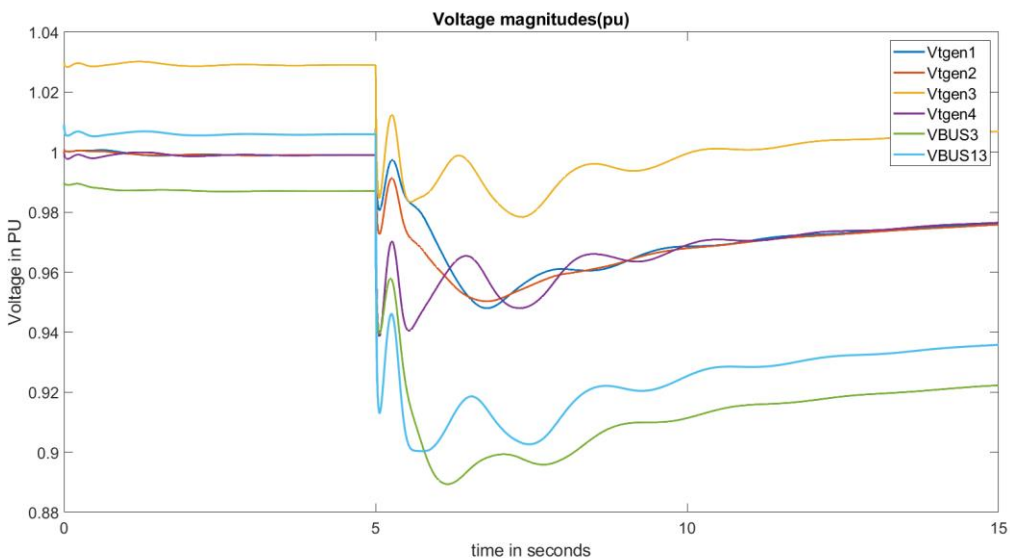


Figure 5.2-9: Voltage levels after a 300MW load increase in area2

Testing with +300MW shows similar relations.

In both examples, but especially the change in load for area 2 the load voltage levels are very low. In a real system this would make it crash.

5.2.4 Testing the limits of the voltage 1000MWs added to load in area1.

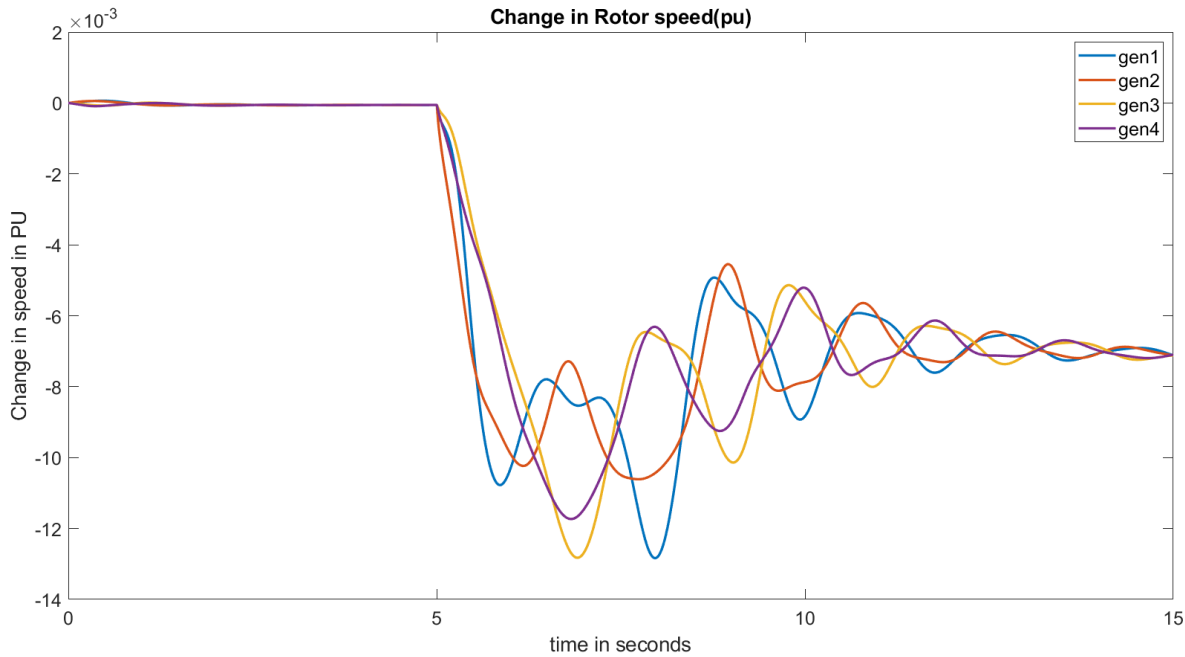


Figure 5.2-10: Speed deviations after a 1000MW load increase in area 1

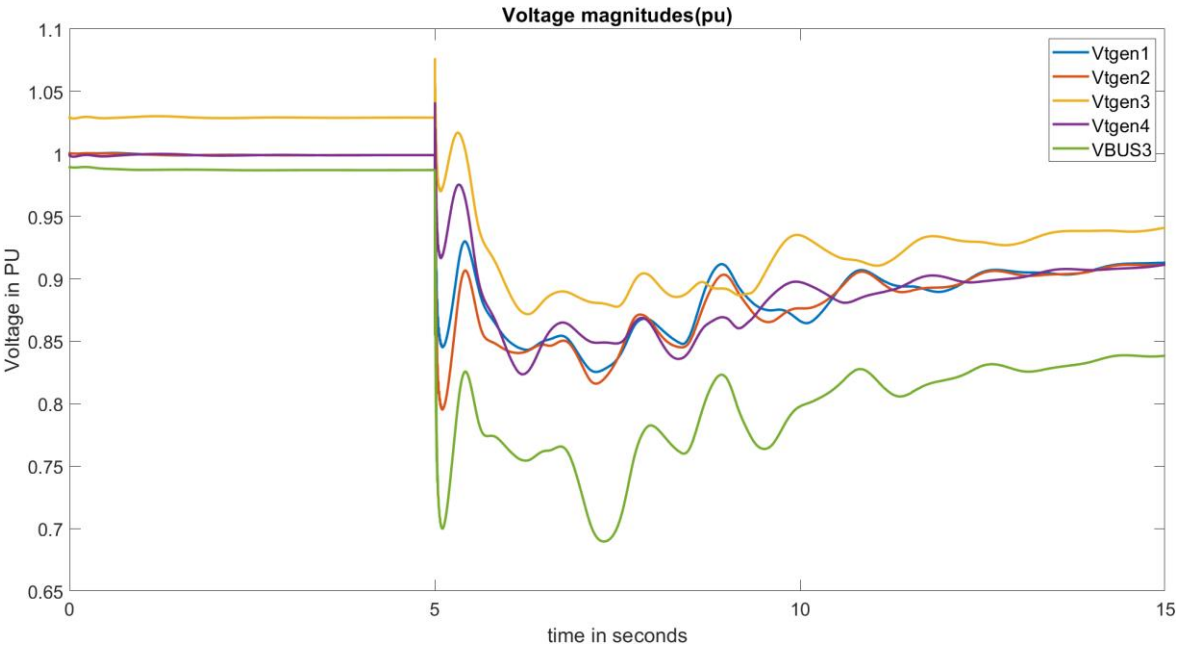


Figure 5.2-11: Voltage levels after a 1000MW load increase in area 1

The system is still running and seems to be stable, but the voltage is so low that in a real system this situation would leave the system unstable. This is a weakness with the variable step model.

5.2.5 Concurrent 50MW increase at both loads

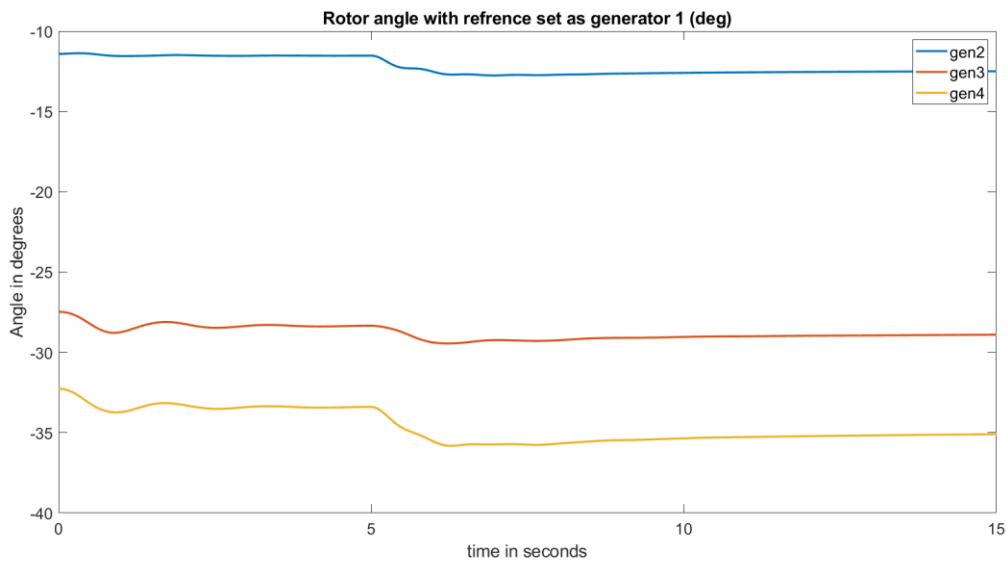


Figure 5.2-12: Rotor angle after a 50MW concurrent load increase in both areas

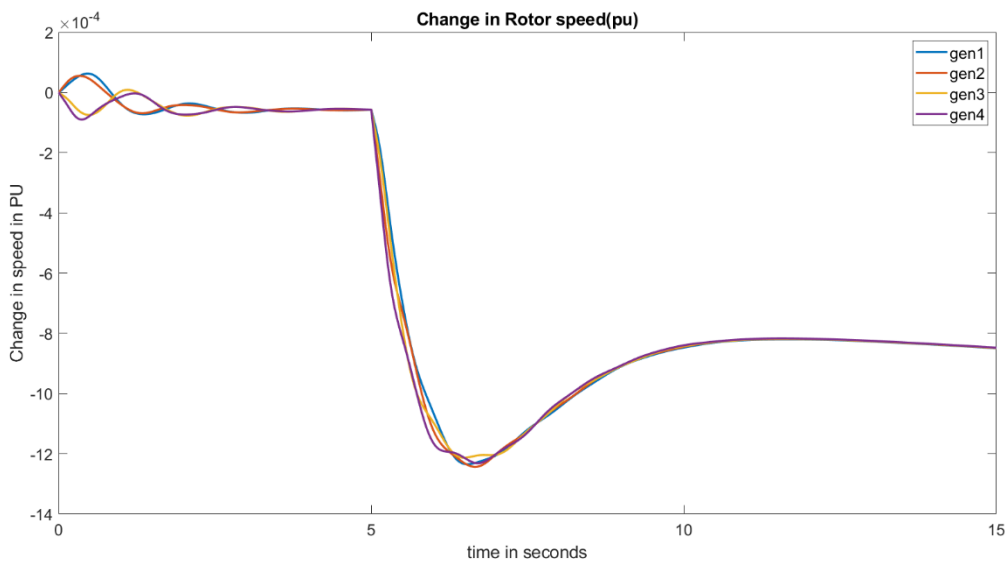


Figure 5.2-13: Rotor speed deviations after a 50MW concurrent load increase in both areas

The speed change plot and Rotor angle plot shows that the concurrent load change dampens most of the oscillations. The reason is destructive interference, since the load change in area 2 produces oscillations that is close to 180 degrees out of phase with the oscillations produced by the change in area 1. In practice some destructive interference will happen since loads in different areas will change up and down at the same regular times every day. The change in each area will rarely be at the same amount, but some destructive interference will still occur to dampen some of the oscillations. Increases in

demand is going to negatively affect the voltage and frequency stability, so it can't be used to improve power system stability in the real world.

5.2.6 Concurrent 100MW increase at both loads

Applying +100MW on each shows the destructive interference will continue at higher load levels.

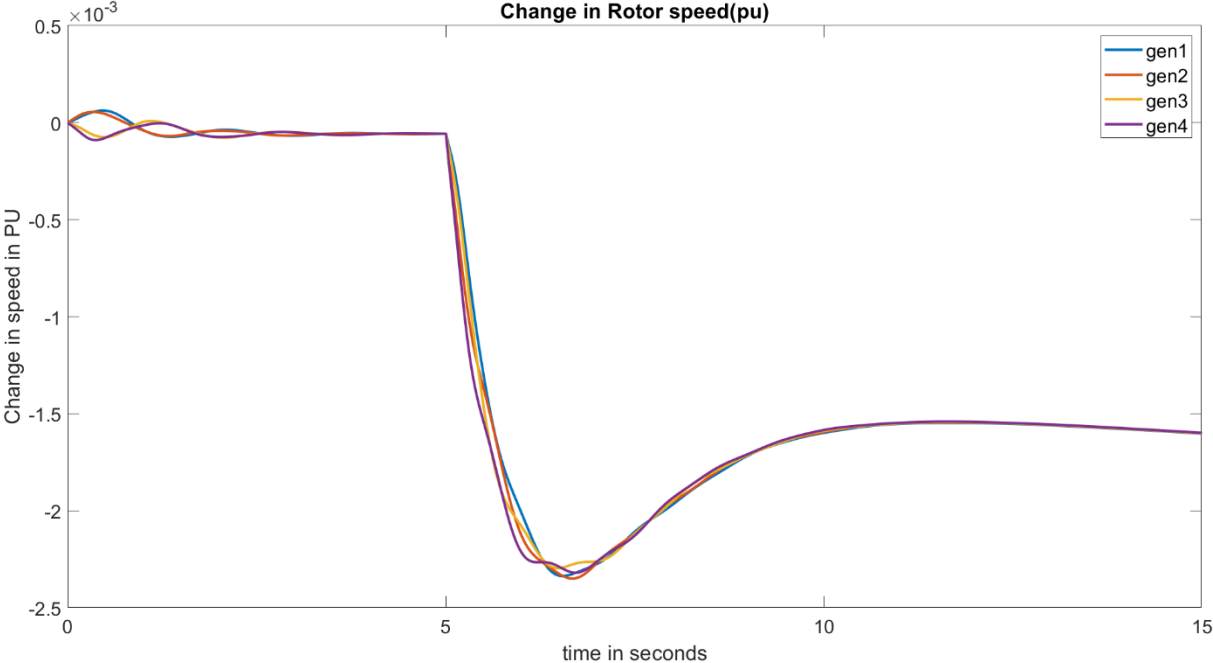


Figure 5.2-14: Rotor speed deviations after a 100MW concurrent load increase in both areas

5.2.7 100MW increase of load in area1, while 100MW decrease of load in area 2

Increasing the load in one area and decreasing it in another will give constructive interference, since the oscillations produced by each change will be in phase with each other, which leads

to higher amplitude oscillations.

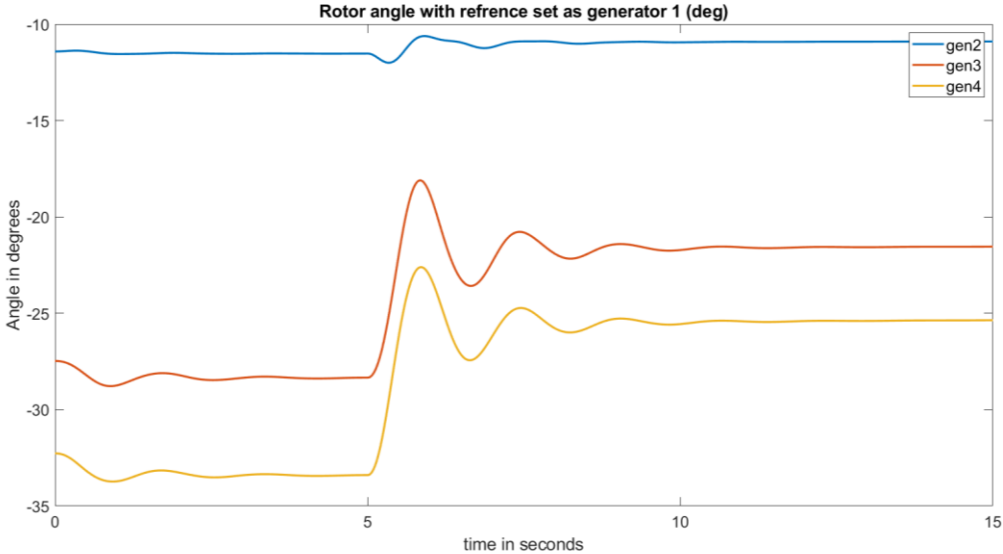


Figure 5.2-15: Rotor angles after a 100MW load increase in area1 and a 100MW load decrease in area 2

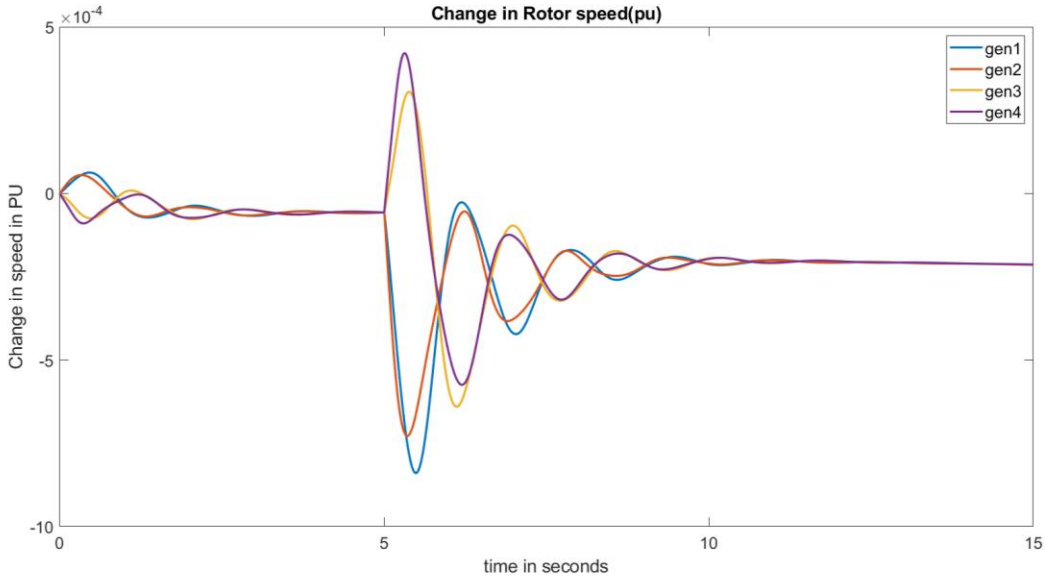


Figure 5.2-16: Rotor speed deviations after a 100MW load increase in area1 and a 100MW load decrease in area 2

Testing it with even larger load changes gives even bigger oscillations.

5.2.8 400MW increase of load in area1, while 400MW decrease of load in area 2

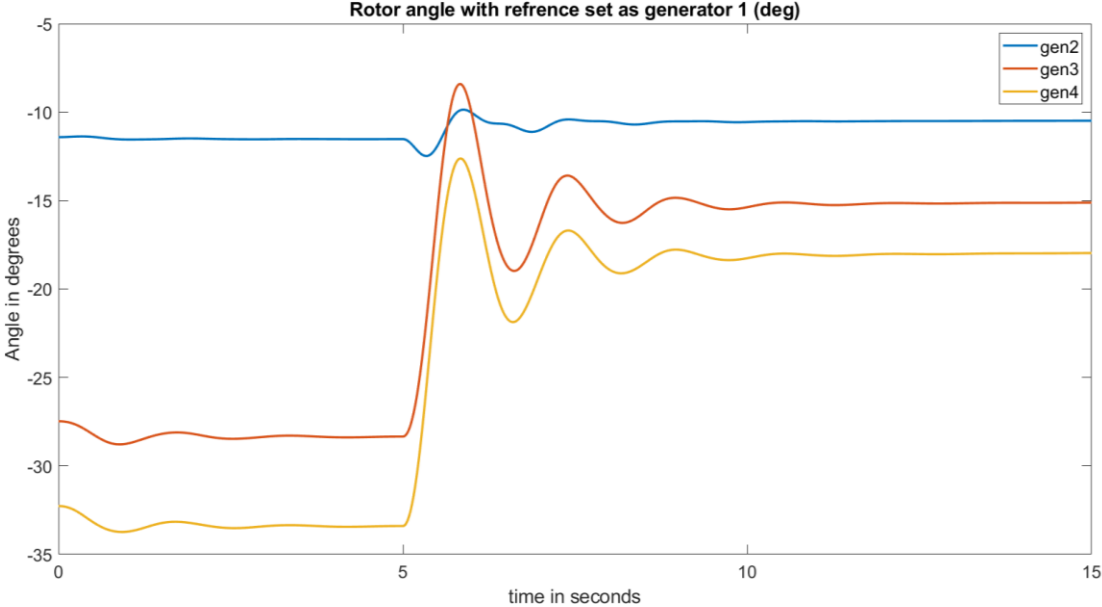


Figure 5.2-17: Rotor angles after a 400MW load increase in area1 and a 400MW load decrease in area 2

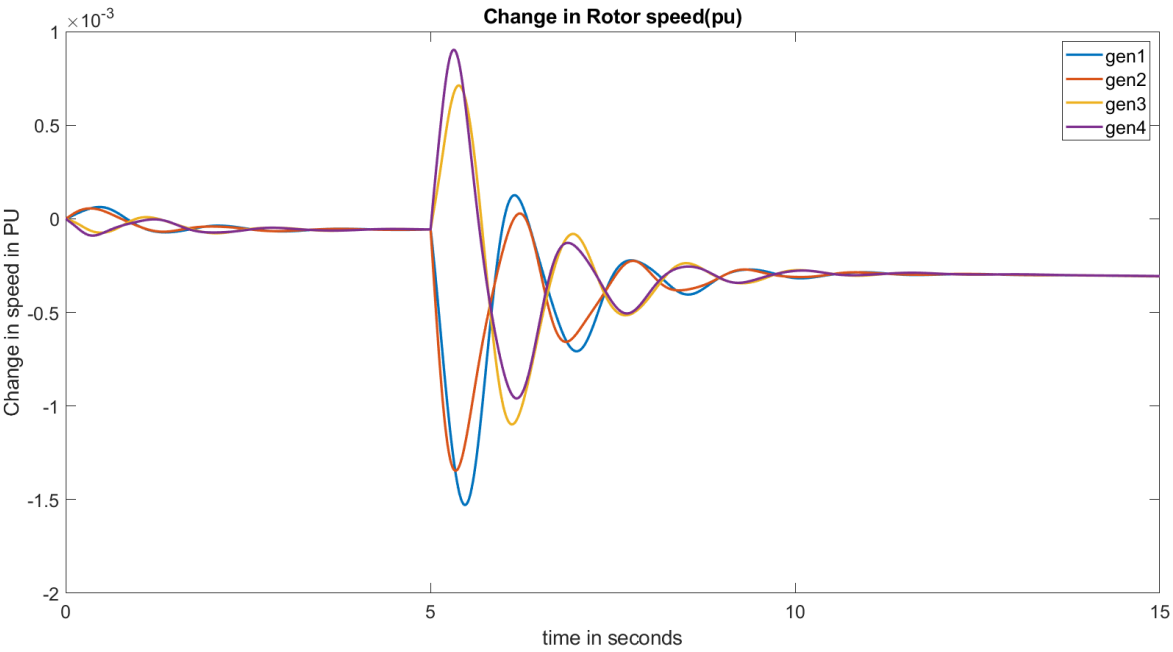


Figure 5.2-18: Rotor speed deviations after a 400MW load increase in area1 and a 400MW load decrease in area 2

Running opposite changes in the two loads is a good way of just looking at the rotor angle stability and the interarea modes, since the frequency and voltage does not get affected much

because there is a zero net gain or loss of load, except for the changes in power losses over the lines.

One can see that with a 400MW concurrent opposite change in each load the system is still stable, and gets dampened out fairly quickly. Increasing the amount of opposite change will at some point be too much since the change in power flow will lead the rotor angle to surpass critical angle which will lead to the generators losing synchronism with each other. For this model, checking in steps of 100MW, the system crashed at a concurrent opposite change of 1000MW. Such a big opposite change, relative for the system, is highly unlikely to happen in a realistic scenario.

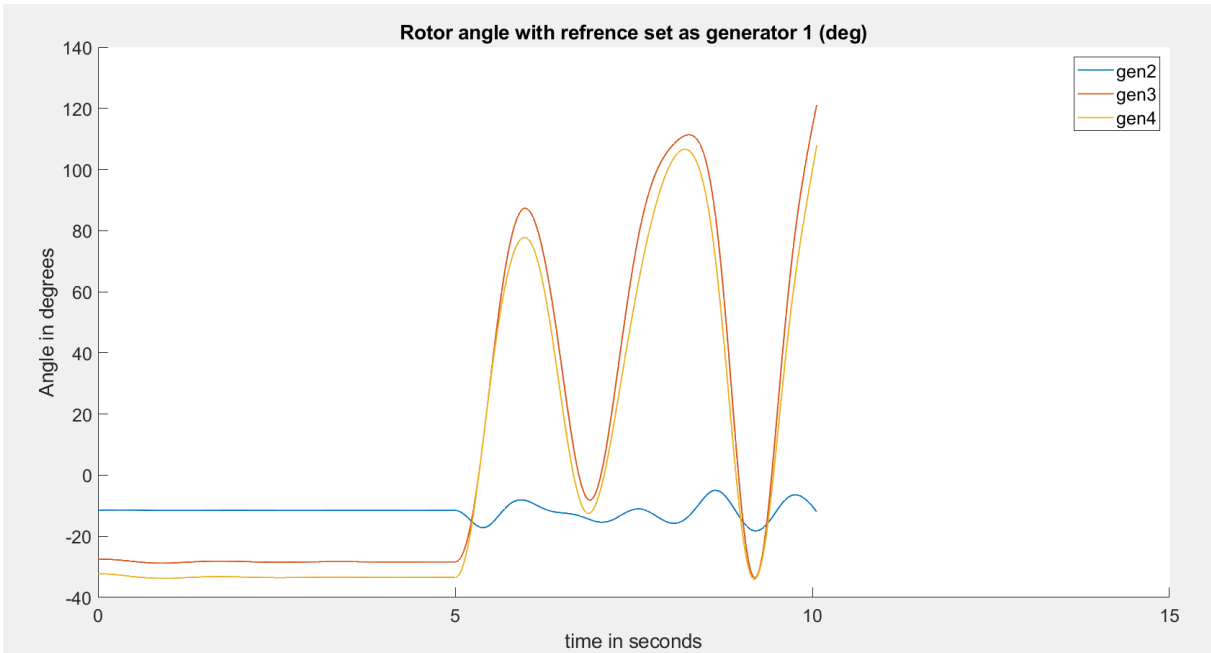


Figure 5.2-19: Rotor angles after a 1000MW load increase in area1 and a 1000MW load decrease in area 2

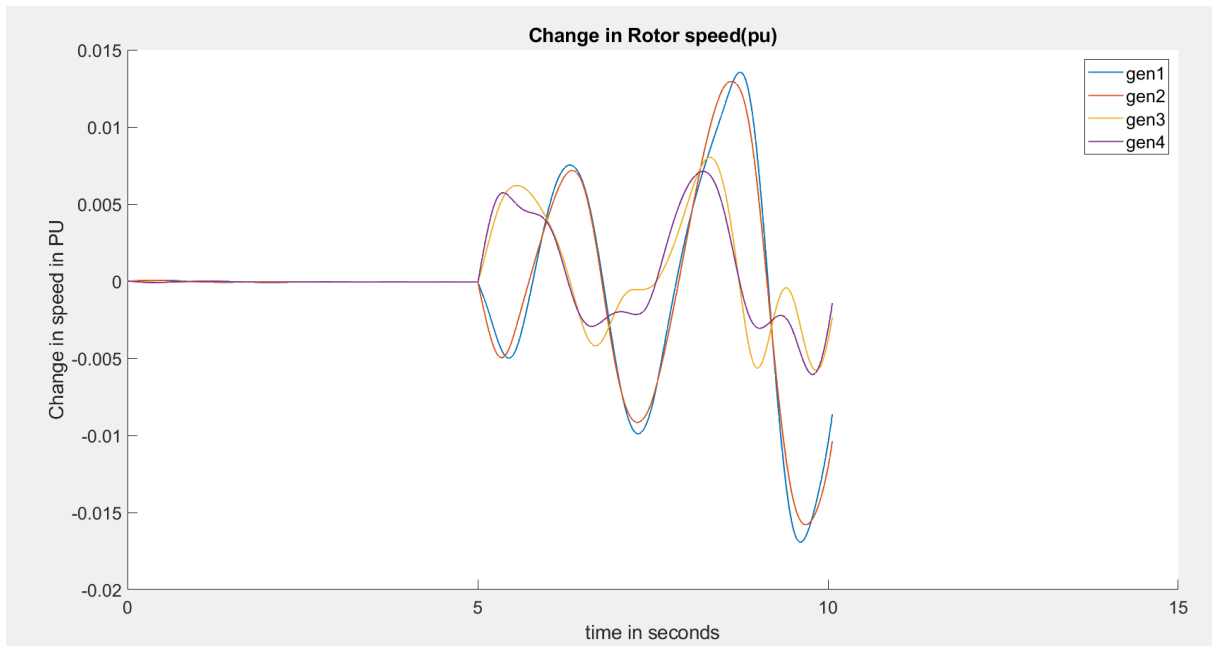


Figure 5.2-20: Rotor speed deviations after a 1000MW load increase in area1 and a 1000MW load decrease in area 2

5.2.9 No PSS tests

For these tests, the load change moment has been moved from 5 seconds into the simulation to 0,01 seconds into the simulation. This has been done since the oscillations from being not perfectly in steady state during initial condition would increase too much if one had to wait for the change for 5 seconds.

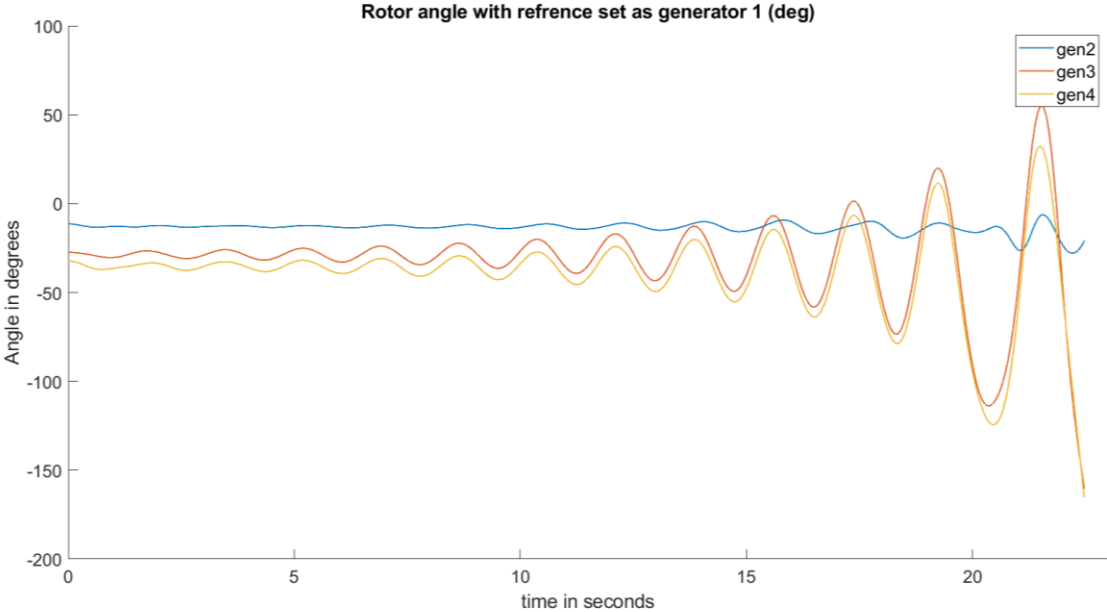


Figure 5.2-21: Rotor angles after a 100MW load increase in area 1 without PSS

Turning off the PSS and increasing load 1 with 100MW gives quite noticeable interarea oscillations that crashes the system 21 seconds after the error occurred when the rotor angles of the generators in area 2 have 180-degree difference from the ones in area 1.

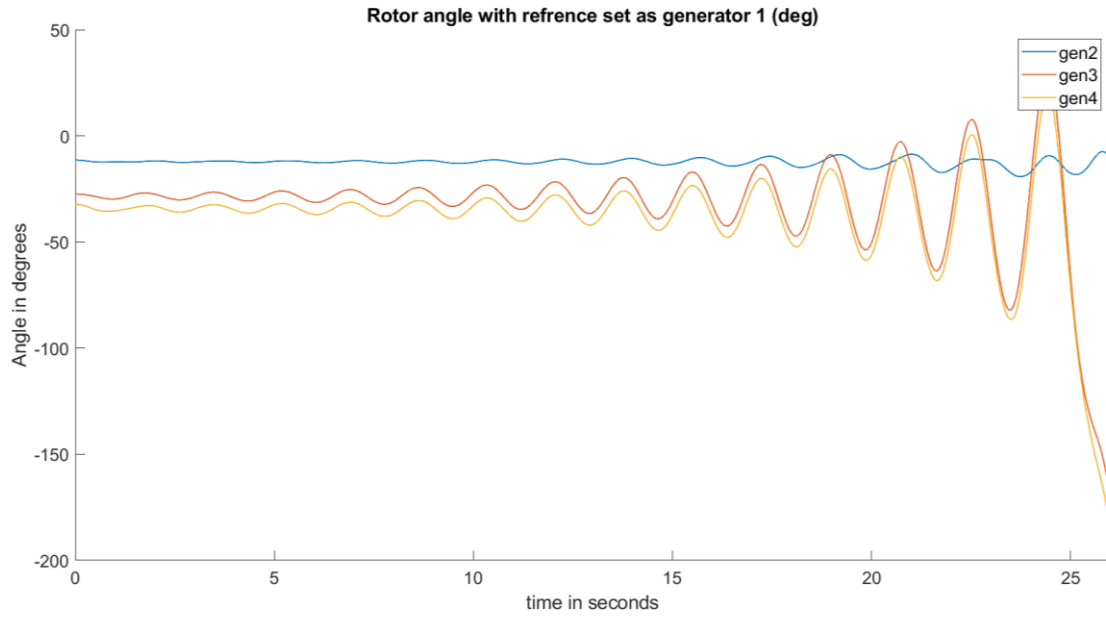


Figure 5.2-22: Rotor angle after a 50MW concurrent load increase in both areas no PSS

A concurrent load change with an increase of 50MW in each area leads to a system crash after 27 seconds.

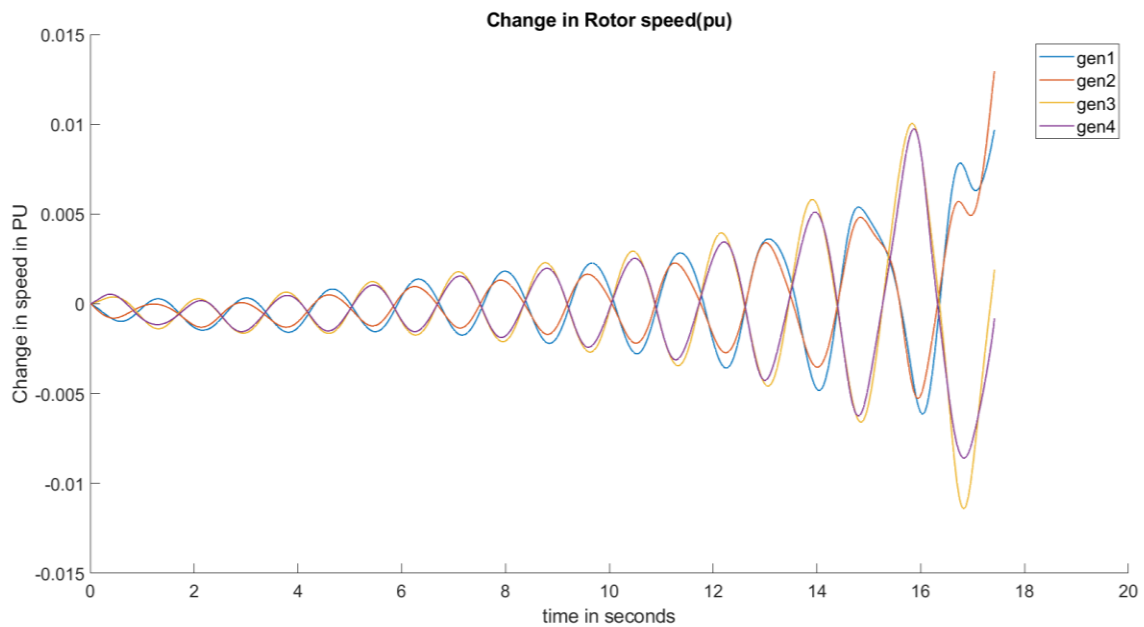


Figure 5.2-23: Rotor speed deviations after a 100MW load increase in area1 and a 100MW load decrease in area 2 without PSS

A concurrent +100MW change on load 1 and a -100MW change on load 2 lead the system to crash after 17 seconds.

5.3 RT lab

5.3.1 With PSS

Running the simulations in RT lab gave very similar results at low changes

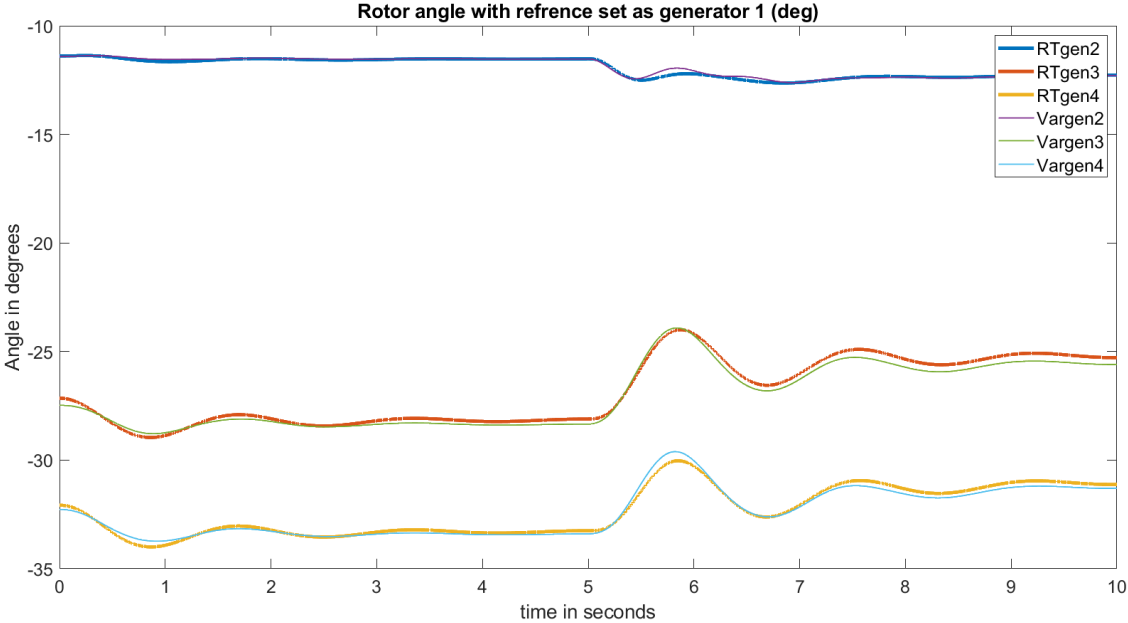


Figure 5.3-1: Rotor angles after a 100MW load increase in area 1 RT/fixed step model versus Variable step model

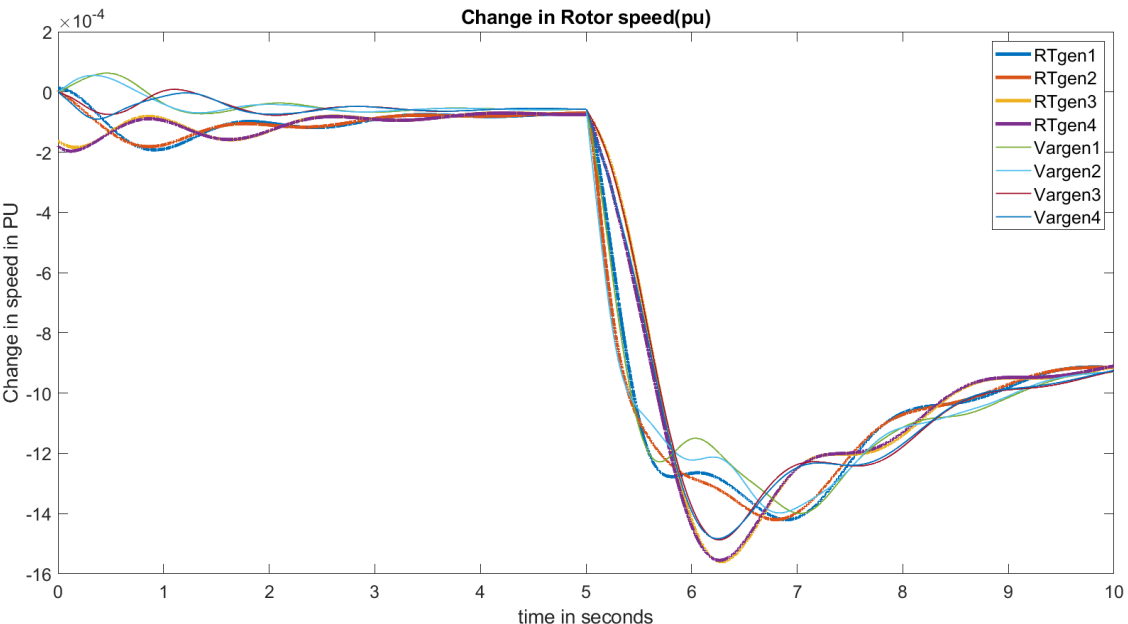


Figure 5.3-2: Speed deviations after a 100MW load increase in area 1 RT/fixed step model versus Variable step model

There are some minor differences, but they originate from various factors, like the slightly different exciters, the additional filters, and the ringing introduced by the load model.

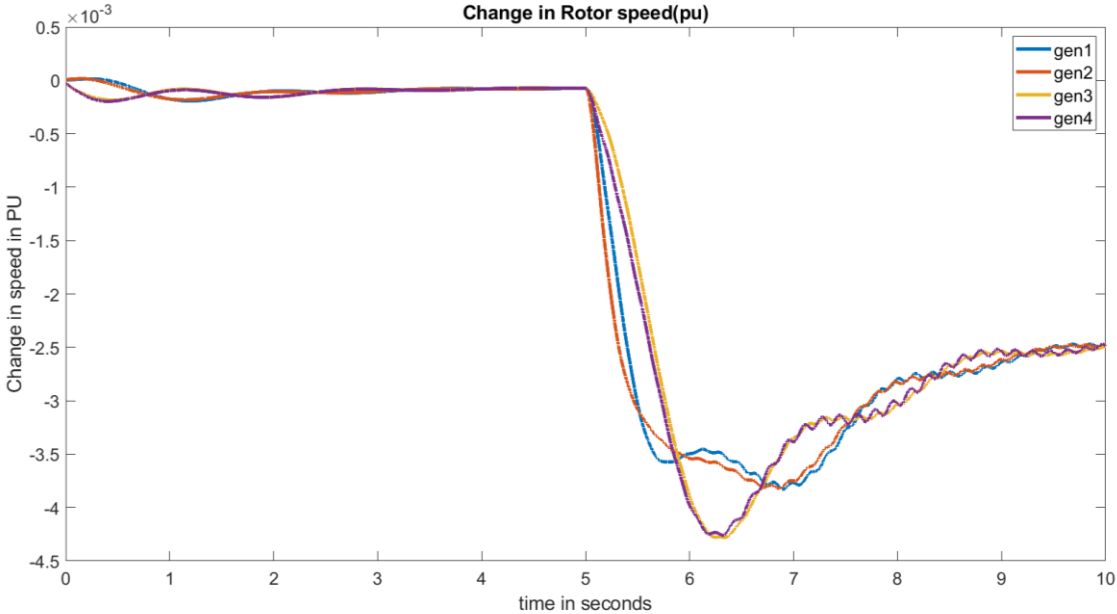


Figure 5.3-3: Speed deviations after a 300MW load increase in area 1 RT

Increasing the load in area 1 to 300MW showed a very noticeable difference from the previous plots. There are some oscillations occurring after the fault, that have a higher

frequency than the inter area modes.

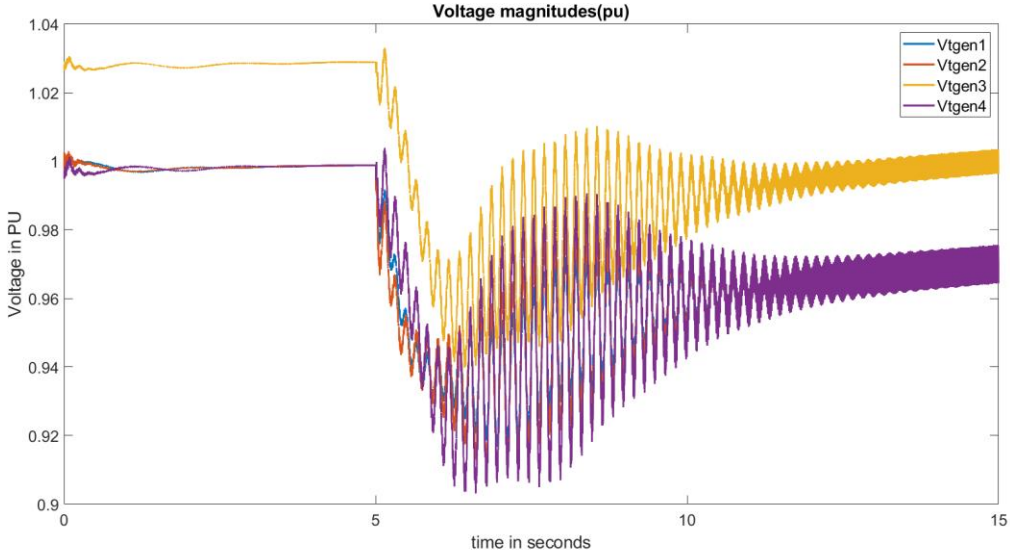


Figure 5.3-4: Terminal voltages after a 300MW load increase in area 1 RT

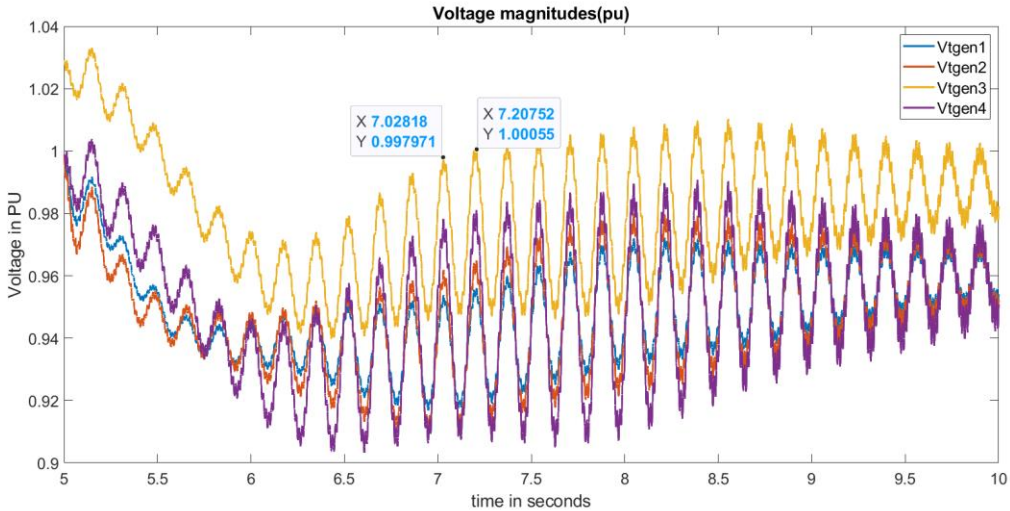


Figure 5.3-5: Terminal voltages after a 300MW load increase in area 1 RT Zoomed in

Looking at the terminal voltages one can see that there is quite strong ringing with a frequency of around 8.333HZ.

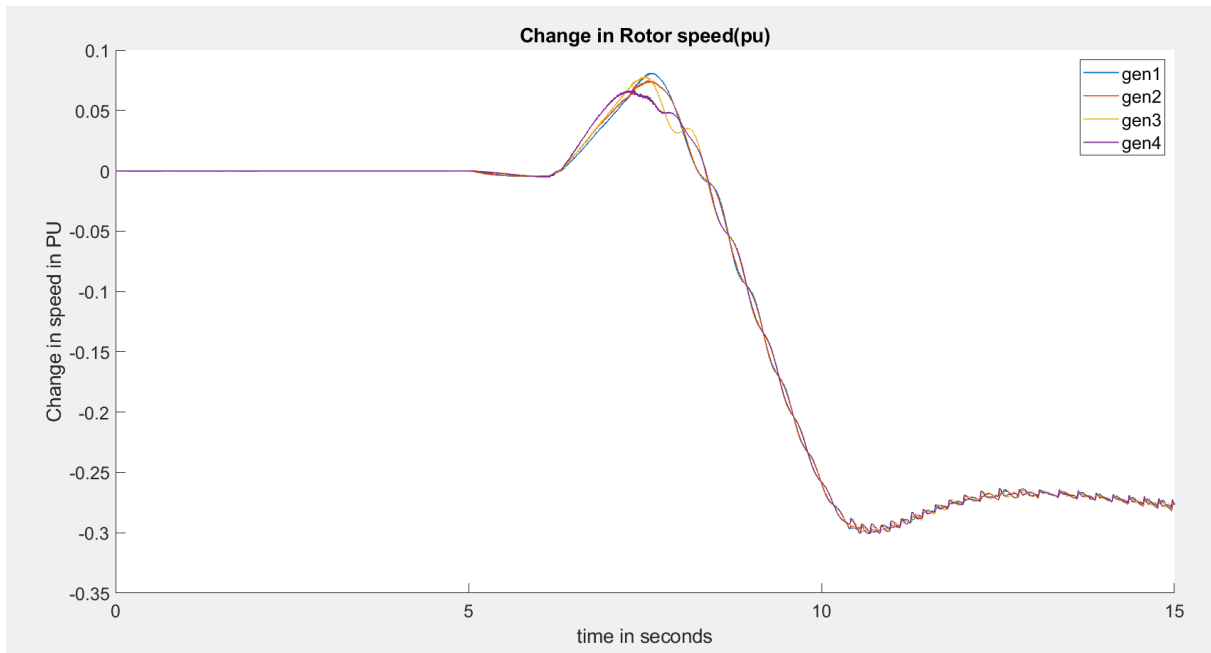


Figure 5.3-6: Rotor speed deviations after a 500MW load increase in area 1 RT

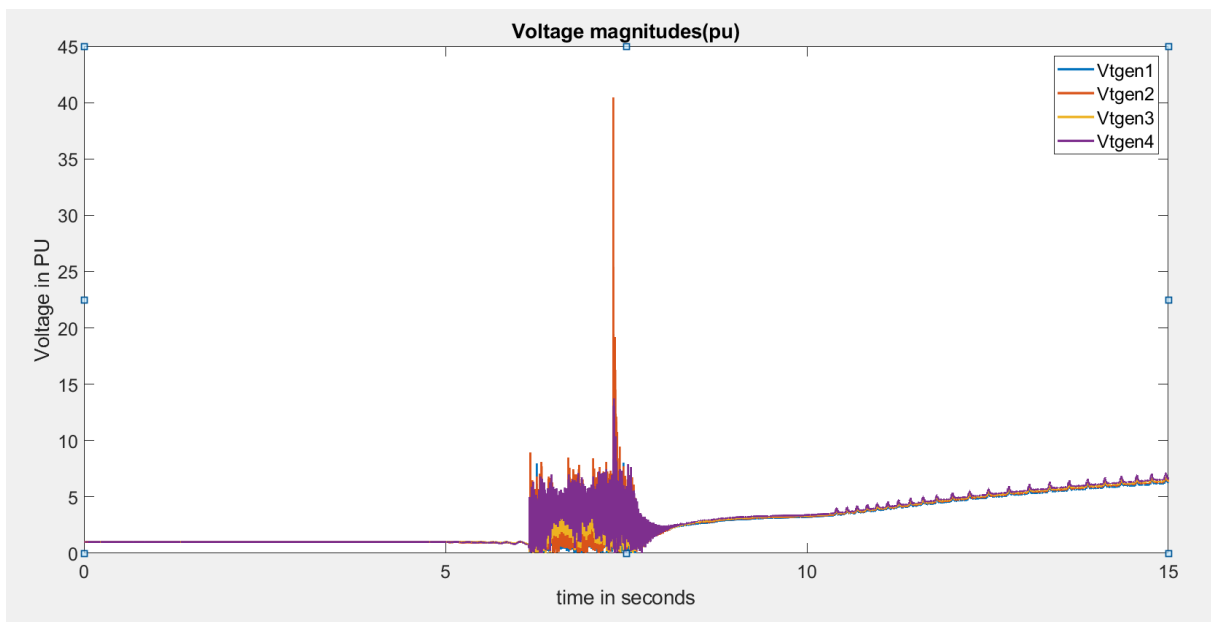


Figure 5.3-7: Terminal voltages after a 500MW load increase in area 1 RT

Pushing the load further, crashes the system as shown here. The terminal voltages gets many times the nominal values. The frequency increases then drops down to 0.7pu of nominal frequency, which means the system has crashed completely. Increasing the time factor of the filter to get an even slower load change does not improve the stability. The system becomes unstable at a certain load value it seems.

The cause of this crash is not clear, but it seems like it is the voltage level rather than the transients that was a cause for the ringing in the system. This would indicate that this version actually considers the voltage stability, unlike the variable step version. Why this might be the result is inconclusive.

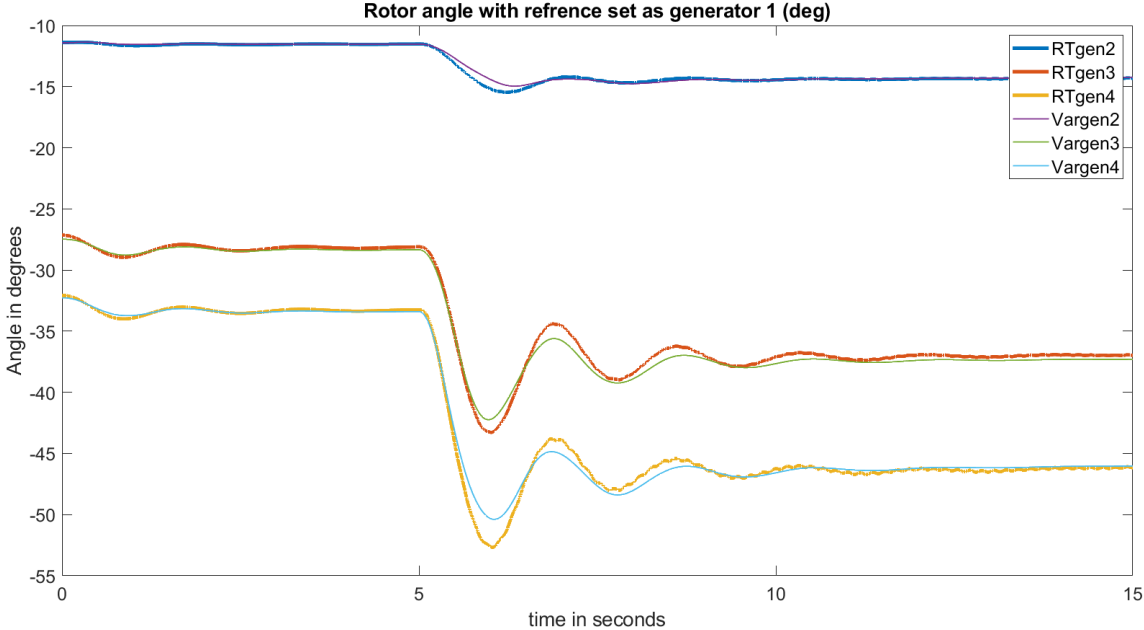


Figure 5.3-8: Rotor angles after a 200MW load increase in area 2 RT/fixed step model versus Variable step model

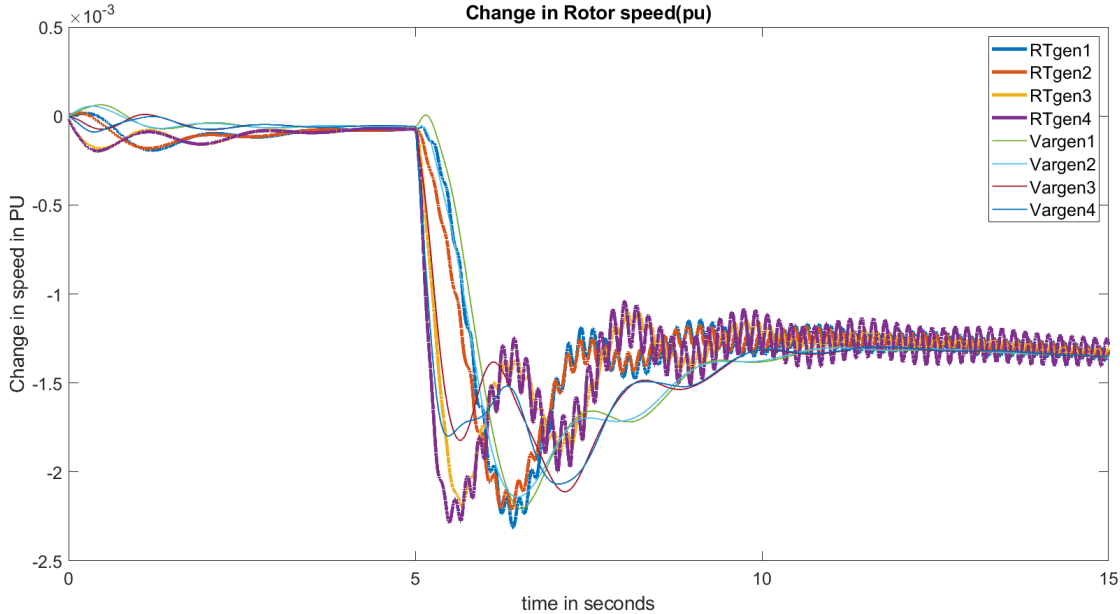


Figure 5.3-9: Speed deviations after a 200MW load increase in area 2 RT/fixed step model versus Variable step model

Testing the second load gives similar results that match the variable step model, but here the system starts getting the oscillations at only +200MW, and crashes at higher load changes in the same way as with changes in area 1. The lower tolerance combined with the results from the variable step model that showed worse voltage levels at the load buses during load changes in area 2, is another sign that it is the lack of voltage stability that causes the system to become unstable.

The RT lab results are very much the same as the variable step results during concurrent load change tests.

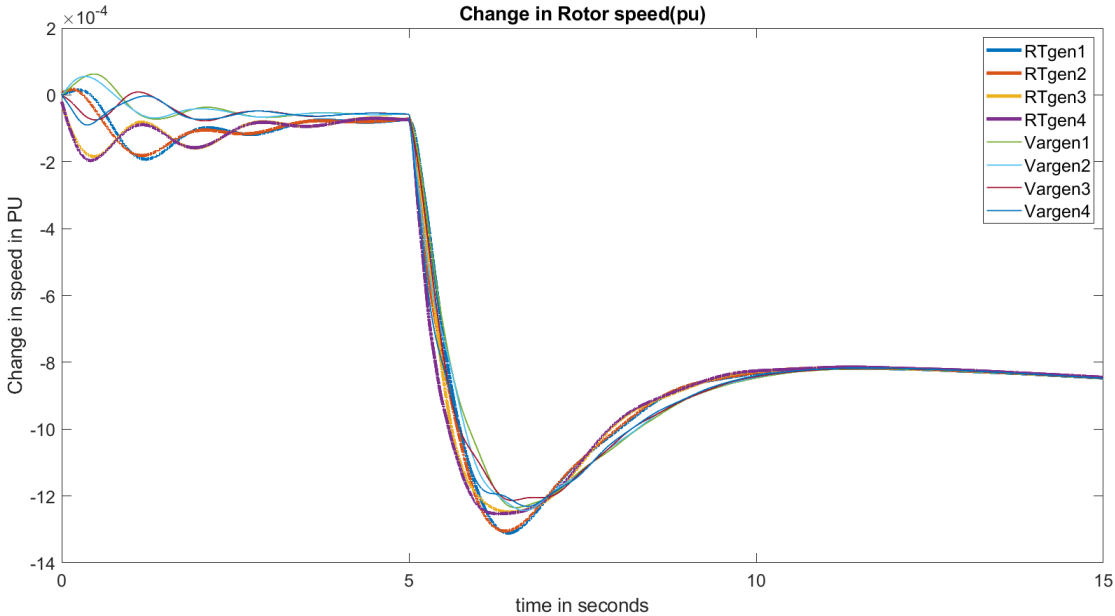


Figure 5.3-10: Rotor speed deviations after a 50MW concurrent load increase in both areas RT lab compared with variable step model

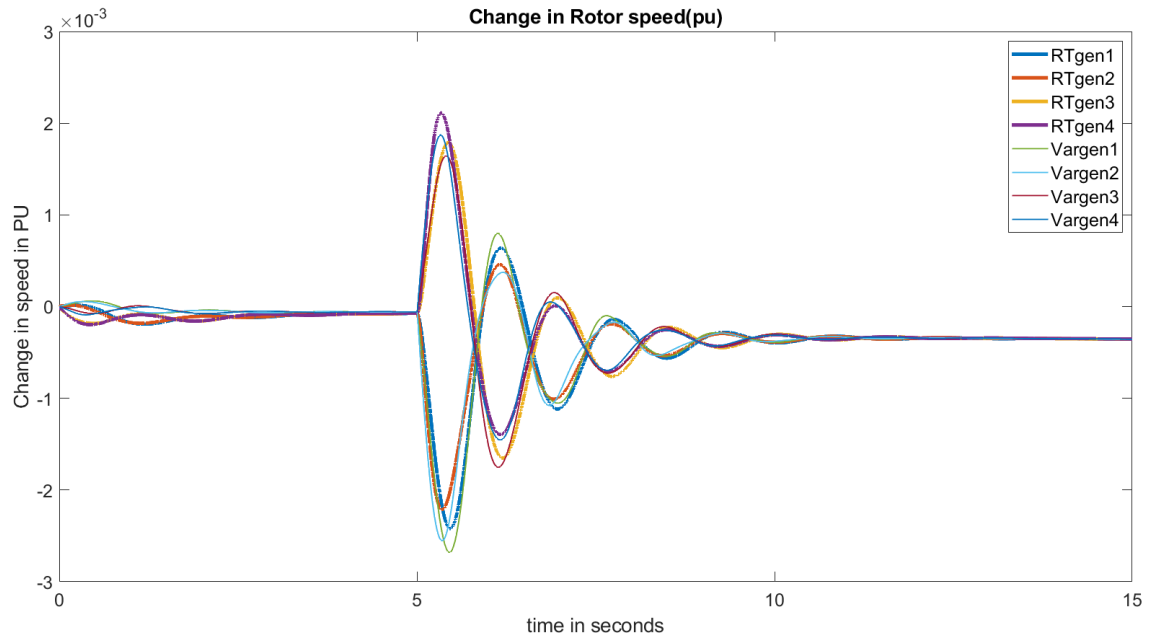


Figure 5.3-11: Rotor speed deviations after a 100MW load increase in area1 and a 100MW load decrease in area 2 RT lab compared with variable step model

5.3.2 Without PSS

The simulations where the PSS was disconnected had more deviations

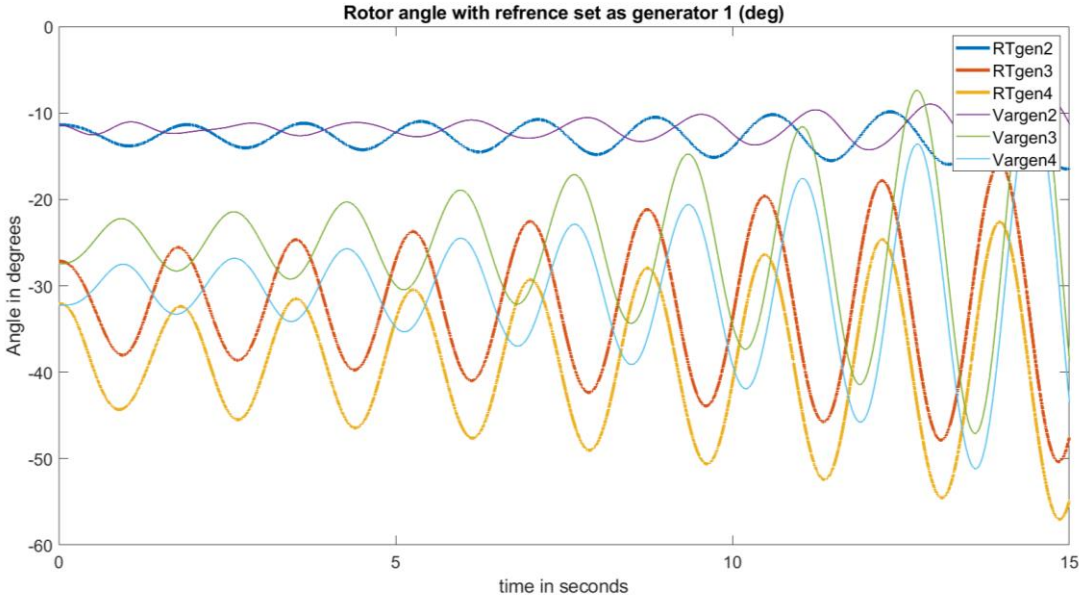


Figure 5.3-12: Rotor angles after a 100MW load increase in area 1 No PSS RT/ fixed step model versus Variable step model

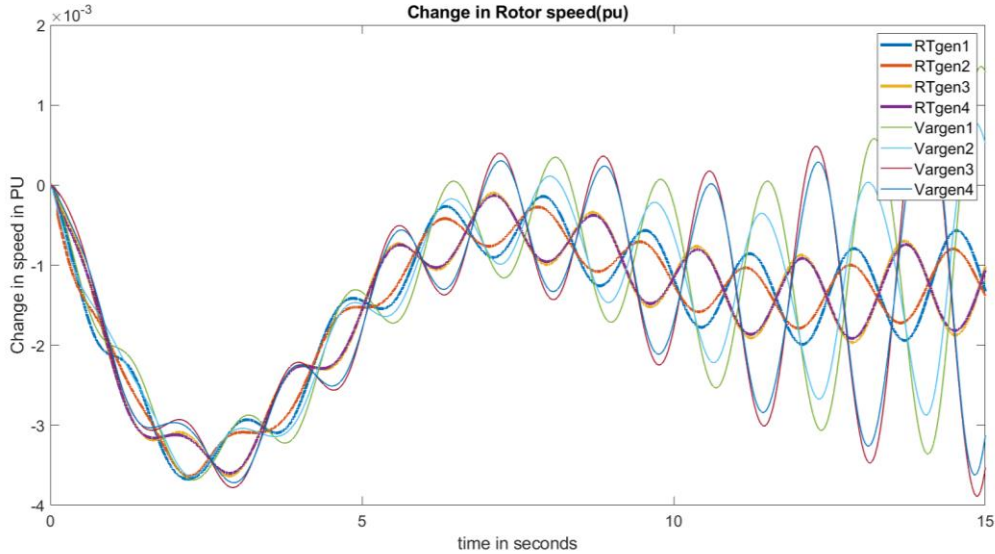


Figure 5.3-13: Speed deviations after a 100MW load increase in area 1 No PSS RT/ fixed step model versus Variable step model

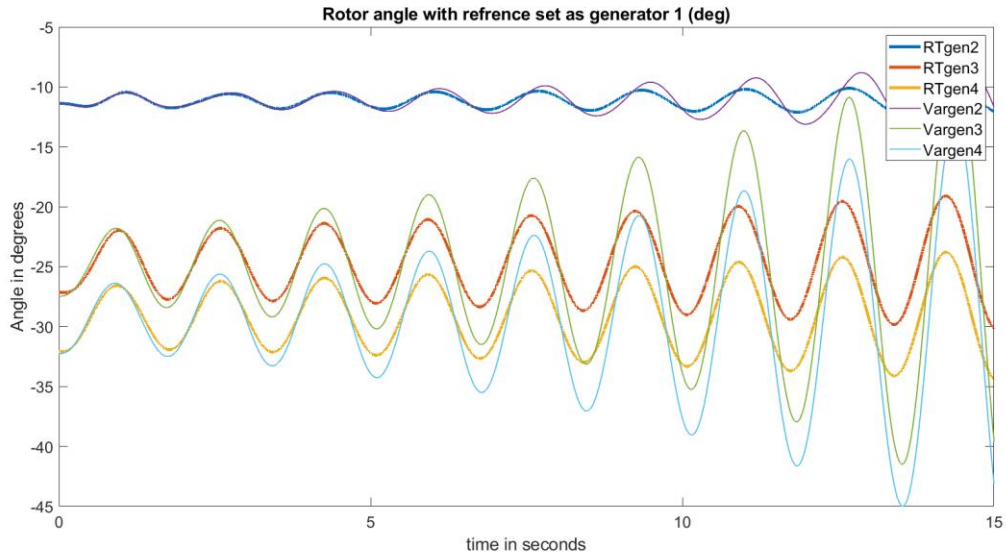


Figure 5.3-14: Rotor angles after a 50MW concurrent load increase in both areas No PSS RT lab compared with variable step model

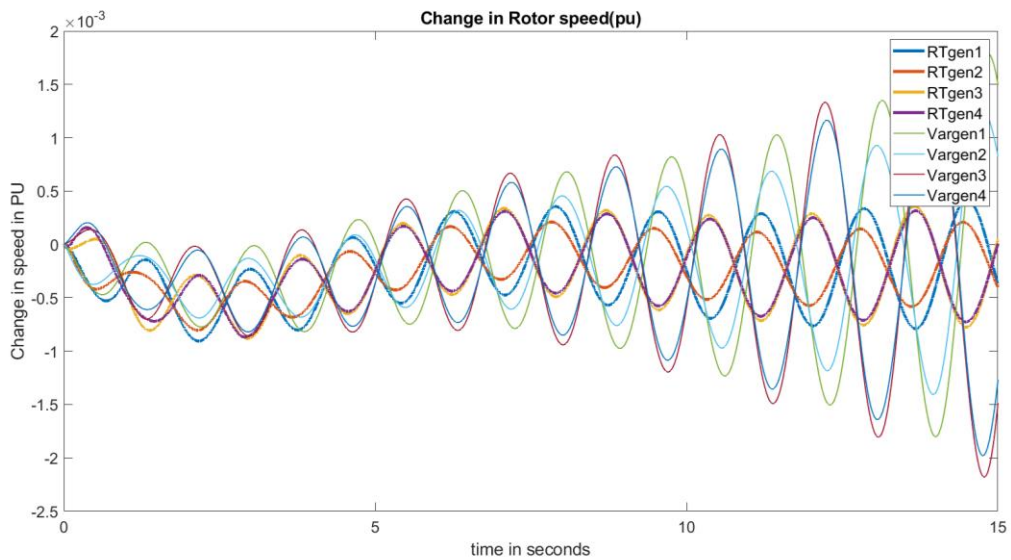


Figure 5.3-15: Rotor speed deviations after a 50MW concurrent load increase in both areas No PSS RT lab compared with variable step model

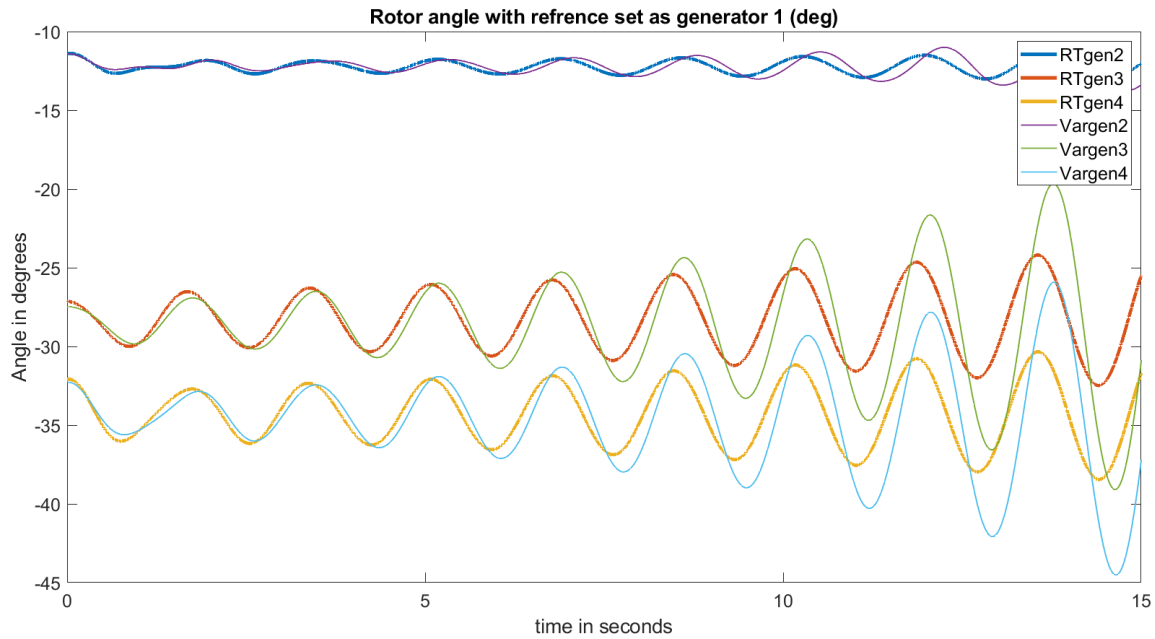


Figure 5.3-16: Rotor angles after a 100MW load increase in area1 and a 100MW load decrease in area 2 No PSS RT lab compared with variable step model

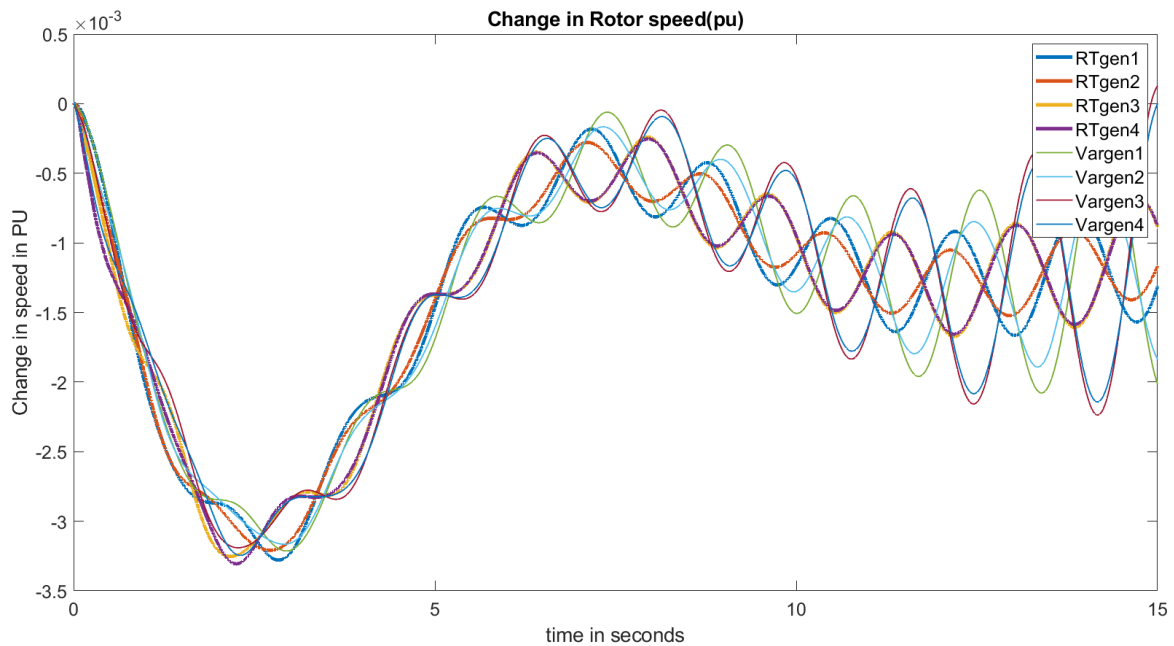


Figure 5.3-17: Rotor speed deviations after a 100MW load increase in area1 and a 100MW load decrease in area 2 No PSS RT lab compared with variable step model

In all cases the oscillations had a higher amplitude in the variable model than the model run on the real time simulator. The difference is not major, but probably originates from the load flow in the network being different leading the RT-lab/fixed step model to have less stressed lines which would help the rotor angle stability.

6 Conclusion and future work

From the results one can see that the different models work very similarly and give results that fits with the theory.

One can see why networks started to implement PSSs since without them long distance networks will have a lot of interarea oscillations that could easily crash the network relatively fast. There are some problems with them, like the ringing in the RT-Lab version, and the lack of consideration for voltage stability in the Variable step model. For the main task of looking only at the interarea oscillations created by load changes the model performs quite well. That the real time simulator is not running in real time is the biggest failure with the project. For future work there needs to be done more studies on the simulator to figure out why it is running so badly.

Using PST for linear analysis is a weakness since it is a very different program from the Simulink model. For future work a way of extracting the solid-state matrix directly from the Simulink model should be found.

Expanding the model with renewable energy sources can also be done in future work, to see how the renewables would affect the rotor angle oscillations. One could also model hydroplants, meaning salient rotors, to make the model more fitting with the current Norwegian power network.

References

- [1] P. Kundur, "Power System Stability and Control". New York, NY, USA: McGraw-Hill, 1994.
- [2] G. Rogers and J. Chow. "Power System Toolbox Version 3.0 Manual". 2008
<https://sites.ecse.rpi.edu/~chowj/PSTMan.pdf>
- [3] G. Rogers, "Power System Oscillations". New York, NY, USA: Kluwer Academic Publisher, 2000.
- [4] Machowski, Jan & Bialek, J.W. & Bumby, J.R.. "Power System Dynamics. Stability and Control". UK: John Wiley & Sons Ltd 2002
- [5] Machowski, Jan & Bialek, J.W. & Bumby, J.R.. "Power System Dynamics. Stability and Control". UK: John Wiley & Sons Ltd 2002 (p. 9)
- [6] P. Kundur, "Power System Stability and Control". New York, NY, USA: McGraw-Hill, 1994. (p. 18)
- [7] Machowski, Jan & Bialek, J.W. & Bumby, J.R.. "Power System Dynamics. Stability and Control". UK: John Wiley & Sons Ltd 2002 (p. 3)
- [8] Machowski, Jan & Bialek, J.W. & Bumby, J.R.. "Power System Dynamics. Stability and Control". UK: John Wiley & Sons Ltd 2002 (p. 5-7)
- [9] Editorial staff. (Publishing date unknown). Rotor Angle Stability of Synchronous Generators in Power System. Instrumentation tools. Last accessed 16th May 2022:
<https://instrumentationtools.com/rotor-angle-stability-synchronous-generators-power-system/>.
- [10] Machowski, Jan & Bialek, J.W. & Bumby, J.R.. "Power System Dynamics. Stability and Control". UK: John Wiley & Sons Ltd 2002 (p. 170-172)
- [11] Machowski, Jan & Bialek, J.W. & Bumby, J.R.. "Power System Dynamics. Stability and Control". UK: John Wiley & Sons Ltd 2002 (p. 176-179)
- [12] Machowski, Jan & Bialek, J.W. & Bumby, J.R.. "Power System Dynamics. Stability and Control". UK: John Wiley & Sons Ltd 2002 (p. 491)

- [13] G. Rogers, "Power System Oscillations". New York, NY, USA: Kluwer Academic Publisher, 2000. (p. 31-33)
- [14] P. Kundur, "Power System Stability and Control". New York, NY, USA: McGraw-Hill, 1994. (p. 711-712)
- [15] B. Pal and B. Chaudhuri, Robust Control in Power Systems. Boston, MA: Springer Science+Business Media, Inc., 2005. (p. 34-35)
- [16] M. Klein, G. J. Rogers and P. Kundur, "A fundamental study of inter-area oscillations in power systems," in IEEE Transactions on Power Systems, vol. 6, no. 3, pp. 914-921, Aug. 1991, doi: 10.1109/59.119229.
- [17] P. Tumino. (October 15, 2020) Frequency Control in a Power System. Instrumentation tools. Last accessed 16th May 2022: <https://instrumentationtools.com/rotor-angle-stability-synchronous-generators-power-system/>.
- [18] Machowski, Jan & Bialek, J.W. & Bumby, J.R.. "Power System Dynamics. Stability and Control". UK: John Wiley & Sons Ltd 2002 (p. 299)
- [19] P. Kundur, "Power System Stability and Control". New York, NY, USA: McGraw-Hill, 1994. (p. 711-400)
- [20] P. Kundur, "Power System Stability and Control". New York, NY, USA: McGraw-Hill, 1994. (p. 711-425)
- [21] Machowski, Jan & Bialek, J.W. & Bumby, J.R.. "Power System Dynamics. Stability and Control". UK: John Wiley & Sons Ltd 2002 (p. 25-26)
- [22] Machowski, Jan & Bialek, J.W. & Bumby, J.R.. "Power System Dynamics. Stability and Control". UK: John Wiley & Sons Ltd 2002 (p. 340)
- [23] Machowski, Jan & Bialek, J.W. & Bumby, J.R.. "Power System Dynamics. Stability and Control". UK: John Wiley & Sons Ltd 2002 (p. 22-23)
- [24] B. Pal and B. Chaudhuri, Robust Control in Power Systems. Boston, MA: Springer Science+Business Media, Inc., 2005. (p. 59-60)

- [25] B. Pal and B. Chaudhuri, Robust Control in Power Systems. Boston, MA: Springer Science+Business Media, Inc., 2005. (p. 65)
- [26] Machowski, Jan & Bialek, J.W. & Bumby, J.R.. "Power System Dynamics. Stability and Control". UK: John Wiley & Sons Ltd 2002 (p. 111-112)
- [27] RT-lab team. (Date unknown) "Building models." OPAL-RT. Last accessed 16th May 2022: <https://wiki.opal-rt.com/display/RD/Building+Models>
- [28] New Mexico EPSCoR (15. June 2021) "OPAL-RT for Beginners". Youtube Last accessed 16th May 2022 <https://www.youtube.com/watch?v=vLljnc6GPSk>
- [29] OPAL-RT . " OP4510 Simulator Manual". (Date unknown) Last accessed 16th May <https://sites.ecse.rpi.edu/~chowj/PSTMan.pdf>
- [30] P. Kundur, "Power System Stability and Control". New York, NY, USA: McGraw-Hill, 1994. (p. 813-814)
- [31] Mathworks . " Performance of Three PSS for Interarea Oscillations". (Date unknown) Last accessed 16th May <https://se.mathworks.com/help/phymod/sps/ug/performance-of-three-pss-for-interarea-oscillations.html>
- [32] Mathworks . " PMU (PLL-based, Positive-Sequence) Kundur's Two-Area System". (Date unknown) Last accessed 16th May <https://se.mathworks.com/help/phymod/sps/ug/pmu-pll-based-positive-sequence-kundur-s-two-area-system.html>
- [33] Mathworks . " Three-Phase Dynamic Load". (Date unknown) Last accessed 16th May <https://se.mathworks.com/help/phymod/sps/powersys/ref/threephasedynamicload.html>
- [33] Mathworks . " Linear System Analyzer". (Date unknown) Last accessed 16th May <https://se.mathworks.com/help/control/ref/linearsystemanalyzer-app.html>

Appendix

MODE DATA WITHOUT PSS

Mode number	Eigenvalue	Dampning factor	Frequency (HZ)
1	-0,0000099702202400672	1	0
2	-0,194973107989279	1	0
3	-0,197661854687224	1	0
4	-0,19768507878681	1	0
5	-0,671750561242661	1	0
6	-0,680557751062714	1	0
7	-0,236545190648605- 0,653677477470661i	0,340274299	0,104036002
8	- 0,236545190648605+0,653677477470661i	0,340274299	0,104036002
9	-0,708438179650606	1	0
10	-0,712084591773498	1	0
11	-1,5509123662052	1	0
12	-1,88952222652482	1	0
13	-1,89398618517934- 0,0115270144289232i	0,99998148	0,001834581
14	- 1,89398618517934+0,0115270144289232i	0,99998148	0,001834581
15	-2,94070849826404	1	0
16	-3,04769159124796	1	0
17	0,135428096532491-3,73054972227586i	-0,036278553	0,593735429
18	0,135428096532491+3,73054972227586i	-0,036278553	0,593735429
19	-3,74815506117902	1	0
20	-3,90501403105687	1	0
21	-0,338283003665267-6,4595046180094i	0,052298139	1,02806209
22	-0,338283003665267+6,4595046180094i	0,052298139	1,02806209
23	-0,383190573999045-6,53953899101425i	0,058495625	1,040799956
24	-0,383190573999045+6,53953899101425i	0,058495625	1,040799956
25	-6,66364073507116	1	0
26	-6,66994499389435	1	0
27	-6,79047047999889	1	0
28	-6,84264317172976	1	0
29	-10,6099056875602	1	0
30	-12,4561278215243-0,742338432545845i	0,99822886	0,118146831
31	-12,4561278215243+0,742338432545845i	0,99822886	0,118146831
32	-8,09349833848268-11,2323729467225i	0,584599139	1,787687677
33	-8,09349833848268+11,2323729467225i	0,584599139	1,787687677
34	-14,6705503874705	1	0
35	-4,79256745441988-14,9464521168633i	0,305336422	2,378801736
36	-4,79256745441988+14,9464521168633i	0,305336422	2,378801736
37	-30,9112761580897	1	0

38	-31,4147993545015	1	0
39	-36,2138523850425	1	0
40	-36,4735121008183	1	0
41	-57,5027242972703-13,2045167116713i	0,974633286	2,101564106
42	-57,5027242972703+13,2045167116713i	0,974633286	2,101564106
43	-57,7800236505628-13,3166896460597i	0,974454572	2,119416983
44	-57,7800236505628+13,3166896460597i	0,974454572	2,119416983
45	-59,8506226756496-16,0366480552302i	0,965926948	2,552311809
46	-59,8506226756496+16,0366480552302i	0,965926948	2,552311809
47	-60,8926953517108-17,8175994673518i	0,959757175	2,835759029
48	-60,8926953517108+17,8175994673518i	0,959757175	2,835759029
49	-69,9662705072471	1	0
50	-70,4564794697491	1	0
51	-71,4720937267452	1	0
52	-71,8301879272459	1	0
53	-166,666666666667	1	0
54	-166,666666666667	1	0
55	-166,666666666667	1	0
56	-166,666666666667	1	0

MODE DATA WITH PSS

Mode	Eigenvalue	Dampningfactor	Frequency (HZ)
1	-9,97119270095471E-06	1	0
2	-0,0527761856259856	1	0
3	-0,103867317428602	1	0
4	-0,106543322553078	1	0
5	-0,106990205278587	1	0
6	-0,170049928279017	1	0
7	-0,170932619623433	1	0
8	-0,175422549054109	1	0
9	-0,192430957673617	1	0
10	-0,196712667954438	1	0
11	-0,198693182976725	1	0
12	-0,198735619603139	1	0
13	-0,681991199022628	1	0
14	-0,681981959264422-0,048238481977079i	0,997507784	0,007677393
15	-		
15	0,681981959264422+0,048238481977079i	0,997507784	0,007677393
16	-0,717791193144085	1	0
17	-0,737240265054267	1	0
18	-1,20116822937311-0,646725847732529i	0,880488554	0,102929615
19	-1,20116822937311+0,646725847732529i	0,880488554	0,102929615
20	-1,66496979641858	1	0
21	-1,71578053993697	1	0
22	-1,87214240130138	1	0
23	-2,24986846349929	1	0
24	-2,31120076750254	1	0
25	-0,830011152197177-3,83468733139147i	0,21154939	0,610309444
26	-0,830011152197177+3,83468733139147i	0,21154939	0,610309444
27	-3,97266343977213-0,0551206697091946i	0,999903756	0,008772727
28	-		
28	3,97266343977213+0,0551206697091946i	0,999903756	0,008772727
29	-6,65952412480618	1	0
30	-6,67389563169097	1	0
31	-6,83853604815388	1	0
32	-6,87314741986814	1	0
33	-7,45842572782974	1	0
34	-7,65875008501223	1	0
35	-0,899638718645128-8,67421818401753i	0,103160752	1,380544701
36	-0,899638718645128+8,67421818401753i	0,103160752	1,380544701
37	-0,928575257389513-8,808460896895i	0,104837635	1,401910093
38	-0,928575257389513+8,808460896895i	0,104837635	1,401910093
39	-6,82211400644901-10,9693681501595i	0,528119352	1,745829164
40	-6,82211400644901+10,9693681501595i	0,528119352	1,745829164
41	-4,08590703546631-15,0155713227772i	0,262564174	2,389802399

42	-4,08590703546631+15,0155713227772i	0,262564174	2,389802399
43	-15,8688677531095	1	0
44	-16,4847063881386	1	0
45	-30,9154082079717	1	0
46	-31,3711624600211	1	0
47	-36,1776560257611	1	0
48	-36,4141560381523	1	0
49	-49,999999999953	1	0
50	-49,999999999981	1	0
51	-49,999999999993	1	0
52	-49,999999999997	1	0
53	-58,303372338224-14,2005586691046i	0,971596156	2,260089107
54	-58,303372338224+14,2005586691046i	0,971596156	2,260089107
55	-58,5345526355117-14,2730480162136i	0,971534368	2,271626145
56	-58,5345526355117+14,2730480162136i	0,971534368	2,271626145
57	-60,1458604385401-16,4135635100999i	0,964722495	2,612299766
58	-60,1458604385401+16,4135635100999i	0,964722495	2,612299766
59	-61,0631350283081-18,058746292844i	0,958943571	2,874138739
60	-61,0631350283081+18,058746292844i	0,958943571	2,874138739
61	-69,8830041646395	1	0
62	-70,3093244045715	1	0
63	-71,1249413444841	1	0
64	-71,4675901333912	1	0
65	-166,666666666667	1	0
66	-166,666666666667	1	0
67	-166,666666666667	1	0
68	-166,666666666667	1	0

